DISS. ETH NO. 20455

LINKING DIFFUSIONAL HETEROGENEITY AND AQUATIC HABITAT FRAGMENTATION WITH MICROBIAL COEXISTENCE AND DIVERSITY IN THE VADOSE ZONE

A dissertation submitted to

ETH ZURICH

for the degree of

Doctor of Sciences

presented by

GANG WANG

MSc in Applied Chemistry, University of Science & Technology of China, China

born March 29, 1979

citizen of China

accepted on the recommendation of

Prof. Dr. Dani Or, examiner
Prof. Dr. Hauke Harms, co-examiner
Prof. Dr. Martin Ackermann, co-examiner

2012

… to my family

ACKNOWLEDGEMENT

There have been so many people helping me during my PhD study! I would now take the opportunity to send my everlasting feeling of gratefulness and thankfulness to all of you. These will be no chance for me to finish my PhD study without your persistent and most kindly help!

It is difficult to overstate my gratitude to my PhD supervisor, Prof. Dr. Dani Or. With his brilliant mind, his inspiration, and his great efforts to explain things clearly and simply, he has helped to make physics and little animals fun for me. Throughout my PhD study time, I would have been lost without his enthusiasm, encouragements, good teaching, and many excellent ideas and advice.

I also would like to thank Prof. Martin Ackermann, the co-examiner of my PhD study. I always enjoyed the fruitful discussions with Martin and his group scientist Dr. Johnson David. My gratitude also goes to co-examiner of my PhD study, Prof. Hauke Harms. I would like to thank him for many last minute proof document sessions on various occasions. I would also like to thank Prof. Barth Smets, Dr. Arnaud Dechesne and Dr. Ganz Gülez, my research partners from the Technical University of Denmark (DTU), for their assistance and productive collaboration. Thanks also go to Prof. Martin Schroth and his research members, Dr. Ruth Henneberger, and Mr. Fabio Ugolini, for their kindly assistance in soil bacteria visualization experiments.

Especially I would like to thank Mr. Daniel Breitenstein and Mr. Hans Wunderli, the great technicians, together with whom we have made interesting laboratory experiments. I would also like to send my gratitude to Mr. Gernot Michlmayr, who is not only sharing the office room with me throughout the last four years, but also a good friend for all sorts of discussions. Spatial thank is due to Ms Christina Häfliger, who is not only my friend, but excellent sources of administrative assistance and many other helps. I would thank my colleagues and fellow PhD students at LASEP (EPF Lausanne) and STEP (ETH Zurich) for providing friendly studying environment and participating in stimulating group exercises developing solutions to all kinds of problems in a wide range of interests. Spatially, I would like to thank Dr. Peter Lehmann and Dr. Stanislaus Schymanski for many fruitful discussions, and also thank Ms Franziska Möbius and Mr. Jonas von Rütte for their numerous kindly assistance for scientific and also for daily problems. Thank is also due to Dr. Yan Jin, from whom I had

received many interesting stories about colloids dynamics sometime behaviors similar with my little animals. Spatial thank also goes to Mr. Fabian Rüdy for his nice graphics distributed throughout the chapters.

I enjoyed my PhD experience that has been extensively interesting, and I would like to express my spatial gratitude to Dr. Papritz Andreas, with whom we have shared many excursion experiences from Swiss mountains and forest.

I wish to gratefully thank my entire extended family for providing a loving environment for me.

Lastly, I wish to thank my parents, they bore me, raised me, taught me, and love me; thank my parents-in-law, who constantly support me and love me; and most importantly, I wish to thank my wife, Guowei Chen and my son, Yizhou Wang, together with whom we have now the most lovely family. To them I dedicate this thesis.

Gang Wang

May 1, 2012, Zurich

TABLE OF CONTENTS

TABLE OF CONTENTS.....I

ABSTRACT V

ZUSAMMENFASSUNG VII

Chapter 1

General Introduction 1

1.1 Microbial diversity and function in soil..... 1

1.2 Modeling hydro-physical microbial interactions in soil..... 2

1.3 Ecological challenges for microbial function in unsaturated soil..... 2

1.3.1 Hydration functions, microbial motility and dispersal on rough surfaces 2

1.3.2 Hydration fluctuations, microbial growth and species coexistence on rough surfaces 3

1.3.3 Linking soil biodiversity with environmental variables, a biophysical metric 4

1.3.4 Trophic interactions, microbial diversity and ecological functions on rough surfaces 4

References..... 6

Chapter 2

Hydration Controlled Bacterial Motility and Dispersal on Surfaces 11

2.1 Introduction 13

2.2 Materials and Methods 13

2.2.1 Bacterial strains..... 13

2.2.2 Experiments on the Porous Surface Model..... 14

2.2.3 Modeling bacterial motility and growth on rough surfaces 15

2.3 Results and Discussion 15

2.3.1 Bacterial motility on rough surface – experimental observations..... 15

2.3.2 Simulation models of bacterial motility on rough surfaces 16

2.3.3 Conclusions and implications..... 20

Acknowledgments..... 21

References..... 22

Appendix: Individual-based simulation of motility and dispersal 25

Chapter 3

Aqueous Films Limit Bacterial Cell Motility and Colony Expansion on Partially Saturated Rough Surfaces 31

3.1 Introduction 33

3.2 Theoretical Considerations 34

3.2.1 Model of heterogeneous rough surface 35

3.2 2 Water configuration on surface roughness network 35

3.2.3 Bacterial motility on partially-saturated rough surface 37

3.2.4 Bacterial growth on partially-saturated rough surface 39

3.2.5 Linking bacterial colony expansion rates with cell motility 40

3.3 Results and Discussion 41

3.3.1 Bacterial cell motility on partially-saturated surface roughness network 41

3.3.2 Bacterial growth on partially-saturated surface roughness network 42

3.3.3 Bacterial colony expansion rates on rough surfaces 43

3.4 Conclusions 46

Acknowledgements 47

References 48

Appendix S1: Capillary pinning force acting on a bacterial cell 54

Appendix S2: Growth kinetics of individual bacterial cell 55

Appendix S3: Bacterial motility on partially-saturated rough surface 56

Chapter 4

Hydration Dynamics Promote Bacterial Coexistence on Rough Surfaces 61

4.1 Introduction 63

4.2 Materials and Methods 64

4.2.1 Modeling heterogeneous rough surface and water configuration 64

4.2 2 Nutrient diffusion and bacterial motility on partially hydrated rough surfaces 65

4.2.3 Simulations of bacterial growth and competition on dynamically-hydrated rough surfaces 67

4.3 Results 68

4.3.1 BMicrobacterial growth and competition on rough surfaces under static hydration conditions 68

4.3.2 Effects of hydration dynamics on microbial growth and species coexistence 70

4.4 Discussion 72

Acknowledgements 76

References 77

Chapter 5

A Hydration-Based Biophysical Index for the Onset of Soil Microbial Coexistence 81

5.1 Introduction 83

5.2 Methods 84

5.2.1 Aqueous-phase configuration on rough surface and analytical prediction 84

5.2.2 Analytical solutions of nutrient diffusivity on rough surfaces 84

5.2.3 Microbial motility and generation length inhabiting unsaturated rough surfaces 85

5.2.4 The definition of predictive microbial coexistence index 86

5.3 Results 86

5.4 Discussion 90

Acknowledgements 91

References 92

Supplementary information 94

Chapter 6

Trophic Interactions and Self-organization of Microbial Consortia on Unsaturated Surfaces 103

6.1 Introduction 105

6.2 Methods 105

6.2.1 Modeling microbial growth on rough surfaces 105

6.2.2 Modeling microbial trophic interactions on unsaturated surfaces 107

6.2.3 Analytical predictions in nutrient diffusion scale and microbial active motility range 107

6.3 Results and Discussion 109

6.3.1 Microbial dynamics and self-organizations of trophically-interacting consortia 109

6.3.2 Hydration and spatial heterogeneity and nutrient concentrations affecting self-organization dynamics 109

6.3.3 Microbial dynamics and self-organizations with multitrophic interactions 112

6.4 Summary and Conclusions 114

Acknowledgements 115

References 116

Chapter 7

Summary and Outlook 121

7.1 Summary 121

7.2 Outlook 123

Curriculum Vitae 125

ABSTRACT

Notwithstanding the inhospitable and nutrient poor environment and the vagaries of ambient and hydration conditions, soil is the most biologically active compartment of the biosphere, hosting unparalleled biodiversity at all scales. Present understanding of soil as a complex and dynamic habitat for microbial life is sketchy and often suffers from misconceptions regarding what constitutes favourable or unfavourable environments. Consequently, understanding of the original patterns of soil microbial diversity represents an immense and uncharted scientific frontier. Progress in resolving mechanisms that promote the unparalleled soil biodiversity and sustain the immense soil ecosystem functions requires transformation of heuristic ecological concepts into process-based models that consider dynamic biophysical interactions at appropriate spatial and temporal scales.

We developed a hybrid modeling framework that couples individual-based modeling approach with diffusion-consumption elements for microbial growth and nutrient consumption, and trophic interactions at individual cell scale on rough surfaces. The model resolves spatial and temporal nutrients diffusion fields defined by boundary conditions, surface geometry features and by local nutrients interceptions by individual cells, and explicitly tracks motions and life histories of individual cells considering primary hydrodynamic and capillary constraints to motility. It enables systematic estimating the effects of hydration status and surface geometrical properties on bacterial cell motility and impacts on surface-attached bacterial colony growth and expansion, and the influence of variable hydration conditions on microbial population interactions and community dynamics on partially hydrated rough surfaces, as well as the effects of trophic interactions on shaping microbial population dynamics and community structure, and their impacts on microbial ecological functioning in unsaturated soils.

Combined experimental observation with simulation models, we have demonstrated that hydration-induced aqueous phase configuration coupling surface geometry properties impose significant physical constraints (cell-wall hydrodynamic and capillary forces) upon microbial cell motility on partially-hydrated rough surfaces, and couples nutrient diffusion limitations, control microbial growth and colony development. The results defined a surprisingly narrow range of hydration conditions (within a few kPa of matric potential value) where motility confers ecological advantage upon microbial life on natural surfaces (seeing chapters 2 and 3). The rapid fragmentation of soil aqueous phase under most natural conditions suppresses microbial growth and cell dispersion thereby balances conditions experienced by competing populations. Additionally, hydration fluctuations intensify localized interactions that lead to

promotion of coexistence by affecting disproportionally densely populated regions during dry periods thereby affecting microbial population dynamics far beyond responses predicted from equivalent stationary hydration values (chapter 4). Based on the knowledge gained from the systematic study of microbial dynamics inhabiting unsaturated rough surfaces, we have successfully developed a novel biophysically-based metric capable for predicting the onset of microbial species coexistence and diversity in soils based on solely quantifiable biophysical variables. The model predicted a surprisingly narrow range of hydration conditions that mark a sharp transition from suppression to promotion of microbial diversity irrespective of soil type or details of surface roughness geometry for the onset of microbial coexistence consistent with limited experimental results and with individual-based simulation models (chapter 5). Simulation models of microbial trophic interactions revealed that trophic interactions among multiple species may increase ecological niche dimensionality through spatial self-organization of microbial consortium. Spatial organization is strongly influenced by the geometry of primary nutrient fluxes and by the nature and rate of release of byproducts essential for other members in the consortium. Not surprisingly, hydration conditions and spatial heterogeneity impose diffusion constraints and motility limitations that influence levels and rates of self-organization. Concentration gradients and inhibitory functions of various substrates relative to species growth rates and tolerance levels are clearly manifested in the emerging spatial patterns of consortia (chapter 6).

The study lay at the intersection of environmental microbiology, vadose zone hydrology, and soil physics. The quantitative estimates offered a potential for improved understanding of microbiological interactions in the most active compartment of the biosphere, and it has broad impact in cutting across disciplinary boundaries and in offering new insights into long standing environmental questions that are critical to soil and water resources quality, the fate of biogenic and anthropogenic contaminants, and global biogeochemical cycles, specifically, shedding lights into the origins of the unparallel soil biodiversity maintenance. The proposed framework would offer instrumental tool in guiding future experiments and data collection.

ZUSAMMENFASSUNG

Trotz unwirtlichen und nährstoffarmen Bedingungen, schnell wechselnden Umwelteinflüssen und veränderlichem Wasserhaushalt ist Boden wohl der biologisch aktivste Bestandteil der Biosphäre und beherbergt unübertroffene Biodiversität. Unser Verständnis von Böden als komplexe und dynamische Lebensräume für Mikroorganismen ist nach wie vor lückenhaft und basiert häufig auf fehlerhaften Auffassungen über die Beurteilung von günstigen beziehungsweise ungünstigen Umweltbedingungen. Dementsprechend stellt das Verständnis von Herkunft und Strukturen mikrobiologischer Artenvielfalt eine grosse wissenschaftliche Herausforderung dar. Um die Erforschung von Mechanismen, welche für die gewaltige Biodiversität im Boden verantwortlich sind, voranzutreiben, ist es erforderlich, heuristische ökologische Konzepte durch Prozess-basierte Modelle zu ersetzen, welche in der Lage sind, biophysikalische Wechselwirkungen auf einer angemessenen räumlichen und zeitlichen Skala zu betrachten.

Wir entwickelten ein Hybrid-Modell, das den Individuen-basierten Ansatz mit Diffusions- und Konsumptionselementen für das microbielle Wachstum und die Nährstoffverfügbarkeit auf rauhen Oberflächen koppelt, und durch trophische Wechselwirkungen auf individueller Zellebene ergänzt. Das Modell beschreibt räumlich und zeitlich aufgelöste Diffusionsprozesse basierend auf gegebenen Randbedingungen, geometrischen Gegebenheiten der rauhen Oberfläche und lokaler Entnahme durch einzelne Mikroben. Die Bewegung und der Lebenszyklus individueller Zellen wird durch das Model verfolgbar gemacht, wobei hier insbesondere Einschränkungen der Bewegungfreiheit durch Kapillarkräfte und hydrodynamische Bedingungen berücksichtigt werden. Das Model erlaubt eine systematische Einschätzung, wie sich der Benetzungsgrad einer rauhen Oberflächen und deren geometrische Beschaffenheit auf die Beweglichkeit von Bakterien auswirkt, sowie deren Einfluss auf das flächenhafte Wachstum von Bakterienkulturen. Ferner ermöglicht es eine quantitative Bewertung des Einflusses von trophischen Wechselwirkungen auf die mikrobielle Populationsstruktur und -dynamik, und deren Auswirkung auf die Erhaltung der Biodiversität und ökologischer Funktionen.

Eine Kombination von experimentellen Beobachtungen und Modellsimulationen zeigte, dass die topographische Oberflächenbeschaffenheit und die räumliche Konfiguration benetzter lächen gemeinsam zu einer erheblichen physikalischen Einschränkung der Bewegungsfreiheit von Mikroorganismen führen (hauptsächlich durch hydrodynamische Interaktionen zwischen Zelle und Untergrund bezwiehungsweise durch Kapillarkräfte). Da zusätzlich der diffusive Transport

von Nährstoffen bei niedrigem Benetzungsgrad limitiert ist, hängt das Wachstum von Zellkulturen und deren Entwicklung auf rauhen Oberflächen zu einem grossen Teil vom Vorhandensein von Wasser ab. Unsere Resultate zeigen eine überraschend schmale Bandbreite von Benetzungsgraden (innerhalb weniger kPa Matrixpotential) einer natürlichen Oberfläche, in der mikrobielle Bewegung ökologische Vorteile bietet (Kapitel 2 und 3). Die rasch zunehmende Fragmentierung von benetzten Flächen bei Abnahme der Oberflächenfeuchte (wie es unter natürlichen Bedingungen häufig auftritt) beschränkt Wachstum und Ausbreitung der Mikroorganismen und gleicht damit die Konkurrenz zwischen einzelnen Populationen aus. Ausserdem intensivieren Schwankungen der Oberflächenbenetzung kleinräumige Interaktionen, die die Koexistenz von Arten dadurch fördern, dass sie dicht besiedelte Populationen ungleich stärker beeinträchtigen, und auf diese Weise die mikrobielle Populationsdynamik weit stäker beeinflussen, als dies bei Betrachtung von äquivalenten stationären Hydrationsverhältnissen zu erwarten wäre (Kapitel 4). Basierend auf dem Wissen, das wir durch die systematische Studie von mikrobieller Populationsdynamik auf rauhen Oberflächen gewannen, konnten wir eine neuartige Kennzahl entwickeln, welche die Möglichkeit mikrobiellen Zusammenlebens und mikrobieller Diversität lediglich aufgrund von biophysikalischen Variablen vorhersagt. Dieses Modell sagt eine überaschend schmale Bandbreite von Benetzungsgraden voraus, bei welcher Biodiversität hemmende und fördernde Mechanismen einander ablösen. Solche Vorhesagen behalten ihre Gültigkeit unabhängig von spezifischen Bodentypen oder geometrischen Details einer rauhen Oberfläche. Unsere Prognosen bezüglich mikrobieller Koexistenz sind ebenfalls im Einklang mit den wenigen verfügbaren experimentellen Beobachtungen und bisherigen Individuen-basierten Modellergebnissen (Kapitel 5). Unsere Simulationsresultate haben ergeben, dass trophische Wechselwirkungen zwischen mehreren Arten die Dimensionalität der ökologischen Nischen durch räumliche Selbstorganisation der mikrobiellen Gemeinschaft erhöhen könnten. Die räumliche Organisation ist stark abhängig von der Richtung des Transports primärer Nährstoffe, sowie von der Ausscheidung sekundärer Nährstoffe, welche von anderen Mitgliedern in einer gegebenen Biozönose genutzt werden. Erwartungsgemäss entscheidet die Menge und Verteilung von Wasser an einer Oberfläche über Einschränkungen für die Nährstoffdiffusion und die mikrobielle Beweglichkeit, und ist dadurch auschaggebend für die Möglichkeit und den Grad der Selbstorganisation. Konzentrationsgradienten von Nährstoffen, sowie die einschränkenden Einfluesse unterschiedlicher Substrate bezüglich Wachstumsraten und Toleranzniveaus verschiedener Bakterienarten spiegeln sich eindeutig in den auftretenden räumlichen Verteilungsmustern der mikrobiellen Gemeinschaften (Kapitel 6).

Diese Studie vereint Elemente der Umweltmikrobiologie, der Bodenhydrologie und der Bodenphysik. Resultierende quantitative Abschätzungen ermöglichen ein vertieftes Verständnis der mikrobiellen Wechselwirkungen im wohl aktivsten Teil der Biosphäre. Diese disziplinübergreifende Studie liefert Antworten auf wichtige und langjährige Fragen der Umweltwissenschaften. Ihre Relevanz erstreckt sich auf Fragen der Qualität unserer natürlichen Wasserressourcen und deren Beeinträchtigung durch natürliche und anthropogene Schadstoffe, sowie auf die Untersuchung des biologischen und geochemischen Kreislaufs. Im Speziellen lässt sie die gewaltige Vielfalt und Diversität von Mikroorganismen in natürlichen Böden in eine neues Licht setzen. Die vorgestellten Konzepte bieten ausserdem einen nützlichen Leitfaden für zukünftige experimentelle Untersuchungen und Datenerhebungen.

Chapter 1

General Introduction

1.1 Microbial diversity and function in soil

Notwithstanding the inhospitable and nutrient poor environment and the vagaries of extreme fluctuations in environmental conditions, soil is the most biologically active compartment of the biosphere hosting unparalleled microbial diversity at all scales (Stotzky, 1997; Fenchel, 2002; Torsvik and Ovreas, 2002; Fierer and Jackson, 2006; Hibbing *et al.*, 2010). Even at very small scale, many thousands to millions of distinct genotypes (or operational taxonomic units - OTU) may inhabit one gram of soil (Torsvik *et al*., 1990; Curtis *et al*., 2002; Schloss and Handelsman, 2006). Results show that soil fungal, archaeal, and viral communities are as diverse as soil bacteria (Schloss and Handelsman, 2006). Soil microbes live in habitats of complex and extremely variable physico-chemical environmental conditions (Curtis & Sloan 2004; Fenchel 2002; Young & Crawford 2004; Prosser *et al*., 2007). The resulting ecological heterogeneity of soils from the interplay of spatiotemporal, physical, chemical and nutritional variables delineating spheres of influence that may separate microbes with respect to location, physiology, or genetics (Dion, 2008). Although spatial and nutritional heterogeneities, and spatial and temporal microhabitat fragmentation are often cited as key factors promoting the immense microbial diversity found in soils, understanding of the original patterns of the dynamics and interplay of mechanisms that sustain such diversity and maintain numerous ecological functions remains sketchy (Zhou *et al*., 2002; Curtis and Sloan, 2004; Torsvik *et al*., 2006; Prosser *et al*., 2007; Dion, 2008).

An important and poorly studied aspect of soil microbial diversity is its temporal component, because molecular-based estimates of microbial diversity in soils are likely to represent a genetic potential most of which may be associated with inactive organisms (similar to the discrepancy between seed bank found in soil relative to actual plant composition - Prosser *et al*., 2007). The ambiguity introduced by the fact that bacteria may be active at different times due to temporal discontinuity of their functional niches (Torsvik *et al*., 1996) presents a challenge establishing direct links between diversity and recent soil environment and also requires revision of elements of ecological theory. The question of how much of molecular-based genetic diversity estimates is directly linked and shaped by present ecological conditions vs. how much of it is shaped by population and interspecies interactions over time remains a central challenge for modern microbial ecology (Prosser *et al*., 2007; Curtis and Sloan, 2005). A promising path of research is

to capitalize on the highly "plastic" physiological and ecological adaptation of microbial life to extreme variations in environmental conditions, even to physico-chemical conditions that define the limit of life, such as desiccation (Torsvik and Ovreas, 2008; Dion, 2008).

1.2 Modeling hydro-physical microbial interactions in soil

Progress in resolving ecological questions pertaining to the origins and mechanisms that promote and sustain soil microbial diversity and the translation of qualitative concepts into predictive tools must rely on quantitative models for integration of main bio-physico-chemical processes considering ecological interactions at appropriate spatial and temporal scales (Kerr *et al*., 2002; Reichenbach *et al.*, 2007; O'Donnell *et al*., 2007; Dion, 2008; Banavar and Maritan, 2009). In a recent review on the role of ecological theory in microbial ecology, Prosser *et al*. (2007) asserts that "*Many pressing questions in microbial ecology require the consideration of both spatial and temporal scale. Growth rates can vary over several orders of magnitude depending on environmental and nutritional conditions, and speciation will depend on both growth and dispersal. Analysis of the combined effects of these factors on microbial community structure, evolution and ecosystem function requires quantitative modeling* ...". In this study, we developed a modeling framework based on spatially- and temporally resolved hybrid model (Long and Or, 2005, 2007, 2009) that couples nutrient diffusion-consumption elements with individual-based modeling approach of microbial growth and dispersion on rough surfaces (or unsaturated soils).

1.3 Ecological challenges for microbial function in unsaturated soil

1.3.1 Hydration functions, microbial motility and dispersal on rough surfaces

Bacterial motility is recognized as a key mechanism for small scale biodiversity maintenance and ecosystem functions (Mills, 2003; Reichenbach *et al*., 2007; Venail *et al*., 2008). In contrast to water-replete environments where bacterial motility is essentially unrestricted, soil bacteria constantly encounter various physical constraints habiting patchy and dynamic soil environments where aquatic microhabitats are often fragmented and connected only by thin liquid films of bacterial size or smaller (Or *et al*., 2007). The limitations to bacterial motility in thin liquid films have long been posited but never directly quantified or described biophysically; and the fitness benefit associated with bacterial motility in partially saturated soils has been debated due to conflicting experimental data (Boelens *et al*., 1994; Turnbull *et al*., 2001). Despite lack of direct observations of bacterial motility in unsaturated soils, evidence suggest

that soil hydration and pore-space characteristics play critical roles in bacterial motility (Barton and Ford, 1997; Chang and Halverson, 2003; Or *et al*., 2007).

Here we experimentally grow bacteria on hydration controlled porous ceramic surface that enables direct observations of individual bacterial dispersal for systematic estimating how surface hydration condition (matric potential) couples surface geometrical properties (pore space heterogeneity) influence bacterial motility, and the impact of such constraints on surface-attached bacterial colony growth and expansion. To mechanistically explain our experimental observations and to provide a predictive tool for bacterial dispersal and colony development on partially-hydrated rough surfaces, we also proposed a hybrid model that couples individual-based modeling approach (Kreft *et al*., 1998) with classical diffusion-reaction elements (Golding *et al*., 1998) for bacterial growth in model heterogeneous nutrient diffusion field where surface roughness and water configuration conspire to impose capillary and viscous constraints affecting bacterial motility. The details of this study are discussed in chapters 2 and 3.

1.3.2 Hydration fluctuations, microbial growth and species coexistence on rough surfaces

It is clear now that statistic hydration status coupling pore-space characteristics may play critical roles in shaping nutrient fields and microbial motility and thereby control microbial growth and dispersal in unsaturated soils and in other porous systems (Barton and Ford, 1997; Wilson *et al*., 2002; Chang and Halverson, 2003; Or *et al*., 2007; Wang and Or, 2010; Chen and Jin, 2011). In addition to spatial heterogeneity of microhabitats formed by complex soil geometrical structures and hydration associated aqueous phase configurations, dynamic fluctuations in hydration conditions are common in natural soil environments. The resulting aqueous phase reconfiguration creates new niches that ate capable of sheltering weaker populations, or cutoff thriving communities from nutrient source diffusion pathways, and thereby balance species evenness and enhance microbial coexistence (Torsvik and Ovreas, 2008). Earlier studies indicated that large fluctuations in hydration conditions cause significant decay in microbial biomass, and alter community composition in general (Fierer and Schimel, 2002; Gordon *et al*., 2008). Nevertheless, most previous studies have focused on microbial survival and population recovery with little consideration of dynamic processes of hydration variations upon microbial community dynamics and population compositions (Prosser *et al*., 2007; Torsvik and Ovreas, 2008). It is no surprise that a mechanistic picture of how soil microbial diversity is promoted and maintained remains largely sketchy (Torsvik and Ovreas, 2008; Ponciano *et al*., 2009).

In this part, we study the combined effects of hydration dynamics and diffusional heterogeneity on microbial growth, motility, competition and species coexistence on partially

hydrated rough surfaces. We employed the hybrid modeling framework as described above and developed new elements of multiple population growth, dispersal and interactions among individual cells. The results and discussions are followed in chapter 4.

1.3.3 Linking soil biodiversity with environmental variables, a biophysical metric

Present understanding of soil as a complex and dynamic habitat for microbial life is sketchy and often suffers from misconceptions regarding what constitutes favorable or unfavorable environments (Stotzky, 1997). The soil physicochemical environment is inherently heterogeneous and patchy, with the aqueous phase essential for microbial life highly dynamic and fragmented (Torsvik *et al*., 2002; Or *et al*., 2007). The complex pore spaces and fragmented aqueous habitats impose constraints on nutrient transport and on microbial motion in unsaturated soils, making molecular diffusion the primary mechanism for nutrient supply relative to transport by infrequent infiltration (e.g., following irrigation or heavy rainfall) episodes (Or *et al*., 2007; Dechesne *et al*., 2010; Wang and Or, 2010). Inhabiting such patchy and ecologically heterogeneous environments even at small scale, motility (however limited) and other strategies for augmenting resource acquisition become critical for survival and functioning (Fenchel, 2002; Olson *et al*., 2004; Mitchell and Kogure, 2006; Or *et al*., 2007; Banavar and Maritan,2009; Hibbing *et al*., 2010). To translate these heuristic ecological concepts, and provide a predictive tool for estimating soil microbial diversity, we developed a novel biophysical index for hydration-mediated microbial coexistence potential in soils that integrates key quantifiable biophysical variables, such as aquatic habitat size and connectivity, nutrient diffusion affecting microbial growth rates, and aqueous films influencing motility and dispersal. We discuss the modeling development and its applications in soil microbiology in chapter 5.

1.3.4 Trophic interactions, microbial diversity and ecological functions on rough surfaces

Microorganisms are the main agents for the majority of soil ecological functions and ecosystem services (Schink, 1997; Dejonghe *et al*., 2003; Curtis & Sloan 2004; Pérez-Pantoja *et al*., 2009; Oren, 2010). Recent advance in microbial biology revealed that microbial communities, that are linked through numerous trophic processes, rather than individual species control the key processes of interactions with local environments in principle (McCann *et al*., 1998; Woyke *et al*., 2006; Miller *et al*., 2010). Although trophic interactions have been long time argued for shaping the immense biodiversity and ecological functioning of macroscale plants and animal ecosystems in detail (Knight *et al*., 2005; Harpole and Tilman, 2007; Alexandrou *et al*., 2011; Cardinale, 2011), understanding of the original patterns and interplay of mechanisms that link

trophic processes and microbial dynamics and ecological implications remains sketchy giving the ambiguity introduced by the fact that soil microbes may be active at different times due to temporal discontinuity of their functional niches (Curtis and Sloan, 2004; Torsvik *et al*., 2006; Prosser *et al*., 2007). Progress in establishing direct links between trophic processes coupling spatial and nutritional variables and microbial community dynamics and ecological implications requires quantitative modeling that integrates revision of elements of ecological theories and bio-physico-chemical processes at appropriate spatial and temporal scales (Prosser *et al*., 2007; O'Donnell *et al*., 2007; Banavar and Maritan, 2009; Gonzalez *et al*., 2011; Morelli *et al*., 2012).

In this part, we study the effects of trophic interactions on shaping microbial population dynamics and community structure, and their impacts on microbial ecological functioning in unsaturated soils. We employed the individual-based modeling framework described above and included new elements of trophic interactions among multiple species, with explicit consideration of interactions among individual cells at local scale of rough surfaces. We discuss the details in chapter 6.

In chapter 7, we provide an overall summary of this study, and an outlook as well.

References

Alexandrou MA, *et al*. Competition and phylogeny determine community structure in Müllerian co-mimics. *Nature* **469**, 84-88 (2011).

Banavar JR, Maritan A. Towards a theory of biodiversity. *Nature* **460**, 334-335 (2009).

Barton JW, Ford RM. Mathematical model for characterization of bacterial migration through sand cores. *Biotechnol. Bioeng.* **53**, 487-496 (1997).

Boelens J, Vandewoestyne M, Verstraete W. Ecological importance of motility for the plant growth-promoting rhizopseudomonas strain-Anp15. *Soil Biol. Biochem.* **26,** 269-277 (1994).

Cardinale BJ. Biodiversity improves water quality through niche partitioning. *Nature* **472**, 86-89 (2011).

Chang WS, Halverson LJ. Reduced water availability influences the dynamics, development, and ultrastructural properties of *Pseudomonas putida* biofilms. *J. Bacteriol.* **185**, 6199-6204 (2003).

Chen J, Jin Y. Motility of Pseudomonas aeruginosa in saturated granular media as affected by chemoattractant. *J. Contam. Hydrol.* **126,** 113-120 (2011).

Curtis TP, Sloan WT, Scannell JW. Estimating prokaryotic diversity and its limits. *Proc. Natl. Acad. Sci. USA* **99,** 10494-10499 (2002).

Curtis TP, Sloan WT. Exploring microbial diversity - a vast below. *Science* **309,** 1331-1333 (2005).

Curtis TP, Sloan WT. Prokaryotic diversity and its limits: microbial community structure in nature and implications for microbial ecology. *Curr. Opin. Microbiol.* **7,** 221-226 (2004).

Dechesne A, Wang G, Güleza G, Or D, Smets BF. Hydration-controlled bacterial motility and dispersal on surfaces. *Proc. Natl. Acad. Sci. USA* **107**, 14369-14372 (2010).

Dejonghe W, *et al.* Synergistic degradation of linuron by a bacterial consortium and isolation of a single linuron-degrading variovorax strain. *Appl. Environ. Microbiol*. **69**, 1532-1541 (2003).

Dion P. Extreme views on prokaryote evolution, In: Dion P, Nautiyal CS (eds), *Microbiology of Extreme Soils*. (Springer, Berlin Heidelberg), pp. 45-70 (2008).

Fenchel T. Microbial behavior in a heterogeneous world. *Science* **296**, 1068-1071 (2002).

Fierer N, Jackson R. The diversity and biogeography of soil bacterial communities. *Proc. Natl. Acad. Sci. USA* **103,** 626-631 (2006).

Fierer N, Schimel JP. Effects of drying-rewetting frequency on soil carbon and nitrogen transformations. *Soil Biol. Biochem.* **34,** 777-787 (2002).

Golding I, Kozlovsky Y, Cohen I, Ben-Jacob E. Studies of bacterial branching growth using reaction-diffusion models for colonial development. *Physica A* **260**, 510-554 (1998).

Gonzalez A, *et al.* Our microbial selves: what ecology can teach us. *EMBO Rep.* **12**, 775-784 (2011).

Gordon H, Haygarth PM, Bardgett RD. Drying and rewetting effects on soil microbial community composition and nutrient leaching. *Soil Biol. Biochem.* **40,** 302-311 (2008).

Harpole WS, Tilman D. Grassland species loss resulting from reduced niche dimension. *Nature* **446**, 791-793 (2007).

Hibbing ME, Fuqua C, Parsek MR, Peterson SB. Bacterial competition: surviving and thriving in the microbial jungle. *Nat. Rev. Microbiol.* **8,** 15-25 (2010).

Kerr B, Riley MA, Feldman MW, Bohannan BJM. Local dispersal promotes biodiversity in a real-life game of rock-paper-scissors. *Nature* **418,** 171-174 (2002).

Knight TM, McCoy MW, Chase JM, McCoy KA, Holt RD. Trophic cascades across ecosystems. *Nature* **437**, 880-883 (2005).

Kreft JU, Booth G, Wimpenny JWT. BacSim, a simulator for individual-based modelling of bacterial colony growth. *Microbiol.-UK* **144,** 3275-3287 (1998).

Long T, Or D. Aquatic habitats and diffusion constraints affecting microbial coexistence in unsaturated porous media. *Water Resour. Res.* **41**, W08408 (2005).

Long T, Or D. Dynamics of microbial growth and coexistence on variably saturated rough surfaces. *FEMS Microbiol. Ecol.* **58**, 262-275 (2009).

Long T, Or D. Microbial growth on partially saturated rough surfaces: simulations in idealized roughness networks. *Water Resour. Res.* **43**, W02409 (2007).

McCann K, Hastings A, Huxel GR. Weak trophic interactions and the balance of nature. *Nature* **395**, 794-798 (1998).

Miller LD, *et al*. Establishment and metabolic analysis of a model microbial community for understanding trophic and electron accepting interactions of subsurface anaerobic environments. *BMC Microbiol*. **10**, 149 (2010).

Mills AL. Keeping in touch: Microbial life on soil particle surfaces. *Adv Agron* **78**, 1-43 (2003).

Mitchell JG, Kogure K. Bacterial motility: links to the environment and a driving force for microbial physics. *FEMS Microbiol. Ecol.* **55**, 3-16 (2006).

Morelli LG, Uriu K, Ares S, Oates AC. Computational approaches to developmental patterning. *Science* **336**, 187-191 (2012).

O'Donnell AG, Young IM, Rushton SP, Shirley MD, Crawford JD. Visualization, modelling and prediction in soil microbiology. *Nat. Rev. Microbiol.* **5**, 689-699 (2007).

Olson MS, Ford RM, Smith JA, Fernandez EJ. Quantification of bacterial chemotaxis in porous media using magnetic resonance imaging. *Environ. Sci. Technol.* **38**, 3864-3870 (2004).

Or D, Smets BF, Wraith JM, Dechesne A, Friedman SP. Physical constraints affecting bacterial habitats and activity in unsaturated porous media - a review. *Adv. Water Resour.* **30,** 1505-1527 (2007).

Oren A. In: Wang LK, Ivanov V, Tay JH, Hung YT, (eds), *Handbook of environmental engineering* (Springer, New York), Vol. 10 (2010).

Pérez-Pantoja D, González B, Pieper DH. In: McGenity T, Meer JR, Lorenzo V, Timmis KN, (eds), *Handbook of Hydrocarbon and Lipid Microbiology* (Springer, Heidelberg), pp. 800-829 (2010).

Ponciano JM, La HJ, Joyce P, Forney LJ. Evolution of diversity in spatially structured *Escherichia coli* populations. *Appl. Environ. Microbiol.* **75,** 6047-6054 (2009).

Prosser JI, Bohannan BJM, Curtis TP, *et al.* The role of ecological theory in microbial ecology. *Nature* **5,** 384-392 (2007).

Reichenbach T, Mobilia M, Frey E. Mobility promotes and jeopardizes biodiversity in rock-paper-scissors games. *Nature* **448,** 1046-1049 (2007).

Schloss PD, Handelsman J. Toward a census of bacteria in soil. *PLoS Comput. Biol.* **2,** 786-793 (2006).

Stotzky G. Soil as an environment for microbial life. In: van Elsas JD, Trevors JT, Wellington EMH (eds), *Modern Soil Microbiology* (Marcel, New York), pp. 1-20 (1997).

Torsvik V, Goksoyr J, Daae FL. High Diversity in DNA of Soil Bacteria. *Appl. Environ. Microbiol.* **56,** 782-787 (1990).

Torsvik V, Ovreas L. Microbial diversity and function in soil: from genes to ecosystems. *Curr. Opin. Microbiol.* **5,** 240-245 (2002).

Torsvik V, Øvreås L. Microbial diversity, life strategies, and adaptation to life in extreme soils. In: Dion P, Nautiyal CS (eds), *Microbiology of Extreme Soils* (Springer Berlin Heidelberg), pp. 15-43 (2008).

Torsvik V, Øvreås L. Microbial phylogeny and diversity in soil. In: van Elsas JD, Jansson JK, Trevors JT (eds), *Modern Soil Microbiology*, 2nd edn (Taylor, Boca Raton), pp. 23-54 (2007).

Torsvik V, Sørheim R, Goksør J. Total bacterial diversity in soil and sediment communities - a review. *J. Ind. Microbiol.* **17,** 170-178 (1996).

Turnbull GA, Morgan JAW, Whipps JM, Saunders JR. The role of bacterial motility in the survival and spread of *Pseudomonas fluorescens* in soil and in the attachment and colonisation of wheat roots. *FEMS Microbiol. Ecol.* **36,** 21-31 (2001).

Venail PA, *et al.* Diversity and productivity peak at intermediate dispersal rate in evolving metacommunities. *Nature* **452,** 210-214 (2008).

Wang G, Or D. Aqueous films limit bacterial cell motility and colony expansion on partially saturated rough surfaces. *Environ. Microbiol.* **12**, 1363-1373 (2010).

Wilson PDG, *et al*. Modelling microbial growth in structured foods: towards a unified approach. *Int. J. Food Microbiol.* **73,** 275-289 (2002).

Woyke T, *et al.* Symbiosis insights through metagenomic analysis of a microbial consortium. *Nature* **443**, 950-955 (2006).

Young IM, Crawford JW. Interactions and self-organization in the soil-microbe complex. *Science* **304,** 1634-1637 (2004).

Zhou J, *et al.* Spatial and resource factors influencing high microbial diversity in soil. *Appl. Environ. Microbiol.* **68,** 326-334 (2002).

Chapter 2

Hydration Controlled Bacterial Motility and Dispersal on Surfaces

Arnaud Dechesne, Gang Wang, Dani Or, Gamze Gülez and Barth F. Smets

Proc. Natl. Acad. Sci. USA **107:** 14369-14372 (2010)

Flagellar motility, a mode of active motion shared by many prokaryotic species, is recognized as a key mechanism enabling population dispersal and resource acquisition in microbial communities living in marine, freshwater, and other liquid-replete habitats. By contrast, its role in variably-hydrated habitats, where water dynamics results in fragmented aquatic habitats connected by micrometric films, is debated. Here we quantify the spatial dynamics of *Pseudomonas putida* KT2440 and its non-flagellated isogenic mutant as affected by the hydration status of a rough porous surface using an experimental system that mimics aquatic habitats found in unsaturated soils. The flagellar motility of the model soil bacterium decreased sharply within a small range of water potential (0 to -2.0 kPa) and nearly ceased in liquid films of effective thickness smaller than 1.5 μm. However, bacteria could rapidly resume motility in response to periodic increases in hydration. We propose a biophysical model that captures key effects of hydration and liquid film thickness on individual cell velocity and use a simple roughness network model to simulate colony expansion. Model predictions match experimental results reasonably well, highlighting the role of viscous and capillary pinning forces in hindering flagellar motility. Although flagellar motility appears to be restricted to a narrow range of very wet conditions, fitness gains conferred by fast surface colonization during transient favorable periods might offset the costs associated with flagella synthesis and explain the sustained presence of flagellated prokaryotes in partially saturated habitats such as soil surfaces.

2.1 Introduction

Dispersal is recognized as a key ecological process enabling populations' access to new sites and pools of resources (Tilman, 2004) thereby affecting structure and productivity of ecosystems (Kerr *et al.*, 2002; Venail *et al*., 2008). Active bacterial motion (motility) takes on many forms that require various appendages (Jarrell and McBride, 2008). If surface-associated modes of motility such as twitching, gliding or swarming appear restricted to some species (Harshey, 2003), the ability to swim by rotating one or more flagella is shared by a large diversity of prokaryotes. This swimming motility has attracted considerable attention, primarily aimed at resolving the biophysical functioning of flagella and, to a lesser degree, at exploring its adaptive value. In marine environments, a large fraction of bacterial populations are flagellated (Grossart *et al*., 2001) and swimming motility is often coupled with chemotaxis, conferring a clear benefit to these cells by allowing them to out-swim diffusion and exploit transient substrate gradients (Fenchel, 2002; Stocker *et al*., 2008).

In contrast to water-replete environments where flagellar motility is essentially unrestricted, there exist strong physical limitations to flagellar motility in partially saturated media where aquatic microhabitats are often fragmented and connected only by thin liquid films of bacterial size or smaller (Or *et al*., 2007). The limitations to bacterial motility in thin liquid films have long been posited but never directly quantified or described biophysically beyond the general notion that flagellar motility requires hydrated pathways. In addition, the fitness benefit associated with flagellar motility in partially saturated soils has been debated due to conflicting experimental data (Boelens *et al*., 1994; Turnbull *et al*., 2001).

Here, to avoid the complexity inherent to natural partially-saturated microbial habitats such as soil matrixes and benefit from direct observation of bacterial dispersal at both individual- and population-scales under conditions of controlled hydration, we employed the Porous Surface Model (PSM) (Dechesne *et al*., 2008a). In this experimental system, bacteria are grown on a porous ceramic surface in thin aqueous films, whose effective thickness is controlled by applying a prescribed suction similar to how matric potential controls hydration in soils. The system allowed a quantitative assessment of the dispersal rate and competition of *Pseudomonas putida* KT2240 and a non-flagellated Δ*fliM* isogenic mutant as influenced by water potential at the colony and the individual scales.

2.2 Materials and Methods

2.2.1 Bacterial strains

Pseudomonas putida KT2440, a flagellated bacterium initially isolated from the rhizosphere (Nakazawa, 2002), was used as model strain. A non-flagellated Δ*fliM* mutant was obtained by allelic exchange with a truncated version of *fliM* carrying the Gm-resistance gene *aacC1* framed by *lox* sequences. The *aacC1* gene was then excised to yield an antibiotic-resistance-free mutant (Quenee *et al*., 2005). Both strains were tagged by inserting a constitutively-expressed fluorescent protein encoding gene at a neutral position of their genome (Lambertsen *et al*., 2004). To increase the fluorescence signal for single cell observations, pJBA128, a multi-copy plasmid carrying a *gfp* gene (Lee *et al*., 2005), was additionally introduced into the *gfp*-expressing wild-type strain. The bacteria were routinely cultivated on FAB medium (Hansen *et al*., 2007) supplemented with 5 mM benzoate.

2.2.2 Experiments on the Porous Surface Model

The Porous Surface Model (PSM) allows growing and observing fluorescent cells at the surface of a porous ceramic plate (diameter, 4.2 cm; maximum pore size, 1.7 µm) under prescribed suction, which controls surface liquid film thickness (Dechesne *et al*., 2008a). Liquid FAB medium with 5 mM of benzoate as the sole carbon source was used to wet the plate and sustain microbial growth. The inoculation of the surface of the PSM was performed as in (Dechesne *et al*., 2008a).

Observations of the PSM surface were realized at different scales using a Leica MZ16FA stereomicroscope. Time lapse videos (27 s, 100 images) were acquired at high magnification (field of view: 0.15 mm^2) to document swimming motility at the cell scale. Individual trajectories were detected and analyzed with Image Pro Plus (MediaCybernetics, Silver Spring, MD). Population-scale dispersal was quantified as previously described (Dechesne *et al*., 2008a).

To measure the relative fitness of the strains we performed competition experiments where the abundance of the strains was measured at coinoculation time and at the end of incubation time. The fitness (W) of the mutant relative to that of the wild-type was calculated as (Kerr *et al*., 2002):

$$W(m,wt) = \ln\left(m_F / m_0\right) \Big/ \ln\left(wt_F / wt_0\right)$$

where m_0 and m_F are initial and final abundances of the mutant and wt_0 and wt_F that of the wild-type. Relative fitnesses were estimated in stirred liquid medium (17 ml FAB benzoate 5 mM) and at the surface of the PSM (same medium). In the later case, the areas colonized by each strain were used as proxy for their abundance to compute relative fitness values.

2.2.3 Modeling bacterial motility and growth on rough surfaces

We modeled a population of motile cells within a surface roughness network of size 17.2 mm × 17.2 mm (100 by 87 sites). The initial substrate concentration in aqueous phase was set to 0.2 mg l^{-1}, and was maintained constant at the top and right boundaries of the domain. The bottom and left boundaries of the simulation domain were no-flux boundaries. Simulations were initiated by inoculating 200 bacterial cells in four sites at the bottom left corner of the domain. Triplicate simulations were conducted for each value of matric potential: -0.0001, -0.5, -1.0, -1.5, and -2.0 kPa for simulating single cells motion, and at -0.5, -1.0, -1.5, -2.0, and -3.6 kPa for colony expansion analyses. Details of the model and its parameters are presented in SI Text.

2.3 Results and Discussion

2.3.1 Bacterial motility on rough surface – experimental observations

At the colony scale, we observed constant front expansion rates, in accordance with the model proposed by Skellam (Skellam, 1951) for a population dispersing by random walk and exponential growth. The average rate of colony expansion for both the wild-type and the non-flagellated mutant decreased with decreasing matric potential (Fig. 1). The most significant differences in expansion rates between the strains were apparent at -0.5 and -1.2 kPa, where the wild-type, capable of flagellar motility, dispersed more than 15 times faster than the mutant, which dispersed by cell shoving and Brownian motion only. This clearly demonstrates the potential of flagellar motility for fast population dispersal on wet surfaces. A role of swarming motility, which in *P. putida* KT2440 relies on short pili rather than on flagella, is unlikely in our experiments because it is expressed only under specific conditions (Matilla *et al*., 2007) and manifests itself by *en masse* cell movements, which we did not observe.

The colony expansion rate of the wild-type decreased exponentially from an average of 521 μm h^{-1} for the wettest conditions (-0.5 kPa) to 14 μm h^{-1} at -2.0 kPa (Fig. 1). Following this sharp decrease, the colonization rate leveled, suggesting that, on the PSM, -2.0 kPa marks a threshold below which the contribution of flagellar motility to population dispersal becomes insignificant. Under drier conditions, we expect both types of bacteria to disperse by cell shoving only and thus their colonies to expand at similar rates. The slightly faster expansion of the wild-type colonies observed at -3.6 kPa (Fig. 1) is attributed to the higher intrinsic growth rate of this organism. Indeed, even though the only difference between mutant and wild-type resides in the *fliM* knock-out, the former presents a significantly reduced growth rate. This was evidenced in competition experiments in stirred liquid medium where the fitness of the mutant

relative to that of the wild-type was significantly smaller than 1 (0.82 ; sd = 0.04, *n*= 3, *P* = 0.016, two-tailed t-test).

The mild matric potential we prescribed does not *per se* restrict bacterial motion (Dechesne *et al*., 2008a) but it acts through its control of the effective liquid film thickness on the ceramic plate surface. The relationship between matric potential and liquid film thickness depends solely on surface wettability and roughness (Or and Tuller, 2000). At -2.0 kPa, which we identified as the limit beyond which the contribution of flagellar motility to colony expansion is negligible on the ceramic plates, the predicted effective liquid film is thinner than 1.5 µm (Dechesne *et al*., 2008a).

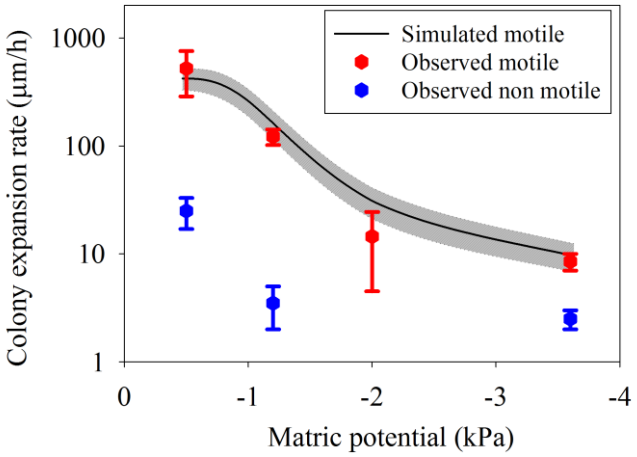

Fig. 1. Matric potential affects colony expansion rates of *P. putida* KT2440 wild-type (flagellated) and its Δ*fliM* isogenic mutant (non-flagellated) measured as radial expansion of colonies initiated from single cells. More negative matric potentials correspond to thinner surface liquid films. Error bars mark one standard deviation (*n* varies from 6 to 14). Simulated colony expansion rates are depicted by line and shaded area (representing one standard deviation).

2.3.2 Simulation models of bacterial motility on rough surfaces

To explain the strong reduction of colony expansion rate observed over a relatively small range of matric potentials and to provide a predictive tool for bacterial dispersal rates on partially saturated rough surfaces, a simple mechanistic model is proposed linking bacterial velocity to viscous and capillary forces acting on motile cells. The key biophysical elements of the proposed model are summarized in Figure 2. The model considers the effects of liquid film thinning on the propulsive force: $F_M = 6\pi R\eta V_0$ (Darnton *et al*., 2007) for flagellar motion at maximum velocity in bulk liquid, V_0.

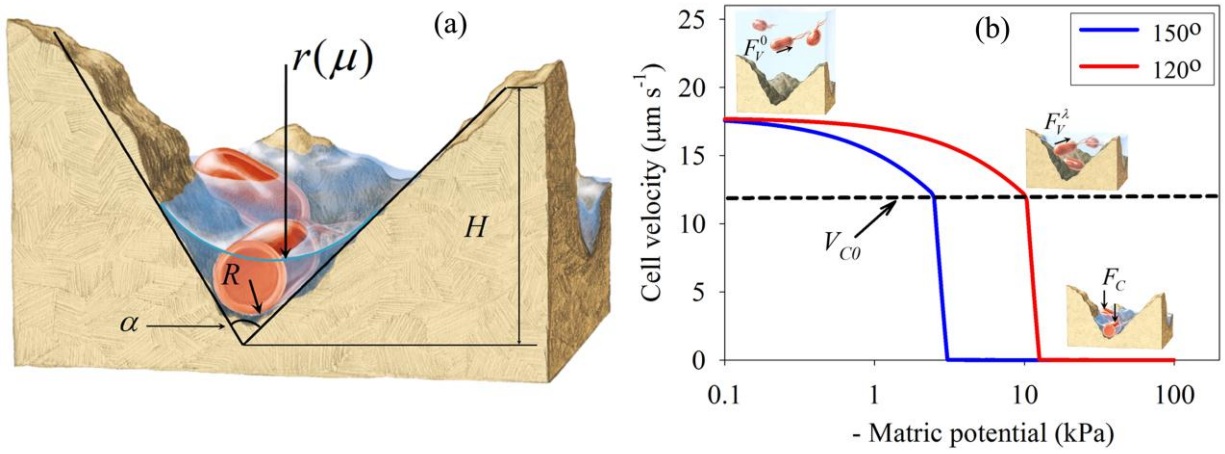

Fig. 2. (a) A roughness element can be abstracted as a channel of triangular section, with depth H and spanning angle α. R is the cell radius and $r(\mu)$ is the radius of curvature of the liquid-air meniscus determined by the ambient matric potential, μ. Depending on the channel geometry, cells can either be fully (left), or partly (right) immersed for a given matric potential. The forces exerted on swimming cells are different in these two situations, as depicted in (b). The cell velocity is modeled for cells swimming in two channels of same depth (H = 100 μm) but contrasting spanning angles (α = 120 or 150°). The maximum average velocity V_0 was fixed to 18 μm s^{-1}, a value typically observed in saturated systems (Berg and Brown, 1972). F_0, F_λ, and F_C are the viscous drag force opposing motion in bulk liquid, the viscous force associated with cell-wall interactions, and the capillary pinning force, respectively. The horizontal dashed line marks the onset of capillarity.

On partially saturated surfaces, hydrodynamic interactions between bacterial cells and solid surface hinder motion, preventing cells from attaining their maximum velocity. Considering, for simplicity, an average 45° angle between the solid surface and cell trajectory we obtain the following hydrodynamic interactions coefficient: $\lambda = \sqrt{\lambda_P^2 + \lambda_N^2}$, given in terms of cell-surface interactions for motion parallel λ_P (Faxen, 1923) and normal λ_N (Maude, 1963) to surface, respectively. These interactions affect bacterial cell velocity according to: $V_\lambda = \frac{V_0}{\lambda}$, and are associated with a corresponding resistive force: $F_\lambda = (1 - \frac{1}{\lambda})F_M$. The most significant hindering force on partially hydrated surfaces sets in when the liquid film becomes thinner than the cell diameter, resulting in interactions with liquid-air interfaces, including formation of a contact line on the cell surface, onset of normal capillary pressure, and introduction of a capillary pinning force (F_C) (Kralchevsky and Nagayama, 2001). We combine hydration-dependent resistive forces into a simple model where attainable bacterial cell velocity is proportional to the residual force available for flagellar propulsion:

$$V = V_0 \frac{F_M - F_\lambda - F_C}{F_M}, \text{ with } V = 0 \text{ for } F_M - F_\lambda - F_C < 0 .$$

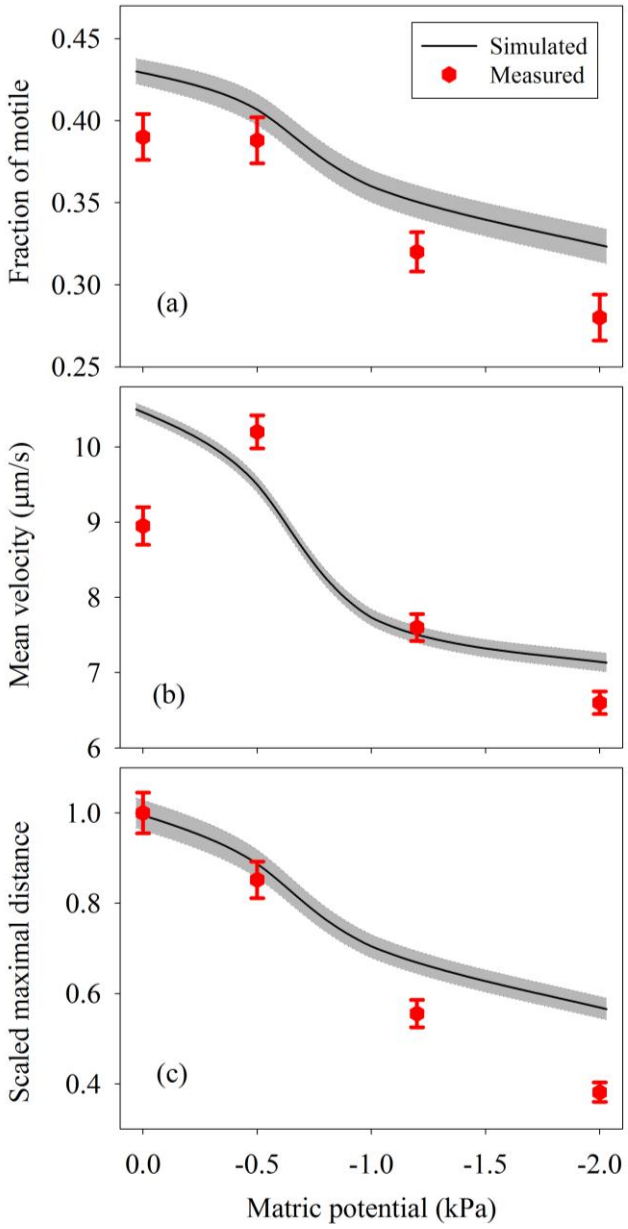

Fig. 3. Comparison of experimentally observed and simulated descriptors of swimming motility on partially saturated rough surfaces. Experimental values were obtained by analyzing the trajectories of individual cells at the surface of the PSM set at various matric potentials. Simulated values are obtained by simulating the motion of 200 cells within an idealized roughness network. All the data are expressed as mean ± s.e.m., with $n > 248$ for experimental trajectories and $n = 600$ for simulations. (a) Fraction of time cells display significant motility (significant motility is defined as velocities larger than 3 µm s^{-1}, the experimental detection limit); (b) Mean cell velocity during phases of significant motility; (c) Scaled maximal cellular travel distance. The maximal travel distance is the distance between the starting point of a cell and the most distant point of its trajectory. The trajectories were recorded over 28 s for experimental measurements and 33 s for simulations. The distance data were scaled by the mean maximal travel distance observed in the wettest conditions (28 and 59 µm, for experiments and simulations, respectively).

This model component provides estimates of the potential cell velocity for local hydration conditions (which may vary spatially over a natural surface) that may then be directed by local chemotactic gradient and a random component (tumble-like) to define the actual direction and extent of displacement during a single run (or a time step). These modifications are implemented by combining the random component (tumble-like change of run direction) and local chemotactic gradients by weighing these by a factor of $(1-\xi)$ and ξ, respectively, depending on normalized local chemoattractant gradient, ξ (defined as the ratio of local to maximal chemotactic gradient, calculated as the concentration difference across the local bond divided by the boundary concentration). The cellular motion is evaluated every 1.1 s (an assumed duration of a run and tumble cycle [Berg, 2004]) and the actual run velocity is obtained as:

$\vec{V} = (\vec{R}(1-\xi) + \vec{N}\xi)V$, with $\vec{R}$ describing a random direction of cell motion, and $\vec{N}$ the displacement component along the chemoattractant gradient.

To validate the proposed model, we experimentally quantified individual cell trajectories at the surface of the PSM for different matric potential values (see Movies S1 and S2 for typical examples). The descriptors of individual trajectories varied considerably due to the specific microtopography experienced by each cell, however the average velocity and dispersal distance clearly decreased with decreasing matric potential (Fig. 3). Single cell motility was simulated by applying the model presented above to cells swimming in an idealized two-dimensional rough surface consisting of a network of angular channels of various geometries that accommodate variable liquid configuration (Long and Or, 2007). The simulated descriptors of cell motility are in good agreement with the experimental results even without specific parameter fitting or other adjustments (Fig. 3). These results highlight the dominant role of capillary pinning forces in constraining bacterial motility.

Subsequently, the cell motility model was implemented to simulate population dispersal and reproduce experimental colony expansion rates. Cell growth and motility were modeled at the individual cell scale (Hellweger and Bucci, 2009) and chemotaxis included by biasing cell movement towards neighboring channels with high nutrient content. An example of colony expansion is shown in Figure S1. The model predictions were consistent with the experimental dispersal rates (Fig. 1), demonstrating that population dispersal correctly emerges from the individual scale behavior, in agreement with previous theoretical derivations (Skellam, 1951; Rivero *et al*., 1989; Phillips *et al*., 1994). See supplementary information for further discussion on the comparison between model and experiments.

As evidenced by our observations and model predictions, thin liquid films such as those found under most circumstances in soils strongly limit the dispersal rate of bacterial populations. Does flagellar motility, then, confer any selective advantage in this physically constrained environment? Competition experiments between the wild-type and the non-flagellated mutant, co-inoculated as randomly distributed single cells at the surface of the PSM, demonstrated hydration conditional fitness effects (Fig. 4). At -3.6 kPa, the two strains developed colonies of similar size and the relative fitness of the mutant was close to 1 (0.91, s.d. = 0.04, n = 9 and 0.96, s.d. = 0.03, n = 12, for low and high inoculation density, respectively). In these relatively dry conditions, the potentially motile wild-type cannot disperse by flagellar motility. Therefore, the sites colonized by each strain remained spatially separated, preventing direct competition, partly alleviating the intrinsic inferiority of the mutant (Dechesne *et al*., 2008b). The situation was different under wet condition (-0.5 kPa), permissive for efficient flagellar motility. In this

condition, the mutant had a very low relative fitness (0.54, s.d. = 0.03, n = 9 and 0.74, s.d. = 0.06, n = 5, for low and high inoculation density, respectively). These values are significantly smaller than those observed in liquid culture (one-tailed t-test, $P = 6.7\ 10^{-8}$ and 0.047, for low and high density, respectively) because the wild-type quickly colonized the surface and thus intercepted substrate fluxes more efficiently than the non-flagellated mutant.

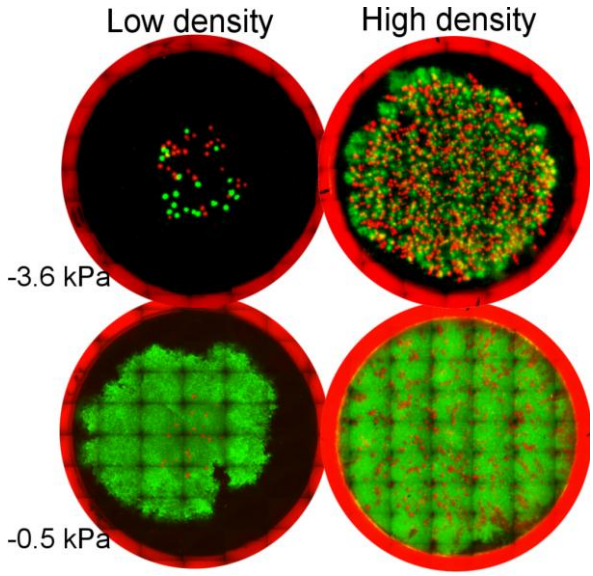

Fig. 4. The competition between *P. putida* KT2440 wild-type (flagellated, green) and its Δ*fliM* isogenic mutant (non-flagellated, red) at the surface of a porous ceramic plate is affected by matric potential and inoculation density. On average, 20 and 1500 cells were inoculated at a 1:1 strain ratio for low and high inoculation densities, respectively. The images were acquired after 2 or 5 days of growth at 22°C for -0.5 and -3.6 kPa, respectively. The plate, 4.2 cm in diameter, is limited by a silicone o-ring, which appears bright red in the pictures. Each mosaic image is composed of about 45 fields of view. The images are representative of observations made on 5 to 12 independent replicate plates. The contrast of the images has been digitally enhanced.

Competition experiments between the wild-type and the non-flagellated mutant, co-inoculated as randomly distributed single cells at the surface of the PSM, demonstrated hydration conditional fitness effects (Fig. 4). At -3.6 kPa, the two strains developed colonies of similar size and the relative fitness of the mutant was close to 1 (0.91, s.d. = 0.04, n = 9 and 0.96, s.d. = 0.03, n = 12, for low and high inoculation density, respectively). In these relatively dry conditions, the potentially motile wild-type cannot disperse by flagellar motility. Therefore, the sites colonized by each strain remained spatially separated, preventing direct competition, partly alleviating the intrinsic inferiority of the mutant (Dechesne *et al.*, 2008b). The situation was different under wet condition (-0.5 kPa), permissive for efficient flagellar motility. In this condition, the mutant had a very low relative fitness (0.54, s.d. = 0.03, n = 9 and 0.74, s.d. = 0.06, n = 5, for low and high inoculation density, respectively). These values are significantly smaller than those observed in liquid culture (one-tailed t-test, $P = 6.7\ 10^{-8}$ and 0.047, for low and high density, respectively) because the wild-type quickly colonized the surface and thus intercepted substrate fluxes more efficiently than the non-flagellated mutant.

2.3.3 Conclusions and implications

Natural partially saturated habitats such as soils and the surface of plant leaves are subject to dynamic variations in hydration conditions, the extent and frequency of which depend on

climate and/or irrigation practices. To address the question of whether the occurrence of short periods of favorable wetness conditions might modify flagellar-based dispersal behavior, we experimentally evaluated the expression of flagellar motility under dry-wet cycles. Inoculated PSMs, maintained at dry conditions (-3.6 kPa), were subjected to two short daily increases in hydration status (2 x 5 min, -0.5 kPa). In spite of the very short duration of the wet periods, the motile strain was able to disperse, yielding larger colonies than on the control surfaces, continuously maintained at -3.6 kPa (Fig. S2). Accelerated surface colonization associated with dry-wet cycles was not observed for the non-flagellated mutant strain. We therefore conclude that *P. putida* KT2440 can take advantage of short and infrequent wet events to disperse by flagellar motility.

Our data demonstrate that under conditions of partial hydration, common in many terrestrial microbial habitats, the thickness and geometry of liquid films control active bacterial motion and dispersal. Viscous and capillary pinning forces reduce the swimming velocity of individual cells, resulting in low surface colonization rates at the population scale. More than bacterial intrinsic growth kinetic parameters, surface micro-topography, hydration status, and bacterial flagellation are essential parameters in surface colonization. Since the fitness gain associated with fast dispersal can be large when nutrient-rich microsites are available (Fig. 4) and since bacteria are able to take advantage of very short wet events to disperse by flagellar motility (Fig. S2), even rare wet events could offset the cost associated with flagellar synthesis and explain the sustained presence of flagellated cells in soil habitats. This demonstrates the very tight couplings between microbial and physical processes in soil, which mediate the emergent properties of soil systems (Young and Crawford, 2004).

Acknowledgments

This work was supported by the Villum Kann Rasmussen Foundation Center of Excellence, Center for Environmental and Agricultural Microbiology (CREAM) and by the Swiss National Science Foundation, project 200021-113442. BFS was supported by Marie Curie Excellence Grant MEXT-CT-2005-024004. We are grateful to Alexis Bazire (UBS, France) for the construction of the Δ*fliM* mutant and to Søren Molin (DTU, Denmark) for the kind gift of pJBA128.

References

Berg HC & Brown DA (1972) Chemotaxis in Escherichia coli analyzed by 3-dimensional tracking. *Nature* 239:500-504.

Berg HC (2004) *E. coli in motion* (Springer, New York).

Boelens J, Vandewoestyne M, & Verstraete W (1994) Ecological importance of motility for the plant growth-promoting rhizopseudomonas strain-Anp15. *Soil Biol. Biochem.* 26:269-277.

Darnton NC, Turner L, Rojevsky S, & Berg HC (2007) On torque and tumbling in swimming *Escherichia coli*. *J. Bacteriol*. 189:1756-1764.

Dechesne A, Or D, Gülez G, & Smets BF (2008a) The porous surface model: a novel experimental system for online quantitative observation of microbial processes under unsaturated conditions. *Appl. Environ. Microbiol.* 74:5195-5200.

Dechesne A, Or D, & Smets BF (2008b) Limited substrate diffusive fluxes facilitate coexistence of two competing bacterial strains. *FEMS Microbiol. Ecol.* 64:1-8.

Faxen H (1923) Die Bewegung einer starren Kugel langs der Achse eines mit zahrer Flüssigkeit, gefüllten Rohres. *Arkiv Mat. Astron. Fys.* 17:1-28.

Fenchel T (2002) Microbial behavior in a heterogeneous world. *Science* 296:1068-1071.

Grossart HP, Riemann L, & Azam F (2001) Bacterial motility in the sea and its ecological implications. *Aquat. Microb. Ecol.* 25:247-258.

Hansen SK, *et al.* (2007) Characterization of a *Pseudomonas putida* rough variant evolved in a mixed-species biofilm with *Acinetobacter* sp strain C6. *J. Bacteriol.* 189:4932-4943.

Harshey RM (2003) Bacterial motility on a surface: Many ways to a common goal. *Annu Rev Microbiol* 57:249-273.

Hellweger FL & Bucci V (2009) A bunch of tiny individuals-Individual-based modeling for microbes. *Ecol. Model.* 220:8-22.

Jarrell KF & McBride MJ (2008) The surprisingly diverse ways that prokaryotes move. *Nat. Rev. Microbiol.* 6:466-476.

Kerr B, Riley MA, Feldman MW, & Bohannan BJM (2002) Local dispersal promotes biodiversity in a real-life game of rock-paper-scissors. *Nature* 418:171-174.

Kralchevsky PA & Nagayama K (2001) *Particles at Fluid Interfaces and Membranes* (Elsevier, Amsterdam).

Lambertsen L, Sternberg C, & Molin S (2004) Mini-Tn7 transposons for site-specific tagging of bacteria with fluorescent proteins. *Environ. Microbiol.* 6:726-732.

Lee B, *et al.* (2005) Heterogeneity of biofilms formed by nonmucoid *Pseudomonas aeruginosa* isolates from patients with cystic fibrosis. *J. Clinic. Microbiol.* 43:5247-5255.

Long T & Or D (2007) Microbial growth on partially saturated rough surfaces: Simulations in idealized roughness networks. *Water Resour. Res.* 43:Art. No. W02409.

Matilla MA, *et al.* (2007) Temperature and pyoverdine-mediated iron acquisition control surface motility of *Pseudomonas putida*. *Environ. Microbiol.* 9:1842-1850.

Maude AD (1963) Movement of a sphere in front of a plane at low Reynolds number. *Brit. J. Appl. Phys.* 14:894-898.

Nakazawa T (2002) Travels of a *Pseudomonas*, from Japan around the world. *Environ. Microbiol.* 4:782-786.

Or D & Tuller M (2000) Flow in unsaturated fractured porous media: Hydraulic conductivity of rough surfaces. *Water Resour. Res.* 36:1165-1177.

Or D, Smets BF, Wraith JM, Dechesne A, & Friedman SP (2007) Physical constraints affecting microbial habitats and activity in unsaturated porous media – A review. *Adv. Water Resour.* 30:1505-1527.

Phillips BR, Quinn JA, & Goldfine H (1994) Random motility of swimming bacteria - Single cells compared to cell-populations. *AIChe J.* 40:334-348.

Quenee L, Lamotte D, & Polack B (2005) Combined *sacB*-based negative selection and *cre-lox* antibiotic marker recycling for efficient gene deletion in *Pseudomonas aeruginosa*. *Biotechniques* 38:63-67.

Rivero MA, Tranquillo RT, Buettner HM, & Lauffenburger DA (1989) Transport models for chemotactic cell-populations based on individual cell behavior. *Chem. Eng. Sci.* 44:2881-2897.

Skellam JG (1951) Random dispersal in theoretical populations. *Biometrika* 38:196-218.

Stocker R, Seymour JR, Samadani A, Hunt DE, & Polz MF (2008) Rapid chemotactic response enables marine bacteria to exploit ephemeral microscale nutrient patches. *Proc. Natl. Acad. Sci. USA* 105:4209-4214.

Tilman D (2004) Niche tradeoffs, neutrality, and community structure: A stochastic theory of resource competition, invasion, and community assembly. *Proc. Natl. Acad. Sci. USA* 101:10854-10861.

Turnbull GA, Morgan JAW, Whipps JM, & Saunders JR (2001) The role of bacterial motility in the survival and spread of *Pseudomonas fluorescens* in soil and in the attachment and colonisation of wheat roots. *FEMS Microbiol. Ecol.* 36:21-31.

Venail PA, *et al.* (2008) Diversity and productivity peak at intermediate dispersal rate in evolving metacommunities. *Nature* 452:210-U257.

Young IM & Crawford JW (2004) Interactions and self-organization in the soil-microbe complex. *Science* 304:1634-1637.

Appendix: Individual-based simulation of motility and dispersal

a) Domain geometry

Bacterial cells were modeled individually within a surface roughness network of size 17.2 mm × 17.2 mm (100 by 87 sites interconnected by channel-like bonds) as described in (Long and Or, 2007). The parameters used to generate networks are listed in SI Table 1.

SI Table1. Parameters of surface roughness network.

Parameters	Mean value	Range	Variance
l (mm, Bond length)	0.2	-	-
H_S (mm, Site height)	0.3*	0.1 to 0.5	0.0033
H_B (mm, Bond height)	0.007**	0 to 0.030	4.9×10^{-5}
α_S (rad, Site spanning angle)	$\pi/2$*	$\pi/3$ to $2\pi/3$	0.018
α_B (rad, Bond spanning angle)	$7\pi/9$**	0 to π	0.56

* truncated normal distribution

** log-normal distribution, the pore size in surface soil being log-normally distributed (Giménez, 2002; Virto *et al*., 2005)

b) Metabolism and growth

Bacterial metabolism and growth were modeled as in (Long and Or, 2007) using the parameters listed in SI Table 2.

SI Table2. Parameters describing bacteria metabolism, adapted from (Kreft *et al*., 1998).

Parameters	**Units**	**Values**
μ_{max}: specific maximum growth rate	hr^{-1}	1.23
K_S: half-saturation constant	fg fl^{-1}	1.17×10^{-3}
Y_{max}: apparent yield at μ_{max}	fg dry mass/fg substrate	0.44
m: apparent maintenance rate at $\mu=0$	fg substrate hr^{-1}/fg dry mass	0.036
B_m: median cell volume at $\mu=0$	fl	0.4
B_d: cell volume at division	fl	$2B_m/1.433$
B_{min}: minimal cell volume of a living bacterium	fl	$B_d/5$
ρ: cell density (dry mass)	fg fl^{-1}	290

c) Motility

All cells are capable of swimming motility and their motion was evaluated every 1.1 s, a value

corresponding to the duration of a run and tumble cycle observed experimentally for *Escherichia coli* (Berg, 2004). However, for simplification, the tumble duration was not explicitly included in our model because it typically amounts only to 1/10 – 1/100 of a run time (Berg, 2004). Reported values for maximum flagellated cell velocity in bulk liquid are in the range of 10-40 μm s^{-1} (Berg and Brown; 1972; Berg, 2004). We have used an average value of 18 μm s^{-1}, a typical value for the experimental results of Berg and Brown (Berg and Brown, 1972). Since cell motion is not entirely random but may exhibit chemotactic behavior, we calculate the actual cell velocity ($\vec{V}$) that depends on local liquid film thickness and local nutrient (chemoattractant) gradient (calculated across a site) by weighing chemotactic and random components of motility using weight factors of ξ and 1- ξ, respectively, where ξ is the dimensionless normalized chemoattractant gradient (defined as ratio of local to maximal chemoattractant gradients). We thus obtain: $\vec{V} = (\vec{R}(1-\xi) + \vec{N}\xi)V$, with $\vec{R}$ (drawn from a uniform distribution between 1 and -1) and $\vec{N}$ (unit vector along chemotactic gradient) describing directions of cell random motion and motion along chemoattractant gradient, respectively, and V is the local, hydration-constrained potential cell velocity as described in the main text.

The sites in the network are considered point-like locations (no length) and are used for nutrient gradient calculations, as well as entry points to connecting bonds, therefore allowing for change of direction. Bacterial motion is consequently limited to bonds only. The resulting random $\vec{R}$ and chemotactic $\vec{N}$ directions of motion are evaluated along the bond axis resulting in net velocity magnitude and direction $\vec{V}$ which then defines net displacement of a cell during a single run. As in (Long and Or, 2007), when a cell displacement exceeds the bond length, the cell enters the corresponding site and waits until its direction and velocity are reevaluated at the next time step. A cell in a site preferentially enters the neighboring bond k with maximal water film thickness and maximum substrate concentration, as described in Eqs.1-3:

$$p_{W,i} = W_i / \sum_{i=1}^{6} W_i \,, \tag{1}$$

$$p_{C,i} = C_i / \sum_{i=1}^{6} C_i \,, \tag{2}$$

$$k = k\{p_{C,W,k} = \underset{i=1:6}{Max}(p_{C,i} \times p_{W,i})\} \,, \tag{3}$$

where W_i and C_i are the water content and the nutrient concentration in the i^{th} neighboring bond, respectively; $p_{W,i}$ and $p_{C,i}$, the distribution of water content and nutrient concentration in the i^{th} bond relative to that of all the bonds connected to the site.

d) Simulations

Triplicate simulations were conducted for each matric potential (-0.0001, -0.5, -1, -1.5, and -2 kPa for single cell motion analysis and -0.5, -1, -1.5, -2, and -3.6 kPa for colony expansion analysis). For each simulation, we generated a new network.

The simulations were initiated by inoculating a total of 200 bacterial cells in four sites at the bottom left corner of the domain.

The initial substrate concentration in aqueous phase was set to 0.2 mg l^{-1}, and was maintained constant at the top and right boundaries of the domain. The bottom and left boundaries of the simulation domain were no-flux boundaries.

e) Descriptors

The characteristics of cell motion were quantified over a 33 s time span after 2 h of simulation. Parameters such as cell velocity and displacement and other physiological properties, were recorded for 600 cells at each time step. The fraction of time a cell displays significant motility (larger than 3 μm s^{-1}) was recorded. The mean cell velocity was calculated taking only the phases of significant motility into account to reflect the way the experimental values have been obtained.

Discussion: comparison of experiments and simulation

The used model is intended for capturing the general phenomenon of bacterial motion and colony expansion on rough unsaturated surfaces (e.g. natural soil/rock surfaces) and not for recreating the specificity of the experimental platform that was used here to quantify hydration control of bacterial motion. Specifically, the fact that bacterial growth is supported by vertical substrate fluxes (i.e., through the pores of the ceramic plate) is not included in the model, which considers surficial diffusive nutrient fluxes. However, a limited set of simulations incorporating vertical nutrient diffusion confirmed that the overarching controlling factor of bacterial spatial dynamics on the PSM is liquid film thickness; the addition of these diffusive fluxes did not markedly modify the simulation outcomes.

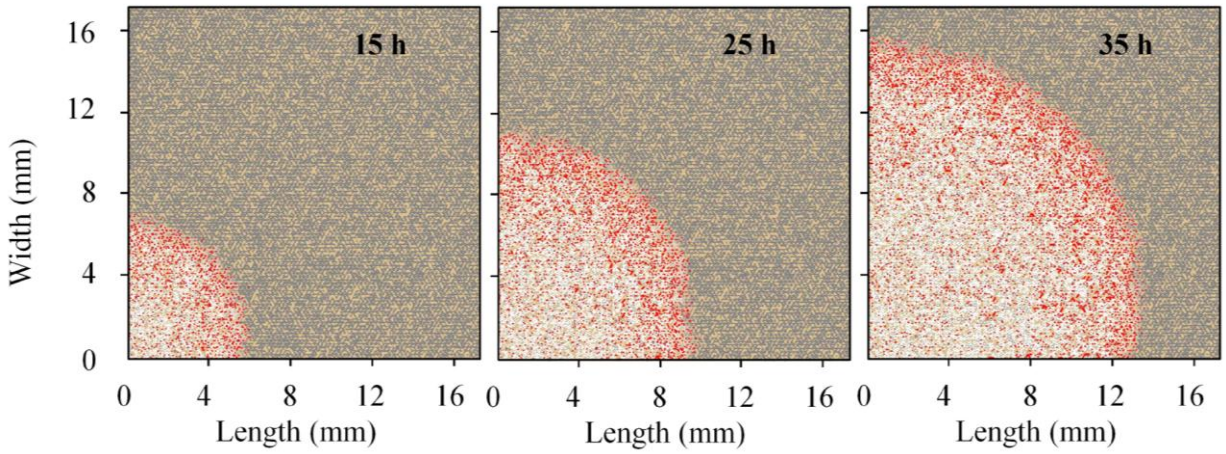

Fig. S1. Simulated colony expansion on an idealized rough surface under a matric potential of -0.5 kPa. Under these wet conditions, population dispersal, which results from a combination of growth and motility, is rapid (the front progresses at about 0.4 mm h^{-1}). Bacteria (in red) were inoculated at the lower-left corner of the domain. The panels present typical simulations after 15, 25, and 35 h of expansion.

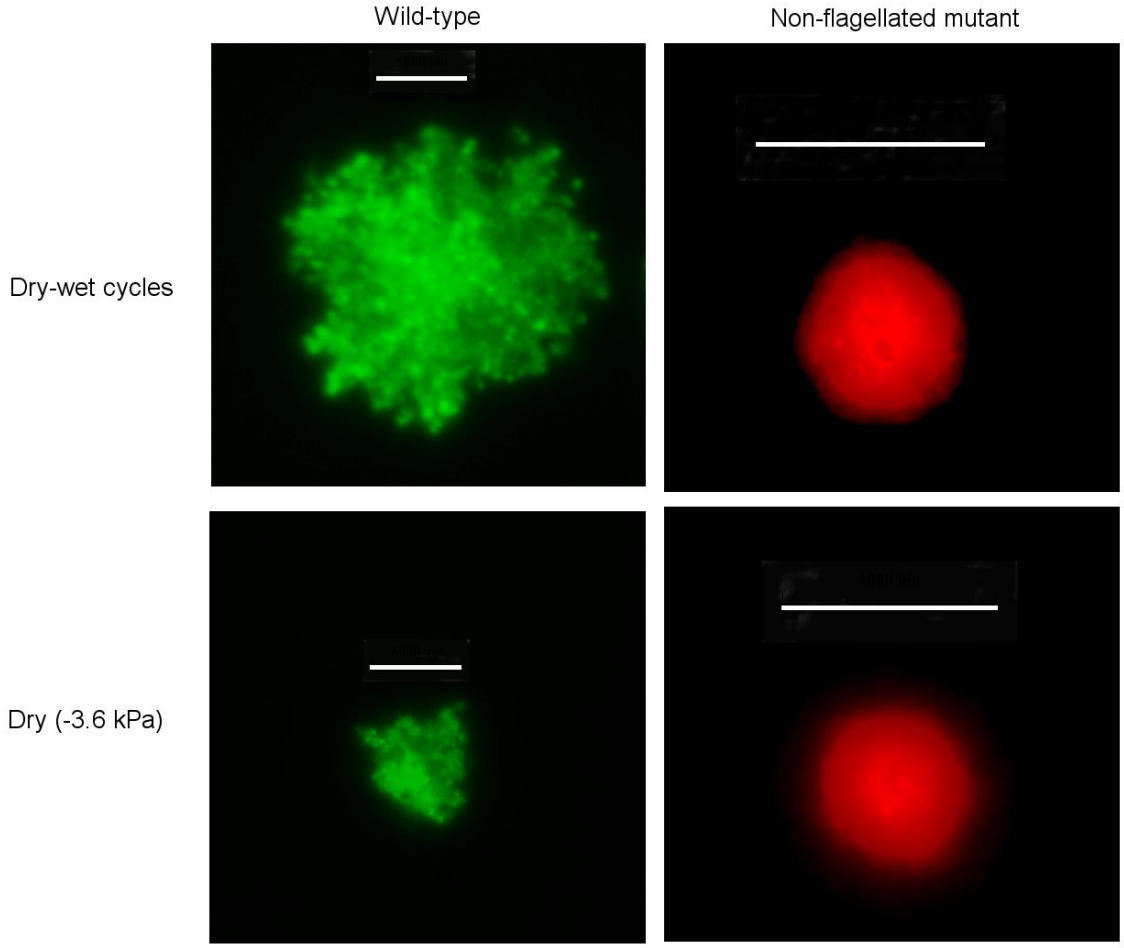

Fig. S2. Five minutes of wet conditions (-0.5 kPa) twice a day (top) allow the flagellated strain, tagged with the GFP (left), to disperse significantly more than when maintained continuously under dry conditions (-3.6 kPa, bottom). This dispersal is linked to flagellar motility since it is not observed with the non-flagellated mutant strain, tagged with the DsRed (right). The images were recorded after three days of incubation and their contrast has been digitally enhanced. The white bars indicate 1 mm.

References

Berg HC & Brown DA (1972) Chemotaxis in *Escherichia coli* analyzed by 3-dimensional tracking. *Nature* 239:500-504.

Berg HC (2004) *E. coli in motion* (Springer, New York).

Giménez D (2002) Macroporosity. *Encyclopedia of Soil Science*, ed Lal R (Marcel Dekker, New York, USA).

Harwood CS, Fosnaugh K, & Dispensa M (1989) Flagellation of *Pseudomonas putida* and analysis of its motile behavior. J. Bacteriol. 171:4063-4066.

Kreft JU, Booth G, & Wimpenny JWT (1998) BacSim, a simulator for individual-based modelling of bacterial colony growth. *Microbiol-Uk* 144:3275-3287.

Long T & Or D (2007) Microbial growth on partially saturated rough surfaces: Simulations in idealized roughness networks. *Water Resour. Res.* 43:Art. No. W02409.

Virto I, Imaz MJ, Bescansa P, & Enrique A (2005) Pore size distribution in relation to soil physical properties in two irrigated semiarid Mediterranean soils as affected by management. *Geophys. Res. Abstr.* 7:03223.

Chapter 3

Aqueous Films Limit Bacterial Cell Motility and Colony Expansion on Partially Saturated Rough Surfaces

Gang Wang and Dani Or

Environ. Microbiol. **12:** 1363-1373 (2010)

Bacterial motility is a key mechanism for survival in a patchy environment and is important for ecosystem biodiversity maintenance. Quantitative description of bacterial motility in soils is hindered by inherent heterogeneity, pore-space complexity and dynamics of microhydrological conditions. Unsaturated conditions result in fragmented aquatic habitats often too small to support full bacterial immersion thereby forcing strong interactions with mineral and air interfaces that significantly restrict motility. A new hybrid model was developed to study hydration effects on bacterial motility. Simulation results using literature parameter values illustrate sensitivity of colony expansion rates to hydration conditions and are in general agreement with measured values. Under matric potentials greater than -0.5 kPa (wet), bacterial colonies grew fast at colony expansion rates exceeding 421±94 μm/hr; rates dropped significantly to 31±10 μm/hr at -2.0 kPa; as expected, no significant colony expansion was observed at -5.0 kPa because of the dominance of capillary pinning forces in the sub-micrometric water film. Quantification of hydration-related constraints on bacterial motion provides insights into optimal conditions for bacterial dispersion and spatial ranges of resource accessibility important for bioremediation and biogeochemical cycles. Results define surprisingly narrow range of hydration conditions where motility confers ecological advantage on natural surfaces.

3.1 Introduction

Bacterial motility is recognized as a key mechanism in small scale biodiversity maintenance of ecosystem (Mills, 2003; Reichenbach *et al*., 2007). Bacteria need to constantly seek optimal conditions in a patchy and dynamic environment (Fenchel, 2002; Alexandre *et al*., 2004), create opportunities for interactions and enhance competition among species within the range of search. Bacteria live in a world with low Reynolds numbers, where molecular diffusion of nutrients is more important than advective transport; therefore, bacteria need to outrun diffusion to survive even in water replete environments (Purcell, 1977; Fenchel, 2002). This need is accentuated in fragmented and heterogeneous environments found in unsaturated soils where nutrient diffusion fields may vary at submillimetric scale (Mitchell and Kogure, 2006). Bacterial motility has been shown to play a dominant role in most aspects of bioremediation, biochemical nutrient cycling, and dispersal of nutrients or waste (Duffy *et al*., 1997; Witt *et al*., 1999; Parales and Harwood, 2002; Wu *et al*., 2003; Madsen, 2005). Pandey and Jain (2002) indicated that effective bioremediation requires movement of active bacteria to access to the target compounds that are present in field. Law and Aitken (2003) and Paul *et al*. (2006) found that bacterial chemotaxis and motility substantially increase the rates of mass transfer and degradation of soil pollutantsl. Gordillo *et al*. (2007) observed that motility of *Pseudomonas* sp. B13 strain, confers clear advantages for bioremediation of contaminated soils relative to non-motile strain of *B. xenovorans* LB400, an advantage attributed to enhanced access to soil-sorbed organic pollutants. Hill and coworkers (2007) found that *Escherichia coli* grown in flowing solution near a surface exhibit a steady propensity of upstream swimming to locate larger nutrient reservoirs. Long and Ford (2009) observed a strong chemotactic bacterial migration up the attractant gradients cultured in saturated porous media. In capillaries containing attractant, bacteria were found to track attractant gradients, gathering near the end where the concentration of attractant is higher (Berg and Brown, 1972; Berg and Turner, 1990).

Despite lack of direct observations of bacterial motility in unsaturated soils, evidence suggest that soil hydration and pore-space characteristics play critical roles in bacterial motility (Barton and Ford, 1997; Chang and Halverson, 2003; Or *et al*., 2007). Other factors, such as temperature (Kurdish *et al*., 2001; Andreoglou *et al*., 2003), and nutrient supply (Sibona, 2007) influence bacterial motion in soil. Soil water, an essential ingredient for bacterial growth (Parr *et al*., 1981; Schjønning *et a*l., 2003), provides the necessary conditions for motility in unsaturated soils (Chang and Halverson, 2003; Or *et al*., 2007; Hill *et al*., 2007). Bacteria in soils inhabit environments dominated by the presence of extensive solid- and gas-water interfacial areas (Mills, 2003). The size of aquatic elements are controlled by hydration conditions and

geometrical features resulting in limited and complex water configurations that preclude full bacterial immersion (Metting and Jr, 1993; Long and Or, 2005; Or *et al*., 2007). Confinement imposed by thin liquid films under unsaturated conditions suppresses free-swimming (planktonian) life forms and promotes bacterial adherence to soil solid surfaces (Mills, 2003). Experimental evidence confirms that bacterial motility in fragmented aquatic environment loosely connected by thin water films is severely limited (Dechesne *et al*., 2008). The key constraints to bacterial motility in thin water films are cell-surface interactions induced viscous and capillary forces due to the proximity of solid and air surfaces inducing hydrodynamic and capillary interactions absent in free solution (Brenner, 1961; Kralchevsky and Nagayama, 2001; O'Donnell *et al*., 2007). As film thickness becomes similar to bacterial size, strong capillary forces emerge and result in pinning resistance hindering bacterial motility (Sur and Pak, 2001).

The limitations of bacterial motility in thin water films, typical of hydration conditions in unsaturated soils, have long been posited (Berg, 2005), and the importance of motility to bacterial life is well established (Vos and Velicer, 2008). However, due to extremely complex biological and physical factors affecting bacterial growth (McBride, 2001; Merz and Forest, 2002; Harshey, 2003; Chang *et a*l., 2009), information regarding mechanisms affecting bacterial motility in partially saturated soils remains sketchy (Potts, 1994). Detailed investigations of bacterial motility, involved in the developmental process from individual cells scattered on a surface to multicellular colonies, are crucial to elaborate bacterial survival strategies on partially-saturated rough surfaces (Diaz *et al*., 2007). Ultimately, the understanding of bacterial activity needs to be viewed in terms of the behavior of individual bacteria (Mitchell and Kogure, 2006). Similarly, quantitative characterization of bacterial motility is necessary for improved understanding of naturally-occurring bacterial transport as well as contemporary biotechnological applications (O'Donnell *et al*., 2007).

The primary motivation for this study was to quantify effects of hydration status and surface geometrical properties on bacterial cell motility and the impact of such constraints on surface-attached bacterial colony growth and expansion. We proposed a hybrid model for bacterial growth in heterogeneous nutrient diffusion field where surface roughness and water configuration conspire to impose capillary and viscous constraints affecting bacterial motility on such partially-saturated rough surfaces. The model incorporates Individual-Based Modeling (IBM) approach (Kreft *et al*., 1998) with classical diffusion-reaction elements of spatial nutrient field supporting bacterial colony growth (Golding *et al*., 1998).

3.2 Theoretical Considerations

3.2.1 Model of heterogeneous rough surface

A key simplification for modeling bacterial motility and growth in partially-saturated porous media, considers an idealized surface roughness network representing real rough surfaces (Fig. 1) and 2-D representation of soil pores. Such relatively simple network retains salient physical process associated with changes in hydration status of soils and other porous media such as capillary water retention in roughness elements, changes in hydraulic connectivity of the network and their effect on associated macroscopic transport properties (e.g., diffusion coefficient) (Blunt, 2001; Long and Or, 2007). The rough surface model consists of a network of conical sites connected by v-shaped bonds, both having isosceles triangular cross sections arranged on a regular grid. Each site connected up to six neighboring bonds to form a hexa-triangular network. The geometry of the network is described by five parameters: site height H_S (mm), site spanning angle θ_S (radian), bond height H_B (mm), bond spanning angle θ_B (radian), and bond length L (mm). Variations in connectivity of the aqueous phase filling this network under various hydration states are determined primarily by bond spanning angles and bond heights (bonds disconnected for $\theta_B \to 0$ and $H_B \to 0$) resulting in spatially heterogeneous geometrical features of the network. The parameters of network used in this study are listed in Table 1. Nutrient distribution and diffusion are supported by the variable aqueous network resulted from various hydration states (Long and Or, 2005).

Table 1. Parameters of surface roughness network.

Parameters	Mean value	Range	Variance
L (mm, Bond length)	0.2	-	-
H_S (mm, Site height)	0.3*	0.1 to 0.5	0.0033
H_B (mm, Bond height)	0.007**	0 to 0.030	4.9×10^{-5}
α_S (rad, Site spanning angle)	$\pi/2$*	$\pi/3$ to $2\pi/3$	0.018
α_B (rad, Bond spanning angle)	$7\pi/9$**	0 to π	0.56

* Truncated normal distribution

** Log-normal distribution, the pore size in surface soil being log-normally distributed (Giménez, 2002; Virto *et al*., 2005).

3.2 2 Water configuration on surface roughness network

The amount of water retained by capillarity within surface roughness elements is a function of ambient matric potential or relative humidity (both linked to the energy state of water) and surface roughness (pore space) geometry (Long and Or, 2007; Or *et al*., 2007). Areal averaged, or effective water film thickness ($\bar{d}$, mm) in a roughness element for a given matric potential is expressed as (Or and Tuller, 2000) (see inset in Fig. 7),

$$\bar{d}(P) = \frac{l(P)\left\{\gamma H + 2[\frac{H}{\cos(\theta/2)} - \frac{r(P)}{\tan(\theta/2)}]\right\}}{H[\gamma + 2\tan(\theta/2)]}, \quad (1)$$

where P (-kPa) is matric potential, H (mm) is the depth of a roughness element, θ (radian) is the spanning angle of the channel, $l(P)$ (mm) is the water film thickness absorbed on a planar surface by van der Waals forces (Iwamatsu and Horii, 1996), γ is a dimensionless geometrical factor for spacing between channel elements scaled by element depth as γH, and $r(P)$ (mm) is the radius of water-vapor interfacial curvature.

Calculated effective water film thickness on a rough element is illustrated in Fig. 2, showing decrease from 100 μm to molecular scale for decreasing matric potential in the rage of 0 to -10

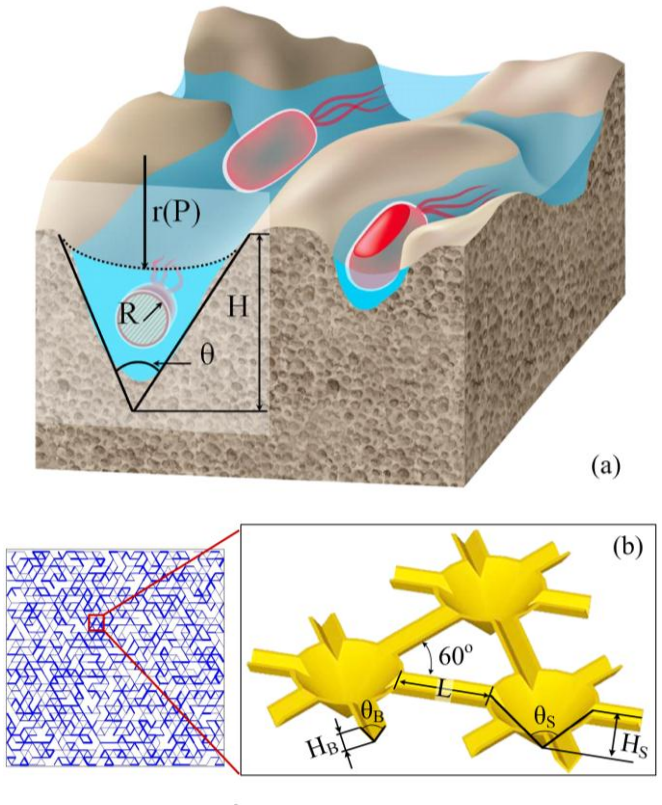

Fig. 1. Conceptualized soil surface roughness for capillary water retention: (a) a conceptualized rough surface; and (b) an idealized roughness network. A surface roughness network is represented by conical sites on a regular lattice each connected with six v-shaped bonds, with H_B, bond height, L, bond length, H_S, site height, θ_B, bond spanning angle, θ_S, site spanning angle, R is cell radius, and $r(P)$ the radius of curvature of water meniscus determined by surface tension.

kPa, consistent with experimental results of Tokunaga and Wan (1997). Naturally, representing the amount of water retained in a surface roughness element as effective film thickness involves averaging; nevertheless, even the largest water element in the system such as the cross section in crevices becomes smaller than average cell size at mild values of matric potential. The maximum size of fully immersed diameter (D*, mm) in a corner behind water-air interface under given matric potential is introduced into this study to evaluate the size of aqueous element for adjusting bacterial cell velocities (Or *et al.*, 2007) (Fig. 7 inset),

$$D^* = -\frac{4\sigma}{P}\frac{(1-\sin(\theta/2))}{(1+\sin(\theta/2))}. \quad (2)$$

In summary, the simple geometry facilitates calculation of an effective aqueous film thickness in which bacterial activity takes place and through which nutrients diffuse to colonies growing on a rough surface. Additionally, capillary behavior in such simple geometry enables estimation of aquatic habitats that become prohibitively small for complete immersion of bacterial cells.

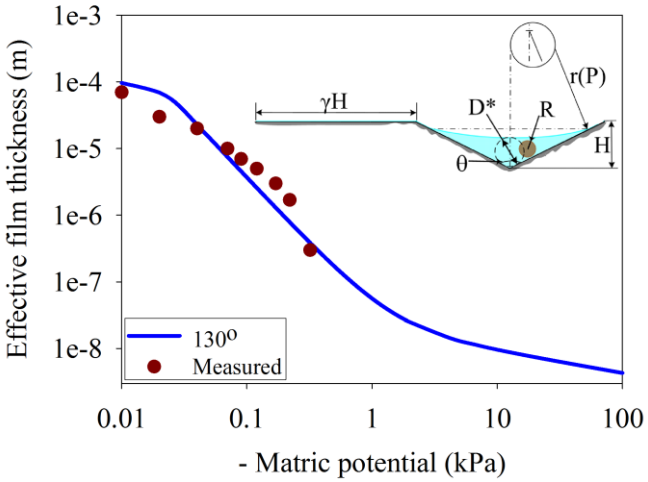

Fig. 2. Model calculations of effective water film thickness on roughness element (Or and Tuller, 2000, using γ = 4, and H = 0.5 mm) and measured values on rough rock surface (Tokunaga and Wan, 1997). A definition sketch for a unit roughness element representing partially-saturated rough surface, with H, the depth of a roughness element, θ, the spanning angle of the channel, γ, a dimensionless scaling factor for film covered spacing between channel elements (γH), R, the bacterial cell radius, D^*, the maximum immersed diameter, and $r(P)$, the radius of curvature of water meniscus determined by surface tension.

3.2.3 Bacterial motility on partially-saturated rough surface

The primary mode of self propulsion of motile bacteria in bulk solution is by means of rotation of flagellar filaments which are firmly anchored to cell body (Berg and Brown, 1972; Darnton and Berg, 2008). On partially-saturated rough surfaces, bacterial motion becomes restricted in thin aqueous films and small capillary-retained liquid elements. The primary impact of thin films is on cell-surface hydrodynamic interactions and emergence of capillary pinning forces (Wan *et al*., 1994; Berg, 2005; Or *et al*., 2007). It is instructive to elaborate key interactions experienced by bacterial cells moving in proximity to solid surface confined by thin aqueous film. Cell-surface hydrodynamic interactions have been succinctly lumped into a function of cell size and water film thickness (Rizk and Elghobashi, 1985),

$$\lambda = f(R,d), \quad (3)$$

where R (mm) is the cell size, d (mm) is liquid film thickness, and λ is the drag coefficient caused by the cell-surface hydrodynamic interactions, which is dependent on cell motion direction. Cell-surface hydrodynamic interactions for a spherical cell moving parallel to a solid wall (Fig. S1a), λ_p, can be simplified as (Lin *et al*., 2000),

$$\lambda_p = 1/[1-\frac{9}{16}(\frac{R}{d})+\frac{1}{8}(\frac{R}{d})^3], \quad (4)$$

and the cell-surface hydrodynamic interaction for a spherical cell moving normal to the solid wall, λ_n, can be expressed as (Maude, 1963),

$$\lambda_n = 1+\frac{9}{8}(\frac{R}{d})+(\frac{9R}{8d})^2. \quad (5)$$

In this model, we assume an average 45° angle between the solid surface and cell trajectory for simplification, thus,

$$\lambda = \sqrt{\lambda_n^2+\lambda_p^2}. \quad (6)$$

Cell-surface hydrodynamic interactions affect bacterial cell velocity according to: $V_\lambda = \frac{V_0}{\lambda}$ (Brenner, 1961), which could also be expressed as a resistive force,

$$F_\lambda = (1-\frac{1}{\lambda})F_M, \quad (7)$$

with F_M the propulsion force for a bacterium swimming at its maximum velocity in bulk solution (Darnton *et al*., 2007),

$$F_M = 6\pi R\eta V_0. \quad (8)$$

As aqueous films become thinner than bacterial cell diameter (i.e., drier ambient conditions), capillary interactions with water-air interfaces emerge and include formation of contact line and onset of a capillary pressure towards the solid surface experienced by the bacterial cell. These are summarized in a composite capillary pinning force (F_C, N), that introduces resistance to cell propulsion and further reduces cell velocity, as described in Appendix A (Kralchevsky and Nagayama, 2001),

$$F_C = (\frac{2\pi\sigma}{R}-\pi P)(R^2-(d+\Delta d-R)^2)\delta, \quad (F_C = 0 \text{ for } d > 2R) \quad (9)$$

where Δd (mm) is the capillary elevation of cell contact line above the flat water film interface, and δ is friction coefficient of cell moving on solid surface (Fig. S1b).

We may combine the hydration-dependent resistive forces into a simple model where bacterial cell velocity is proportional to the residual force available for propulsion,

$$V = V_0 \frac{F_M - F_\lambda - F_C}{F_M}, \tag{10}$$

with $V = 0$ for $F_M - F_\lambda - F_C < 0$.

3.2.4 Bacterial growth on partially-saturated rough surface

Despite the prescribed water-filled volumes of sites that are typically bigger than water held in bonds, for simplicity, we assume that sites do not support bacterial life but these structures are used as nutrient reservoirs and mixers providing boundary conditions for nutrient fluxes in and out of bonds (Aker *et al.*, 2000). We thus assume that nutrient concentrations at sites are constant for a small time increment (a few seconds) based on the large disparity between larger volumes in sites (average size of site is over 50 times bigger than bond) relative to bonds. Nutrient diffusion and bacterial nutrient consumption in a bond are solved using a well-established Reaction-Diffusion Method (RDM) (Golding *et al.*, 1998; Long and Or, 2005),

$$\begin{cases} \dfrac{\partial b}{\partial t} = D_b \nabla^2 b + \dfrac{\mu_{Max} S}{K_S + S} b \\ \dfrac{\partial S}{\partial t} = D_S \nabla^2 S - \dfrac{Y \mu_{Max} S}{K_S + S} b \end{cases}, \tag{11}$$

where b is bacteria number or concentration, S (mg/L) is nutrient concentration, D_b and D_S (mm^2/hr) are diffusion coefficients of bacteria and nutrient, respectively, t (hr) is elapsed time, K_S (mg/L) is half-saturation constant, μ_{Max} (hr^{-1}) is maximum specific growth rate, and Y is the yield term (linking bacterial growth with consumed nutrient).

Table 2. Parameters describing bacterial growth and metabolism.

Parameters	**Units**	**Values**
μ_{max}: maximum specific growth rate	hr^{-1}	1.23
K_S: half-saturation constant	fg/fl	1.17×10^{-3}
Y_{max}: apparent yield at μ_{max}, corrected for maintenance	fg dry mass/fg substrate	0.44
m: apparent maintenance rate at μ=0	fg substrate/(fg dry mass × hr)	0.036
$\bar{V}_B$: median cell volume at μ=0	fl	0.4
$V_{B,d}$: cell volume at division	fl	$2\bar{V}_B$/1.433
$V_{B,min}$: minimal cell volume of an active bacterium	fl	$V_{B,d}$/5
ρ: cell density (dry mass)	fg/fl	290

Bacterial growth on the surface roughness network is modeled by using the IBM framework (Kreft *et al*., 1998), as described in Appendix B. The biological parameters used for bacterial growth and consumption are summarized in Table 2. The parameters are selected on the basis of the Kreft *et al*. (1998) which cited typical batch growth values of *Escherichia coli*, but with a lower K_S value, to enhance population growth during the limited simulation time.

To quantify the combined effects of hydration conditions on diffusion and bacterial motility, and their manifestation in rates of colony growth and expansion, we inoculated 50 cells in four sites of the network for all simulations. Initial nutrient concentration in the aqueous phase was set to 0.2 mg/L (Long and Or, 2009), and similar and constant nutrient concentration was maintained at the upper and right boundaries of the simulation domain throughout simulations. Triplicate simulations with six different matric potential values of -0.01, -0.5, -1.0, -2.0, -3.5, and -5.0 kPa, were conducted, respectively.

3.2.5 Linking bacterial colony expansion rates with cell motility

The IBM framework allows tracking of motion and growth status of each bacterial cell in the simulation domain. Cells maintain their trajectory within a time step; however they are not allowed to traverse an entire bond length. If a cell's displacement length exceeds bond length within a time step it is placed at the nearest site for redirection at next time step according to criteria outlined in Appendix C (see Fig. S2a). The velocity of an individual cell is determined using Eq. 10 by estimating bacterial cell size and local water film thickness. Bacterial chemotaxis are considered in this model by preferentially selecting neighboring bonds with higher nutrient concentration and water contents for motion of an individual cell, as described in Appendix C.

Population-scale dispersal of motile bacteria on rough surfaces was linked with single cell motility (Korber *et al*., 1994). Skellam (1951) has derived an expression for population dispersal on surfaces as,

$$\bar{V}_R = \sqrt{4\mu D_B}\,, \tag{12}$$

where D_B (mm^2/s) is bacterial random diffusion coefficient expressed as (Lovely and Dahlquist, 1975; Othmer *et al*., 1988),

$$D_B = \frac{\langle l \rangle^2}{2T[1-\cos(\omega)]}\,, \tag{13}$$

where T (s) is time interval, $\langle l \rangle$ (mm) is mean travel distance between turns, and ω (radian) is the angle between successive trajectories.

In this study, bacterial motility is not entirely random, but includes a chemotactic component. In the presence of chemical attractant, bacterial chemotactic velocity can be expressed as (Rivero *et al*., 1989),

$$V_C = \frac{1}{2}\chi_0 v \frac{N_T}{(K_d + S)^2}\frac{\partial S}{\partial x}, \tag{14}$$

where χ_0 (mm/receptor) is the chemotactic sensitivity, K_d (mM) is the receptor/ligand dissociation equilibrium constant, and N_T is the total number of cell receptors for the ligand.

Considering these expressions and network properties, we proposed a simple analytical prediction model to estimate the rate of bacterial colony expansion on partially-saturated surface roughness network as (Appendix C),

$$\bar{V} = (1-\zeta)\sqrt{2\mu_{Max}\frac{D_{eff,S} v L^{1.6}}{D_{0,S}\Gamma[1-\cos(\omega)]}} + \frac{1}{2}\zeta\chi_0 v \frac{N_T S_0}{(K_d + S)^2 L\Gamma}, \tag{15}$$

where ζ is a dimensionless factor, $D_{eff,S}$ and $D_{0,S}$ are effective nutrient diffusion coefficient and diffusion coefficient in bulk water, respectively, and v (mm/s) is the mean cell velocity (details see Appendix S3).

3.3 Results and Discussion

3.3.1 Bacterial cell motility on partially-saturated surface roughness network

Theoretical relationship between hydration status (matric potential) and bacterial motility within surface roughness elements (Eq. 10) is depicted in Fig. 3. Calculations show bacterial cell velocity decreases from 18 μm/s (a typical experimental value for flagellar motility in bulk solution – Berg and Brown, 1972) to near 0 with decreasing matric potential from -0.1 to -10.0 kPa, respectively. For wet conditions (matric potential values higher than -0.5 kPa), bacteria move in aqueous phase at velocities close to maximum velocity in bulk solution, V_0. Cell velocity decreases gradually with decreasing matric potential and thinning of liquid films that result in increased drag due to cell-surface hydrodynamic interactions. At a critical matric potential value (intersection of the velocity curve with the dashed line in Fig. 3), aqueous film thickness is equal to bacterial cell size and capillary force becomes dominant. Subsequent reduction in matric potential and associated film thickness results in sharp decrease in cell velocity to near zero values at only a few kPa. These theoretical predictions are consistent with experimental observations that indicated that cell velocity in thin aqueous film decreases with increasing resistive forces (Goldstein and Charon, 1988; Biondi *et al*., 1998; Miyata *et al*., 2002).

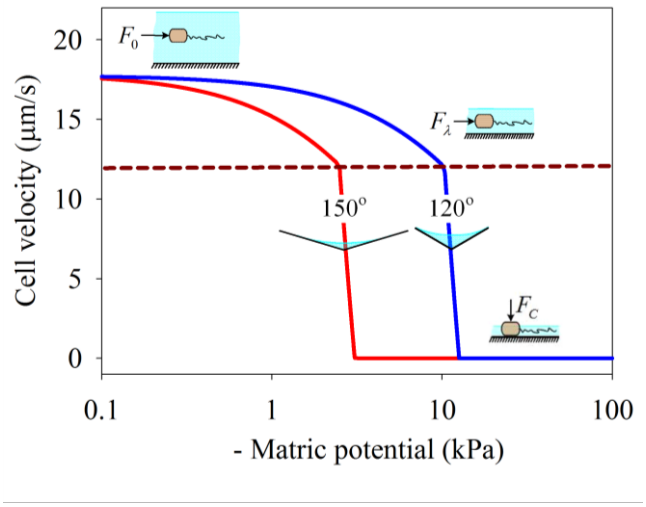

Fig. 3. Effect of hydration status on bacterial motility (cell velocity) as a function of matric potential for rough elements with two spanning angles and identical bond height, $H = 100\mu m$. The dashed line marks cell velocity corresponding to film thickness equals to one cell diameter, and intersection of velocity model with dashed line occurs at critical matric potential that varies with pore geometry. F_0 , F_λ , and F_C are the viscous drag force opposing motion in bulk water, the viscous force associated with cell-surface hydrodynamic interactions, and the capillary pinning force, respectively.

3.3.2 Bacterial growth on partially-saturated surface roughness network

Figure 4 depicts bacterial colony patterns after 25 hrs of growth under various hydration (matric potential) conditions. Under wet conditions (matric potential greater than -0.5 kPa), bacterial colonies expand relatively fast, resulting in bacterial population size exceeding 55,600±26,000 individual cells forming colonies with mean radius of 13.8±3.5 mm. In contrast, drier conditions limited bacterial colony growth, where for matric potential of -3.5 kPa, mean bacterial population size dropped to 220, and mean colony radius was only 0.3 mm after 25 hours. No significant colony growth was observed at matric potential value of -5.0 kPa, which marks practical limitation for bacterial colony growth on partially hydrated rough surfaces with effective water film thickness of 0.1 μm (Biondi *et al*., 1998; Sur and Pak, 2001). The critical matric potential for measurable bacterial growth was -2.0 kPa below which, bacterial colony radius decreased sharply. Similar phenomena have been reported indicating that bacteria that were motile in culture may exhibit non-migrating growth pattern in dry soils due to limiting aqueous phase configuration (Gray and Williams, 1971). Matsuyama and Nakagawa (1995) observed significantly restricted colony growth for *Serratia marcescens*, a motile bacterium, on dehydrated rough surface, indicating that aqueous surface tension (capillarity) exerted significant influence on limiting bacterial colony extension on partially-saturated rough surfaces. More recent experimental observations show suppressed colony growth of *Pseudomonas putida*, a flagellated bacterium: on rough surfaces with aqueous film controlled by matric potential, colony radii showed a consistent decrease from 21.0 to 0.4 mm after 40 hrs of incubation with decreasing matric potential from -0.5 to -3.6 kPa, respectively (Dechesne *et al*., 2008).

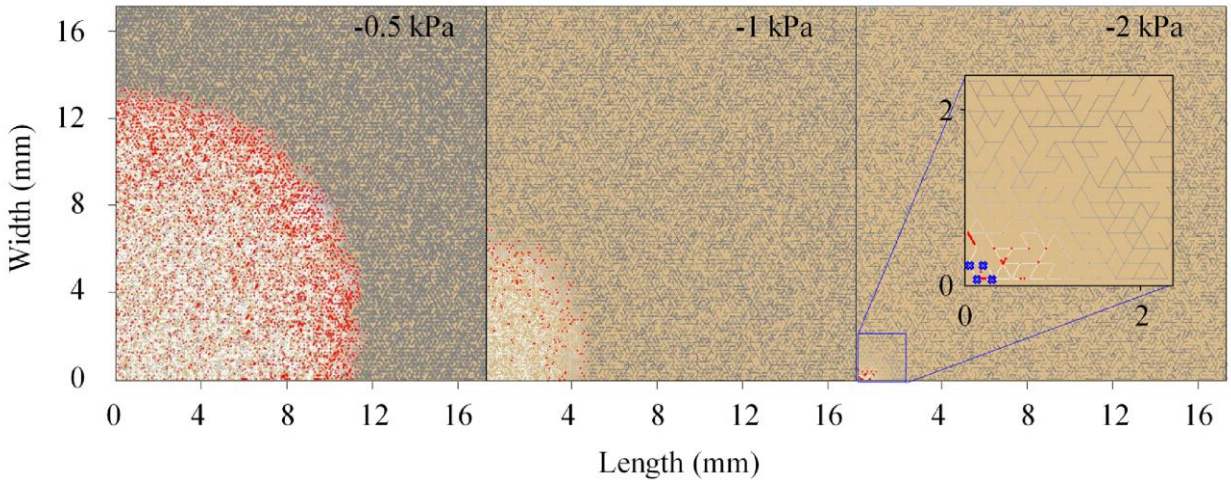

Fig. 4. Patterns of bacterial colonies grown on rough surfaces under various hydration statuses 25 hrs after inoculation. Blue spots mark inoculation sites (same inoculation locations for all simulations in this study).

3.3.3 Bacterial colony expansion rates on rough surfaces

Figure 5 illustrates the effect of hydration status on simulated and measured rates of bacterial colony expansion on rough surfaces. Under wet conditions (matric potential greater than -0.5 kPa), bacterial population dispersed at high rates with colony front velocity exceeding 421±92 μm/hr. A significant decline in colony expansion rate from 262±74 to 31±10 μm/hr was simulated for when matric potential was reduced from -1 to -2.0 kPa, respectively. Following this relatively large decline, the rate of colony expansion leveled at values of less than 31±10 μm/hr.

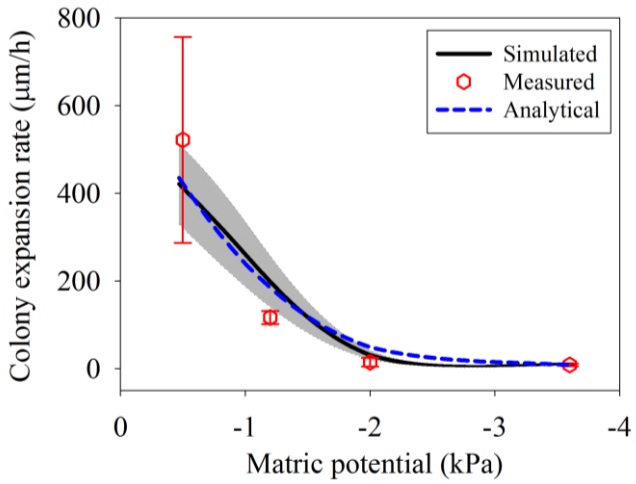

Fig. 5. Effect of hydration status (expressed as matric potential) on bacterial colony expansion rates on rough surface: measured (data from Dechesne et al. 2008), simulated and analytical prediction. Error bars indicate one standard deviation (sample number, n, varies from 6 to 14). Simulated colony expansion rates depicted by lines with shaded area representing one standard deviation.

The large decline in colony expansion rate reflects effects of water configurations on the rough surface especially the thinning of water films. The calculated effective water film thickness was less than 1 μm (allowing for only partial cell immersion) for matric potential less than -2.0 kPa, at which bacterial motility is severely constrained due to onset of capillary-induced pinning forces. Bacterial colony growth on surfaces is generally dependent on surface hydration

conditions (Senesi *et al*., 2002; Berg, 2005; Or *et al*., 2007). Colonies of *Pseudomonas putida*, a flagellated bacterium, grown on ceramic surfaces under controlled matric potential conditions experienced a sharp reduction in expansion rates from 521 to 9 μm/hr when matric potential decreased from -0.5 to -3.6 kPa, respectively (Dechesne *et al*., 2008) (Fig. 5).

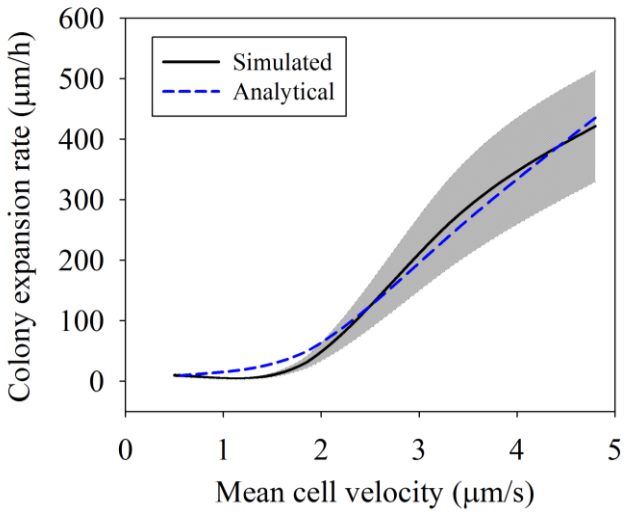

Fig. 6. Effect of individual cell motility on bacterial colony expansion rates on partially-saturated rough surface. Simulated colony expansion rates are depicted by line (shaded area represents one standard deviation), and analytical predicted colony expansion rate is represented as dashed line. The mean cell velocity represents the statistical mean of individual cell velocities at each bond of the network.

Bacterial population dispersal or colony expansion rates are linked to- and driven by individual cell motility (Eq. 15). Wolfe and Berg (1989) found that dispersal of bacterial population was promoted by increased individual cell velocity for motile *Escherichia coli* grown on agar. Phillips *et al.* (1994) also reported colony expansion rates of motile bacteria, *Escherichia coli*, and proportional to individual cell velocity. Dispersal of motile bacterial colonies on partially-saturated rough surface could be reasonably well predicted with simple model, as illustrated in Fig. 6, showing decreasing mean colony expansion rate from 421 to 9 μm/hr with decreasing mean cell velocity from 4.8 to 0.5 μm/s, respectively. Spatially, the highest density of bacterial population occurs at the periphery of a colony (Fig. 7a) consistent with experimental observations where also most flagellated cells are found (Park *et al*., 2003; Macnab, 2003; Harshey, 2003). Such spatial colony structure is also linked with bacterial chemotaxis behavior where motile bacteria move towards higher nutrient (attractant) concentration and form high-density population bands (Brown and Kraus, 1974; Medvinsky *et al*., 1993; Fenchel, 2002). The shape of population bands or waves was attributed to cell motility (Matsushita *et al*., 1999), cell-cell signaling, chemotaxis interactions in complex mechanisms (Harshey, 2003), and nutrient properties (Hiramatsu *et al*., 2005).

Following prolonged growth periods, colony expansion rate becomes nonlinear as depicted in Fig. 7b. Bacterial colony radius scales as a power-law with growth time as t^{β}, with β assuming values up to 0.88 under wettest condition (-0.01 kPa). The simulation results are in agreement with observations showing reduced colony expansion rates of *Escherichia coli* and *Serratia*

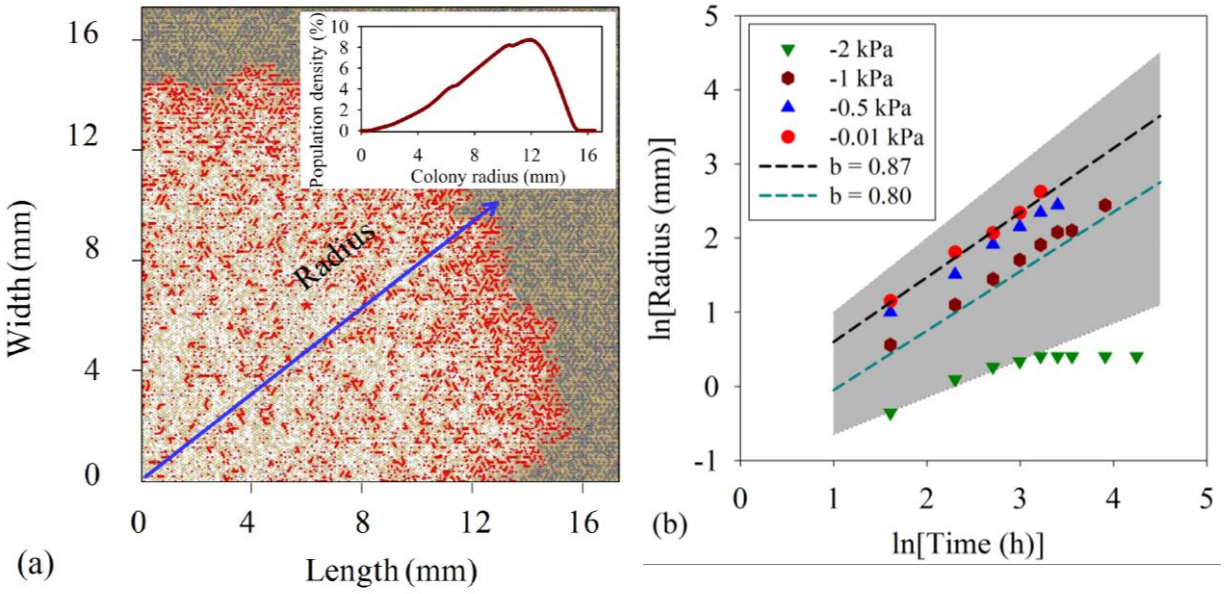

Fig. 7. Effect of hydration status on bacterial colony expansion: (a) pattern of bacterial colony growth under -0.01 kPa 25 hrs after inoculation (the red spots represent individual bacterial cells, and the population density marks the population distribution along the colony radius); and (b) power-law relationship between colony radius growth and time. The shaded area represents power exponent values spanning 0.5 to 1.0. The dash lines are observations by Pipe and Grimson (2008).

marsescens on agar with power values (β) varying in the range of 0.80 to 0.87 for *Escherichia coli* and *Serratia marsescens*, respectively (Pipe and Grimson, 2008). We found power values for colony growth reduced from 0.88 to 0.47 with decreasing matric potential from -0.01 to -2.0 kPa, respectively. These changes are attributed to restrictive role of hydration conditions on both bacterial motility and on nutrient diffusion processes (Koch, 1990). As rough surfaces become progressively less saturated nutrient amounts retained in aqueous solutions are reduced and nutrient diffusional pathways are restricted and reconfigure (Young et al., 1999), resulting in impaired bacterial motility and growth rate (Parr *et al*., 1981; Koch, 1990). For instance, as matric potential was decreased from -0.01 to -2.0 kPa, the corresponding mean cell velocity and mean bacterial population size were reduced from 7.2 to 2.0 μm/s, and from 55,600 to 272, respectively.

Bacterial motility is recognized as a key mechanism for survival in patchy and heterogeneous environments at small scale and is important for biodiversity maintenance of ecosystems (Mills, 2003; Reichenbach *et al*., 2007). Understanding the extremely complex interactions between physico-chemical characteristics of soil matrix and bacterial motility are keys to understanding how these survival and biodiversity are maintained *in situ*. Vos and Velicer (2008) reported that motility variations in bacterial population of *Myxococcus Xanthus*, may result in alternate motility forms such as social-motility and adventurous-motility, reflecting diversifying

adaptation to various soil microenvironments. Dechesne and coworkers (2008) found that flagellated bacterial strain, *Pseudomonas putida*, exhibited significant reduction in colony expansion rates with decreasing matric potential on rough surfaces. These were attributed to physical constraints imposed on individual bacterial cells under drier conditions. However, these observations did not attempt to quantify the phenomenon which is elucidated in this study.

Spatial and temporal variations in nutrient availability at small scales are ubiquitous in natural soils, where bacterial motility is a foraging strategy in the limited and patchy nutrient environment, and thus plays a fundamental role in competition and survival ability (Mitchell and Kogure, 2006). Simulation results show motile bacteria prefer to congregate at most favorable nutrient gradient consistent with experimental observations (Adler, 1966; Zhulin *et al*., 1995; Fenchel, 2002; Barbara and Mitchell, 2003). High motility could potentially provide a means for rapid and uniform dissemination of bacteria in polluted environments (Witt *et al*., 1999), and enhance biochemical processes by increasing sufficient interactions between bacteria and patchy resources. In harsh and dry soil environments, lower bacterial motility would be expected to increase isolation among local populations and reduce interactions between neighboring colonies, thus enhancing the formation of microcolonies and increasing soil biodiversity (Paul, 2006; Long and Or, 2009).

3.4 Conclusions

We explicitly consider effects of physical constraints imposed on motility of bacterial cells inhabiting partially-saturated rough surfaces, considering primarily cell-surface hydrodynamic interactions and capillary pinning forces. A new hybrid model for bacterial growth and nutrient consumption was proposed to systematically evaluate influences of surface hydration and pore features on bacterial motility and the further impact on bacterial growth and colony expansion on partially-saturated rough surfaces. Simulation results indicate that capillarity and water configuration play key roles in affecting bacterial activities on partially-saturated rough surfaces, and define a surprisingly narrow range of hydration conditions where motility confers ecological advantage in identical systems. Bacteria experience reduced cell motilities with decreasing matric potential on rough surfaces resulting in suppressed growth and colony expansion. Reduced bacterial motility under drier conditions is expected to increase isolation among local populations, thus enhancing potential of biodiversity by sheltering less competitive species. Including fundamental mechanisms representing physical constraints composed of cell-surface hydrodynamic interactions and capillary pinning forces on bacterial growth and colony

expansion on partially-saturated rough surfaces should guide future experiments and improve predictions of bacterial activities in partially-saturated porous media.

Acknowledgements

We gratefully acknowledge the financial support of the Swiss National Science Foundation (200021-113442), and thank Barth Smets and Arnaud Dechesne (DTU, Denmark) for their assistance and for a productive collaboration.

References

Adler, J. (1966) Chemotaxis in bacteria. *Science* **153**: 708-716.

Aker, E., Måløy, K.J., Hansen, A., and Basak, S. (2000) Burst dynamics during drainage displacements in porous media: simulations and experiments. *Europhys Lett* **51**: 55-61.

Alexandre, G., Greer-Phillips S., and Zhulin I.B. (2004) Ecological role of energy taxis in microorganisms. *FEMS Microbiol Rev* **28**: 113-126.

Andreoglou, F.I., Vagelas, I.K., Wood, M., Samaliev, H.Y., and Gowen, S.R. (2003) Influence of temperature on the motility of *Pseudomonas oryzihabitans* and control of *Globodera rostochiensis*. *Soil Biol Biochem* **35**: 1095-1101.

Barbara, G.M., and Mitchell, J.G. (2003) Marine bacterial organisation around point-like sources of amino acids. *FEMS Microbiol Ecol* **43**: 99-109.

Barton, J.W., and Ford, R.M. (1997) Mathematical model for characterization of bacterial migration through sand cores. *Biotechnol Bioeng* **53**: 487-496.

Berg, H.C. (2005) Swarming motility: it better be wet. *Curr Bio* **15**: 599-600.

Berg, H.C., and Brown, D.A. (1972) Chemotaxis in *Escherichia coli* analysed by three-dimensional tracking. *Nature* **239**: 500-501.

Berg, H.C, and Turner, L. (1990) Chemotaxis of bacteria in glass capillary assays. *Biophys J* **58**: 919-930.

Biondi, S.A., Quinn, J.A., and Goldfine, H. (1998) Random motility of swimming bacteria in restricted geometries. *AIChE J* **44**: 1923-1929.

Blunt, M.J. (2001) Flow in porous media: pore-network models and multiphase flow. *Curr Opin Colloid Interface Sci* **6**: 197-207.

Brenner, H. (1961). The slow motion of a sphere through a viscous fluid towards a plane surface. *Chem Eng Sci* **16**: 242-251.

Brown, W.J., and Kraus, S.J. (1974) Gonococcal conlony types. *Jama-J Am Med Assoc* **228**: 862-863.

Chang, W.S., and Halverson, L.J. (2003) Reduced water availability influences the dynamics, development, and ultrastructural properties of *Pseudomonas putida* biofilms. *J Bacteriol* **185**: 6199-6204.

Chang, W.S., Li, X.H., and Halverson, L.J. (2009) Influence of water limitation on endogenous oxidative stress and cell death within unsaturated *Pseudomonas putida* biofilms. *Environ Microbiol* **11**: 1482-1492.

Darnton, N.C., Turner, L., Rojevsky, S., and Berg, H.C. (2007) On torque and tumbling in swimming *Escherichia coli*. *J Bacteriol* **189**: 1756-1764.

Darnton, N.C., and Berg, H.C. (2008) Bacterial flagella are firmly anchored. *J Bacteriol* **190**: 8223-8224.

Dechesne, A., Or, D., Gulez, G., and Smets, B.F. (2008) The porous surface model, a novel experimental system for online quantitative observation of microbial processes under unsaturated conditions. *Appl Environ Microb* **74**: 5195-5200.

Diaz, C., Schilardi, P.L., Salvarezza, R.C., and de Mele, M.F.L. (2007) Nano/Microscale order affects the early stages of biofilm formation on metal surfaces. *Langmuir* **23**: 11206-11210.

Duffy, K.J., Ford, R.M., and Cummings, P.T. (1997) Residence time calculation for chemotactic bacteria within porous media. *Biophys J* **73**: 2930-2936.

Fenchel, T. (2002) Microbial behavior in a heterogeneous world. *Science* **296**: 1068-1071.

Giménez, D. (2002) Encyclopedia of Soil Science, R. Lal, Ed. Marcel Dekker, New York.

Golding, I., Kozlovsky, Y., Cohen, I., and Ben-Jacob, E. (1998) Studies of bacterial branching growth using reaction-diffusion models for colonial development. *Physica A* **260**: 510-554.

Goldstein, S.F., and Charon, N.W. (1988) Motility of the *Spirochete Leptospira*. *Cell Motil Cytoskel* **9**: 101-110.

Gong, J.P., Kagata, G., and Osada, Y. (1999) Friction of gels. 4. friction on charged gels. *J Phys Chem B* **103**: 6007-6014.

Gordillo, F., Chávez, F.P., and Jerez, C.A. (2007) Motilityand chemotaxis of *Pseudomonas* sp. B4 towards polychlorobiphenyls and chlorobenzoates. *FEMS Microbiol Ecol* **60**: 322-328.

Gray, T.R.G., and Williams, S.T. (1971) Microbial productivity in soil. In: D.E. Hughes and A.H. Rose, Editors, *Microbes and Biological Productivity*, University Press, Cambridge, pp. 255-286.

Harshey, R.M. (2003) Bacterial motility on a surface: many ways to a common goal. *Annu Rev Microbiol* **57**: 249-273.

Hill, J., Kalkanci, O., McMurry, J.L., and Koser, H. (2007) Hydrodynamic surface interactions enable *Escherichia coli* to seek efficient routes to swim upstream. *Phys Rev Lett* **98**: 068101.

Hiramatsu, F., Wakita, J.I., Kobayashi, N., Yamazaki, Y., Matsushita, M., and Matsuyama, T. (2005) Patterns of expansion produced by a structured cell population of *Serratia Marcescens* in response to different media. *Microbes Environ* **20**: 120-125.

Iwamatsu, M., and Horii, K. (1996) Capillary condensation and adhesion of two wetter surfaces. *J Colloid Interface Sci* **182**: 400-406.

Koch, A.L. (1990) Diffusion: the crucial process in many aspects of the biology of bacteria. *Adv Microb Ecol* **11**: 37-70.

Korber, D.R., Lawrence, J.R., and Caldwell, D.E. (1994) Effect of motility on surface colonization and reproductive success of *Pseudomonas fluorescens* in dual-dilution continuous culture and batch culture systems. *Appl Environ Microb* **60**: 1421-1429.

Kralchevsky, P.A., and Nagayama, K. (2001) Lateral Capillary Forces between Partially Immersed Bodies. Chapter 7 in the book: "Particles at Fluid Interfaces and Membranes" (P. A. Kralchevsky and K. Nagayama, Authors) Elsevier, Amsterdam, pp. 287-350.

Kreft, J.U., Booth, G., and Wimpenny, J.W.T. (1998) BacSim, a simulator for individual-based modelling of bacterial colony growth. *Microbiology-UK* **144**: 3275-3287.

Kurdish, I.K., Antonyuk, T.S., and Chuiko, N.V. (2001) Influence of environmental factors on the chemotaxis of *Bradyrhizobium japonicum*. *Microbiology* **70**: 91-95.

Law, A.M.J., and Aitken, M.D. (2003) Bacterial chemotaxis to naphthalene desorbing from a nonaqueous liquid. *Appl Environ Microb* **69**: 5968-5973.

Lin, B.H., Yu, J., and Rice, S.A. (2000) Direct measurements of constrained Brownian motion of an isolated sphere between two walls. *Phys Rev E* **62**: 3909-3919.

Long, T., and Ford, R.M. (2009) Enhanced transverse migration of bacteria by chemotaxis in a porous T-sensor. *Environ Sci Technol* **43**: 1546-1552.

Long, T., and Or, D. (2005) Aquatic habitats and diffusion constraints affecting microbial coexistence in unsaturated porous media. *Water Resour Res* **41**: W08408.

Long, T., and Or, D. (2007) Microbial growth on partially saturated rough surfaces: simulations in idealized roughness networks. *Water Resour Res* **43**: W02409.

Long, T., and Or, D. (2009) Dynamics of microbial growth and coexistence on variably saturated rough surfaces. *FEMS Microbiol Ecol* **58**: 262-275.

Lovely, P.S., and Dahlquist, F.W. (1975) Statistical measures of bacterial motility and chemotaxis. *J Theor Biol* **50**: 477-496.

Macnab, R.M. (2003) How bacteria assemble flagella. *Annu Rev Microbiol* **57**: 77-100.

Madsen, E.L. (2005) Identifying microorganisms responsible for ecologically significant biogeochemical processes. *Nat Rev Microbiol* **3**: 439-446.

Matsushita, M., Wakita, J., Itoh, H., Watanabe, K., Arai, T., Matsuyama, T., Sakaguchi, H., and Mimura, M. (1999) Formation of colony patterns by a bacterial cell population. *Physica A* **274**: 190-199.

Matsuyama, T., and Nakagawa, Y. (1995) Bacterial wetting agents working in colonization of bacteria on surface environments. In Symposium on Biosurfactants and Biosurfaces, at the 1995 International Chemical Congress of Pacific Basin Societies. Honolulu, Hi, pp. 207-214.

Maude, A.D. (1963). The movement of a sphere in front of a plane at low Reynolds number. *British J Appl Phys* **14**: 894-898.

McBride, M.J. (2001) Bacterial gliding motility: multiple mechanisms for cell movement over surfaces. *Annu Rev Microbiol* **55**: 49-75.

Medvinsky, A.B., Tsyganov, M.A., Kutyshenko, V.P., Shakhbazian, V.Yu., Kresteva, I.B., and Ivanitsky, G.R. (1993) Instability of waves formed by motile bacteria. *FEMS Microbiol Lett* **112**: 287-290.

Merz, A.J., and Forest, K.T. (2002) Bacterial surface motility: Slime trails, grappling hooks and nozzles. *Curr Biol* **12**: R297-R303.

Metting, F., and Jr, B. (1993) Soil microbial ecology. Marcel Dekker, New York, p. 11-17.

Mills, A.L. (2003) Keeping in touch: Microbial life on soil particle surfaces. *Adv Agron* **78**: 1-43.

Mitchell, J.G., and Kogure, K. (2006) Bacterial motility: links to the environment and a driving force for microbial physics. *FEMS Microbiol Ecol* **55**: 3-16.

Miyata, M., Ryu, W.S., and Berg, H.C. (2002) Force and velocity of *Mycoplasma* mobile gliding. *J Bacteriol* **184**: 1827-1831.

O'Donnell, A.G., Young, I.M., Rushton, S.P., Shirley, M.D., and Crawford, J.D. (2007) Visualization, modelling and prediction in soil microbiology. *Nat Rev Microbiol* **5**: 689-699.

Or, D., and Tuller, M. (2000) Flow in unsaturated fractured porous media: hydraulic conductivity of rough surfaces. *Water Resour Res* **36**: 1165-1177.

Or, D., Smets, B.F., Wraith, J.M., Dechesne, A., and Friedman, S.P. (2007) Physical constraints affecting bacterial habitats and activity in unsaturated porous media - a review. *Adv Water Resour* **30**: 1505-1527.

Othmer, H., Dunbar, S., and Alt, W. (1988) Models of dispersal in biological systems. *J Math Biol* **26**: 263-298.

Pandey, G., and Jain, R.K. (2002) Bacterial chemotaxis toward environmental pollutants: role in bioremediation. *Appl Environ Microb* **68**: 5789-5795.

Parales, R.E., and Harwood, C.S. (2002) Bacterial chemotaxis to pollutants and plant-derived aromatic molecules. *Curr Opin Microbiol* **5**: 266-273.

Park, S., Wolanin, P.M., Yuzbashyan, E.A., Silberzan, P., Stock, J.B., and Austin, R.H. (2003) Motion to form a quorum. *Science* **301**: 188-188.

Parr J.F., Gardner, W.R., and Elliott, L.F. (ed.) (1981) *Water Potential Relations on Soil Microbiology. SSSA-Special Publication Number 9*. Madison, USA: Soil Science Society of America.

Paul, E.A. (2006) *Soil microbiology, ecology, and biochemistry*, 3rd edn. Boston, USA: Elsevier Academic Press.

Paul, D., Singh, R., and Jain, R.K. (2006) Chemotaxis of *Ralstonia* sp. SJ98 towards *p*-nitrophenol in soil. *Environ Microbiol* **8**: 1797-1804.

Phillips, B.R., Quinn, J.A., and Goldfine, H. (1994) Random motility of swimming bacteria: single cells compared to cell- populations. *AIChE J* **40**: 334-348.

Pipe, L.Z., and Grimson, M.J. (2008) Spatial-temporal modelling of bacterial colony growth on solid media. *Mol Biosyst* **4**: 192-198.

Potts, M. (1994) Desiccation tolerance of prokaryotes. *Microbiol Rev* **58**: 755-805.

Purcell, E.M. (1977) Life at low Reynolds number. *Am J Phy*s **45**: 3-11.

Reichenbach, T., Mobilia, M., and Frey, E. (2007) Mobility promotes and jeopardizes biodiversity in rock-paper-scissors games. *Nature* **448**: 1046-1049.

Rivero, M., Tranquillo, R., Buettner, H., and Lauffenburger, D. (1989) Transport models for chemotactic cell populations based on individual cell behaviour. *Chem Eng Sci* **44**: 2881-2897.

Rizk, M., and Elghobashi, S. (1985) The motion of a spherical particle suspended in a turbulent flow near the wall. *Phys Fluids* **28**: 806-817.

Schjønning, P., Thomsen, I.K., Moldrup, P., and Christensen, B.T. (2003) Linking soil microbial activity to water- and air-phase contents and diffusivities. *Soil Sci Soc Am J* **67**: 156-165.

Senesi, S., Celandroni, F., Salvetti, S., Beecher, D.J., Wong, A.C.L., and Ghelardi, E. (2002) Swarming motility in *Bacillus cereus* and characterization of a fliY mutant impaired in swarm cell differentiation. *Microbiol-Sgm* **148**: 1785-1794.

Sibona, G.J. (2007) Evolution of microorganism locomotion induced by starvation. *Phys Rev E* **76:** 011919.

Skellam, J.G. (1951) Random dispersal in theoretical populations. *Biometrika* **38**: 196-218.

Sur, J., and Pak, H.K. (2001) Capillary force on colloidal particles in a freely suspended liquid thin film. *Phys Rev Lett* **86**: 4326-4329.

Tokunaga, T.K., and Wan, J. (1997) Water film flow along fracture surfaces of porous rock. *Water Resour Res* **33**: 1287-1295.

Virto, I., Imaz, M.J., Bescansa, P., and Enrique, A. (2005) Pore size distribution in relation to soil physical properties in two irrigated semiarid mediterranean soils as affected by management. *Geophys Res Abstr* **7**: 03223.

Vos, M., and Velicer, G.J. (2008) Natural variation of gliding motility in a centimeter-scale population of *Myxococcus xanthus*. *FEMS Microbiol Ecol* **64**: 343-350

Wan, J.M., Wilson, J.L., and Kieft, T.L. (1994) Influence of the gas-water interface on transport of microorganisms through unsaturated porous media. *Appl Environ Microb* **60**: 509-516.

Witt, M.E., Dybas, M.J., Worden, R.M., and Criddle, C.S. (1999) Motility-enhanced bioremediation of carbon tetrachloride-contaminated aquifer sediments. *Environ Sci Technol* **33**: 2958-2964.

Wolfe, A.J., and Berg, H.C. (1989) Migration of bacteria in semisolid agar. *Proc Natl Acad Sci USA* **86**: 6973-6977.

Wu, G., Feng, Y., and Boyd, S.A. (2003) Characterization of bacteria capable of degrading soil-sorbed biphenyl. *Environ Cont Toxicol* **71**: 768-775.

Young, G.M., Smith, M.J., Minnich, S.A., and Miller, V.L. (1999) The *Yersinia enterocolitica* motility master regulatory operon, flhDC, is required for flagellin production, swimming motility, and swarming motility. *J Bacteriol* **181**: 2823-2833.

Zhulin, I.B., Lois, A.F., and Taylor, B.L. (1995) Behaviour of *Rhizobium meliloti* in oxygen gradients. *FEBS Lett* **367**: 180-182.

Appendix S1: Capillary pinning force acting on a bacterial cell

The frictional force, F_C (N), acting on a small spherical cell partially immersed in thin water film due to capillary stress (Kralchevsky and Nagayama, 2001) is expressed as,

$$F_C = (2\pi\sigma r_C \cos(\theta + \pi/2 - \alpha) + \pi r_C^2 \Delta P)\delta, \quad \text{(A1)}$$

where ΔP is the pressure difference across the free surface (equals to minus of matric potential, P), θ and α (radian) is contact angle and central cone angle, respectively, δ is friction coefficient of cell moving on solid surface (take 0.01 in this study, from Gong *et al*., 1999), and r_C (mm) is immersed radius of cell which can be expressed as (Fig. S1b),

$$r_C = \sqrt{R^2 - (d + \Delta d - R)^2}\,. \quad \text{(A2)}$$

In this model, we assume a zero contact angle at cell surface for simplification. Therefore, Eq. A1 can be rewritten as,

$$F_C = (2\pi\sigma r_C \sin\alpha + \pi r_C^2 \Delta P)\delta\,. \quad \text{(A3)}$$

Noting that $\sin\alpha = \sqrt{1 - (\frac{d + \Delta d - R}{R})^2}$, and substituting Eq. A2 into Eq. A3, one get,

$$F_C = (\frac{2\pi\sigma}{R} - \pi P)(R^2 - (d + \Delta d - R)^2)\delta\,. \quad (F_C = 0 \text{ for } d > 2R) \quad \text{(A4)}$$

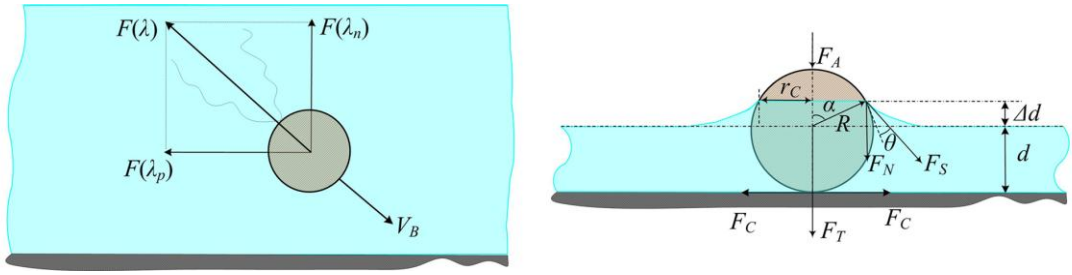

Fig. S1. Definition sketches of bacterial cell moving in thin water film: (a) sketch of a bacterial cell swimming in thin water film. V_B is cell velocity, $F(\lambda_p)$ and $F(\lambda_n)$ are viscous resistive forces due to cell-surface hydrodynamic interactions for a cell moving parallel to- and normal to solid wall, respectively, and $F(\lambda)$, the resultant force; and (b) sketch of capillary meniscus formed around a partially immersed spherical cell which is situated on a thin water film. Where d is water film thickness at infinite distance, Δd is capillary elevation of the contact line at the particle surface, θ and α is contact angle and central cone angle, respectively, r_C is immersed radius of the cell, R is cell radius, ΔP is the pressure difference across the free surface, and F_A, F_S, F_N, F_T, and F_C is capillary force due to the pressure difference across the free surface, surface tension force acting tangentially to the interface along the contact line, the vertical component of the surface tension force, the total normal capillary stress, and frictional force caused by total normal capillary stress, respectively.

Appendix S2: Growth kinetics of individual bacterial cell

The growth kinetics of a single bacterium is described by (Kreft *et al*., 1998),

$$X(t+1) = X(t) + X(t)\mu_B \Delta t \,, \tag{B1}$$

where X (mg) is the dry cell mass, Δt (hr) is the time interval, and μ_B (hr^{-1}) is the specific growth rate, which can be described as,

$$\mu_B = \frac{\mu_{Max} S}{K_S + S} - mY \,, \tag{B2}$$

with m (hr^{-1}) the maintenance rate.

The cell growth is then evaluated by estimating its volume (Long and Or, 2007). When a cell's volume, V_B (mm^3), becomes larger than a critical division volume, $V_{B,d}$ (mm^3), the cell reproduces a new cell. While V_B becomes less than a critical minimum volume, $V_{B,min}$ (mm^3), a cell is deemed dead. The $V_{B,d}$ and $V_{B,min}$ are determined based on the Donachie model (Kreft *et al*., 1998),

$$V_{B,d} = \frac{2}{1.433}\bar{V}_B \,, \tag{B3}$$

$$V_{B,\min} = \frac{1}{5}V_{B,d} \,, \tag{B4}$$

where $\bar{V}_B$ (mm^3) is the average volume of an active bacterium.

Appendix S3: Bacterial motility on partially-saturated rough surface

A cell is not allowed to traverse a bond length within a single time step. If a cell's displacement length exceeds bond length within a time step ($V_1\Delta t \geq L_2$ or $V_2\Delta t \geq L_2$) it is placed at the nearest site (site1 or site2) for redirection (see Fig. S2a).

Motion of a bacterial cell is not entirely random but cells have a chemotactic preference towards substrate-rich bonds. A cell in a site preferentially enters the neighboring bond k with higher nutrient concentration and water content, as described in Eqs. C1-3:

$$p_{W,i} = W_i / \sum_{i=1}^{6} W_i \,, \tag{C1}$$

$$p_{C,i} = C_i / \sum_{i=1}^{6} C_i \,, \tag{C2}$$

$$k = k\{p_{C,W,k} = \underset{i=1:6}{Max}(p_{C,i} \times p_{W,i})\}, \tag{C3}$$

where W_i and C_i are water content and nutrient concentration in the i^{th} neighboring bond, respectively; $p_{W,i}$ and $p_{C,i}$ are the components of water content and nutrient concentration in the i^{th} neighboring bond relative to that of all the bonds connected to a site.

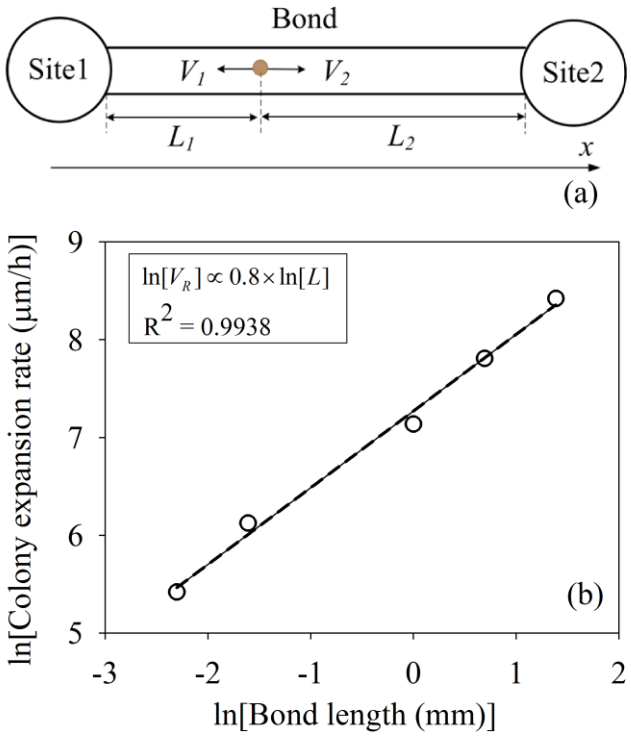

Fig. S2. (a) Definition sketch for bacterial cell motion within a roughness bond; and (b) effect of bond length on the rate of bacterial colony expansion within partially-saturated surface roughness network.

The rate of bacterial population-scaled dispersal on a two dimensional surface, $\bar{V}_R$, can be described as (Skellam, 1951),

$$\bar{V}_R = \sqrt{4\mu D_B}\,, \tag{C4}$$

where D_B (mm^2/s) is bacterial random diffusion coefficient, which can be described as (Lovely and Dahlquist, 1975; Othmer *et al*., 1988),

$$D_B = \frac{\langle l \rangle^2}{2T[1-\cos(\omega)]}\,, \tag{C5}$$

where T (s) is the mean persistence time, $\langle l \rangle$ (mm) is the mean persistence length, and ω (radian) is the angle between successive trajectories. Noting that $\langle l \rangle / T = v$, with v (mm/s) the mean cell velocity, one gets,

$$D_B = \frac{\langle l \rangle v}{2[1-\cos(\omega)]}\,. \tag{C6}$$

On partially-saturated rough surface, bacterial growth is controlled by the limited aqueous configuration and heterogeneous diffusion field (Mills, 2003; Or *et al*., 2007). Under nutrient limiting conditions, we may assume that bacterial growth rate is proportional to effective nutrient diffusion coefficient as,

$$\mu = \mu_{Max}\left(\frac{D_{eff,S}}{D_{0,S}}\right), \tag{C7}$$

where $D_{0,S}$ (mm^2/s) is nutrient diffusion coefficient in bulk water, and $D_{eff,S}$ (mm^2/s) is effective nutrient diffusion coefficient on the rough surface, which can be expressed as (Moldrup *et al*., 1997),

$$D_{eff,S} = 0.66 D_{0,S}\varepsilon\left(\frac{\varepsilon}{\Phi}\right)^{\frac{8}{3}}, \tag{C8}$$

where ε is volumetric water content, and Φ is total porosity of the rough surface.

The effective bacterial diffusion coefficient on rough surface can be expressed as,

$$D_{eff,B} = D_B / \Gamma\,, \tag{C9}$$

where Γ is the tortuosity of the rough surface, which can be expressed as (Moldrup *et al*., 2001),

$$\Gamma = \sqrt{\frac{\varepsilon D_{0,S}}{D_{eff,S}}}\,, \tag{C10}$$

Substituting Eq. C6 into C9,

$$D_{eff,B} = \frac{\langle l \rangle v}{2[1-\cos(\omega)]\Gamma}\,. \tag{C11}$$

Substituting Eqs. C7 and C11 into Eq. C4 to obtain the rate of bacterial colony expansion on the rough surface,

$$\bar{V}_R = \sqrt{2\mu_{Max} \frac{D_{eff,S} \langle l \rangle \nu}{D_{0,S} \Gamma [1 - \cos(\omega)]}} \,. \tag{C12}$$

Since a cell moving in a bond doesn't change its direction, the mean turning angle between successive trajectories only dependents on the coordination number of the network, N (for a hexa-triangular network, $N = 6$), then, $\cos(\omega) = 0.5$.

Noting that a cell doesn't change its direction in a bond, we let $\langle l \rangle = L$ for simplification. Such assumption will link the predicted colony expansion rate to the bond length. Therefore, estimations of the influence of bond length on the rate of bacterial surface colony expansion are essential. Simulations with different bond length were conducted to estimate the effect of bond length on the rate of colony expansion under matric potential of -0.5 kPa. The simulated rate of surface colony expansion increases nonlinear with the increasing of bond length. Nonlinear regression gives out a power-law relationship between the rate of colony expansion and the bond length as (Fig. S2b),

$$\bar{V}_R \propto L^{0.8} \,. \tag{C13}$$

Therefore, we take Eq. C14 for simplification,

$$\bar{V}_R = \sqrt{2\mu_{Max} \frac{D_{eff,S} \nu L^{1.6}}{D_{0,S} \Gamma [1 - \cos(\omega)]}} \,. \tag{C14}$$

In the presence of chemical attractant, bacterial chemotactic velocity can be expressed as (Rivero et al., 1989),

$$V_C = \frac{1}{2} \chi_0 \nu \frac{N_T}{(K_d + S)^2} \frac{\partial S}{\partial x} \,, \tag{C15}$$

where χ_0 (mm/receptor) is the chemotactic sensitivity, K_d (mM) is the receptor/ligand dissociation equilibrium constant, and N_T is the total number of cell receptors for the ligand. Here, we considering the maximum spatial gradient within a bond as,

$$\left(\frac{\partial S}{\partial x}\right)_{Max} = \frac{S_0}{L} \,, \tag{C16}$$

where S_0 is the initial nutrient concentration. Considering the heterogeneity of the rough surface, the chemotactic velocity can be rewritten as,

$$V_C = \frac{1}{2} \chi_0 \nu \frac{N_T S_0}{(K_d + S)^2 L \Gamma} \,. \tag{C17}$$

By weighting the random motility and chemotactic motility with 1-ζ and ζ, respectively, one get the analytical predicted bacterial colony expansion rate on the partially-saturated rough surface,

$$\bar{V} = (1-\zeta)\sqrt{2\mu_{Max}\frac{D_{eff,S}vL^{1.6}}{D_{0,S}\Gamma[1-\cos(\omega)]}} + \frac{1}{2}\zeta\chi_0 v\frac{N_T S_0}{(K_d+S)^2 L\Gamma}, \quad \text{(C18)}$$

where ζ is a dimensionless factor.

The biological and physical parameters for analytical prediction of surface colony expansion are listed in Table S1.

Table S1. Biological and physical parameters for predictions of surface colony expansion .

Parameters	Values
χ_0, bacterial chemotactic sensitivity (mm/receptor)	5×10^{-5} (Rivero *et a*l., 1989)
S_0, initial nutrient concentration (mM)	0.2
K_d, the receptor/ligand dissociation constant (mM)	0.1 (Rivero *et al*., 1989)
N_T, total number of cell receptors for the ligand	2500 (Clarke and Koshland, 1979)

Chapter 4

Hydration Dynamics Promote Bacterial Coexistence on Rough Surfaces

Gang Wang and Dani Or

ISME J. 2012, doi:10.1038/ismej.2012.115

Identification of mechanisms that promote and maintain the immense microbial diversity found in soil is a central challenge for contemporary microbial ecology. Quantitative tools for systematic integration of complex biophysical and trophic processes at spatial scales relevant for individual cell interactions are essential for making progress. We report a modeling study of competing bacterial populations cohabiting soil surfaces subjected to highly dynamic hydration conditions. The model explicitly tracks growth, motion and life histories of individual bacterial cells on surfaces spanning dynamic aqueous networks that shape heterogeneous nutrient fields. The range of hydration conditions that confer physical advantages for rapidly growing species and support competitive exclusion is surprisingly narrow. The rapid fragmentation of soil aqueous phase under most natural conditions suppresses bacterial growth and cell dispersion thereby balancing conditions experienced by competing populations with diverse physiological traits. Additionally, hydration fluctuations intensify localized interactions that promote coexistence through disproportional effects within densely populated regions during dry periods. Consequently, bacterial population dynamics is affected well beyond responses predicted from equivalent and uniform hydration conditions. New insights on hydration dynamics could be considered in future designs of soil bioremediation activities, affect longevity of dry food products, and advance basic understanding of bacterial diversity dynamics and its role in global biogeochemical cycles.

Key words: bacterial coexistence/diffusion/hydration dynamics/motility

4.1 Introduction

Notwithstanding the vagaries of extreme environmental fluctuations affecting the harsh and nutrient poor environment, soil emerges as the most biologically active compartment of the biosphere hosting unparalleled bacterial diversity at all scales (Stotzky, 1997; Fenchel, 2002; Torsvik and Ovreas, 2002; Fierer and Jackson, 2006; Hibbing *et al.*, 2010). Understanding bacterial diversity patterns and function, and determining biophysical processes that shape and maintain diversity represents a central challenge for contemporary microbial ecology (Fenchel, 2002; Hibbing *et al.*, 2010; Fierer and Lennon, 2011). Curtis and Sloan (2004) have commented that this challenge is "an immense and unexplored frontier in science of astronomical dimensions and of astonishing complexity".

Soil bacteria inhabit complex and heterogeneous pore spaces where water and nutrient resources essential for bacterial life may significantly vary across micrometeric spatial scales or entirely change within a single bacterial generation (Crawford *et al.*, 2005; Mitchell and Kogure, 2006; Or *et al.*, 2007; Banavar and Maritan, 2009). Hydration status and pore-space characteristics are critical factors shaping nutrient fields and bacterial motility, and are thus key to understanding bacterial interactions in soil and other porous media such as dry food products (Barton and Ford, 1997; Dens and Van Impe, 2000; Wilson *et al.*, 2002; Chang and Halverson, 2003; Or *et al.*, 2007; Chen and Jin, 2011). Although motility has long been argued as a key factor for survival in heterogeneous environments and for biodiversity maintenance (Fenchel, 2002; Reichenbach *et al.*, 2007; Vos and Velicer, 2008), it is only recently that crucial processes regulating bacterial motility within liquid films forming on partially hydrated rough surfaces have been quantified (Dechesne *et al.*, 2010; Wang and Or, 2010). These studies have shown that surface roughness and aqueous-phase configuration impose capillary and hydrodynamic constraints limiting bacterial motility, and defined a surprisingly narrow range of hydration conditions where motility could confer ecological advantage on rough surfaces. These are but preliminary steps towards development of a broader understanding of hydration effects on bacterial population interactions, and species coexistence in unsaturated soil.

In addition to inherent spatial heterogeneity of complex soil pore spaces and the resulting configuration of the aqueous phase retained therein, dynamic fluctuations in hydration conditions common in most natural soils affect microhabitats and thus greatly influence growth rates and community compositions. Such fluctuations and associated aqueous phase reconfiguration may create new niches that may shelter less competitive communities, or restrict diffusion in support of thriving communities thereby enhancing bacterial diversity (Torsvik and Ovreas, 2008). Like in other ecological systems, studies have shown that fluctuations in

hydration conditions could lead to significant decay in bacterial biomass, and alter community composition (Fierer and Schimel, 2002; Gordon *et al.*, 2008). Nevertheless, most previous studies have focused on bacterial survival and population recovery with little consideration of the role of hydration dynamics on interactions among competing bacterial populations (Prosser *et al.*, 2007; Torsvik and Ovreas, 2008). Not surprisingly, a mechanistic picture of how soil bacterial diversity is promoted and maintained remains sketchy (Torsvik and Ovreas, 2008; Ponciano *et al.*, 2009). Progress in resolving mechanisms responsible for promoting or limiting bacterial competition and diversity, and the development of predictive tools require quantitative modeling capable of systematic consideration of bio-physico-chemical processes and ecological interactions at appropriate spatial and temporal scales (Prosser *et al.*, 2007; O'Donnell *et al.*, 2007; Banavar and Maritan, 2009).

We study interactions between hydration dynamics and diffusional heterogeneity affecting bacterial growth, motility, competition and species coexistence on partially hydrated rough surfaces. We employed a hybrid model that couples individual-based description of cell growth, motion and interactions within a nutrient field described by a (continuum-based) reaction-diffusion model (Kreft *et al.*, 1998; Dechesne *et al.*, 2010). The model resolves spatial and temporal nutrient diffusion fields subjected to prescribed boundary conditions, heterogeneity and local nutrient interception by individual cells. Additionally, the model explicitly tracks motions and life histories of all individual cells within a population considering local hydrodynamic and capillary constraints to motility (due to aqueous phase configuration).

4.2 Materials and Methods

4.2.1 Modeling heterogeneous rough surface and water configuration

Natural surfaces are represented as two dimensional (2D) networks of roughness elements with different characteristics arranged on a lattice (Dechesne *et al.*, 2010) in which bacterial populations grow, interact and compete. The roughness network captures salient aspects of aqueous phase retention and spatial organization of real surfaces while providing a tractable representation of physical processes such as water films, hydraulic connectivity, and effective diffusion of real porous media (Blunt, 2001; Dechesne *et al.*, 2010). The amount of aqueous phase retained within roughness element was calculated as a function of ambient matric potential value (or relative humidity in the air) and surface roughness geometry (Or *et al.*, 2007). The connectivity of aqueous networks and the effective sizes of connected aqueous elements capable of supporting bacterial motility were deduced from roughness element geometry and invoking universal percolation theory arguments for network fragmentation (Berkowitz and

Ewing, 1998). An example of the resulting connected clusters of water-filled channels are depicted in Figure 1a and 1b for a roughness network under different matric potential values, highlighting increased fragmentation of aquatic habitats as the surface becomes drier.

4.2 2 Nutrient diffusion and bacterial motility on partially hydrated rough surfaces

The effective diffusion coefficient D_S for nutrients varies with hydration conditions (higher for wetter conditions) and thus is a key parameter for determining bacterial growth rate and population carrying capacity of unsaturated surfaces. For simplicity, we expressed the relative diffusion coefficient as a function of hydration state (water content or matric potential) according to the classical Millington and Quirk (MQ) model that was originally developed for soil (Moldrup *et al.*, 2003),

$$D_{eff} = D_0 \frac{\theta^2}{\Phi^{2/3}}, \tag{1}$$

where D_0 is nutrient diffusion coefficient in bulk water, Φ is effective "porosity" of rough surface (relative to smooth surface), that is calculated according to,

$$\Phi = \frac{2\sqrt{3}}{3\langle H \rangle l} \int_{\Omega_\alpha} \int_{\Omega_H} H^2 \tan(\frac{\alpha}{2}) d\alpha dH, \tag{2}$$

where $\langle H \rangle$ is the expected value of channel/bond height (considering the effective height of the domain equals to the value of 3 times of the mean height of channels/bonds), l is the length of a roughness element (channel/bond), α and H are spanning angle and height of a roughness element, with the intervals of Ω_α and Ω_H, respectively (Dechesne *et al.*, 2010), and θ is volumetric water content which can be estimated as a function of ambient hydration status (matric potential, ψ) and surface roughness characteristics according to,

$$\theta = \sum_i \theta_i(\psi) / (3\langle H \rangle A), \tag{3}$$

where $\theta_i(\psi)$ is volumetric water content of a certain roughness element at matric potential value ψ (Dechesne *et al.*, 2010), A is the surface area (summation is over all elements in the network). Monte Carlo simulations of diffusive fluxes across the unsaturated roughness network yield effective nutrient diffusion coefficient similar to those obtained from macroscopic MQ model (Moldrup *et al.*, 2003), as depicted in Figure 1c. For high matric potential values (wet conditions) large nutrient diffusive fluxes are supported across the roughness network, with effective nutrient diffusion coefficient of up to 0.5 mm^2 h^{-1} under -0.0001 kPa (wettest conditions considered) similar to values in the range of 0.4 to 0.8 mm^2 h^{-1} for soils at near saturation found by Darrah (1991) and Moldrup *et al.* (2003). The drying of a rough surface (lower matric

potential) is associated with a significant decline in effective nutrient diffusion coefficient within a few kPa drop in matric potential value.

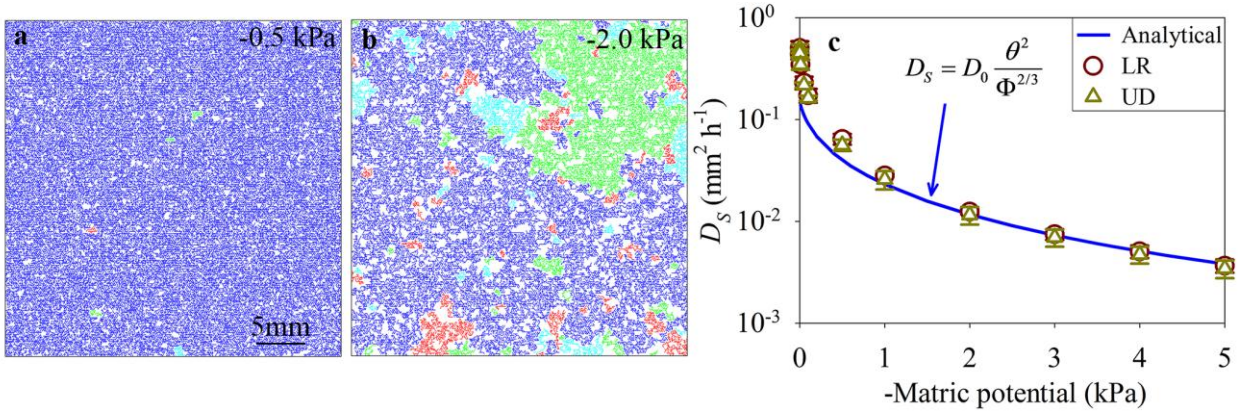

Fig. 1. Aqueous configurations and nutrient diffusive flux on roughness network. Aqueous phase configuration on a model roughness network under (**a**) wet and (**b**) dry conditions; and (**c**) simulated (mean ± s.d., n=5) and analytical effective nutrient diffusion coefficients as a function of matric potential value. UD (Up to Down) and LR (Left to Right) represent simulated diffusion coefficients with flux from up to down and from left to right boundaries of the simulation domain, respectively. Colors in (a) and (b) mark different water-filled bond clusters (aqueous fragmentation) available for cell motility (with effective water film thickness larger than a typical cell size of 1 μm). Clusters containing bond numbers less than 10 are not plotted.

Flagellated motility is the primary mode of self-propulsion of bacterial cells in planktonian form within aqueous films (Darnton and Berg, 2008; Dechesne *et al.*, 2010). On partially hydrated rough surfaces, flagellated motion is gradually restricted due to cell-wall viscous drag and capillary pinning forces experienced by cells within thin aqueous films. These effects are succinctly lumped into relationship between cell size and effective water film thickness – $d(\psi)$ (which can be calculated as a function of matric potential and geometrical features of a roughness element according to $d(\psi) = R(\psi)\frac{1-\sin(\alpha/2)}{1+\sin(\alpha/2)}$, with $R(\psi)$ of the radius of the liquid interfacial meniscus formed in a roughness element, see Long and Or, 2005 for more detail). We explicitly consider capillary and hydrodynamic limitations to cell motility (expressed as cell velocity, V) as a function of matric potential in the following expression: $V(\psi) = V_0 \frac{F_M - F_C(d(\psi)) - F_\lambda(d(\psi))}{F_M}$ ($V(\psi) = 0$, while $F_M - F_C(d(\psi)) - F_\lambda(d(\psi)) < 0$), with V_0 of mean cell velocity in bulk water, and F_M, F_C and F_λ are the viscous drag force opposing motion in bulk water (equal to the maximum flagellar propulsive force), the viscous force associated with cell-wall hydrodynamic interactions, and the capillary pinning force, respectively (Dechesne *et al.*, 2010). Additionally, the receding air-water interfaces results in thinning of film thickness effectively disconnecting bacterial aqueous habitats previously

hydraulically connected under wet conditions and further limit bacterial motion (Or *et al.*, 2007; Dechesne *et al.*, 2010; Wang and Or, 2010). Therefore, cell velocity within each roughness element is determined by matric potential value and geometrical features of a roughness element. Nutrient diffusion, bacterial growth and nutrient consumption within a channel/bond are solved based on the well-established reaction-diffusion model (Kreft *et al.*, 1998; Dechesne *et al.*, 2010).

4.2.3 Simulations of bacterial growth and competition on dynamically-hydrated rough surfaces

The hybrid modeling framework discussed above supports highly resolved description of spatial and temporal nutrient diffusion fields shaped by surface and aqueous phase heterogeneity and by local nutrient interception by individual cells. To provide a baseline for the joint effects of physico-chemical heterogeneity at microscale with variations in hydration status on bacterial motility, growth, and population interactions on rough surfaces, we conducted Monte Carlo simulations for various (static) hydration conditions expressed as matric potential values of -0.5, -0.9, -2.0 and -3.5 kPa (10 replicates for each matric potential value using newly generated roughness network for each replicate). The baseline static simulation results were compared with simple dynamic hydration cycles (three simulations for each hydration sequence), starting with water potential at -2.0 kPa that was subsequently varied between -2.0 and -0.5 kPa every 12 and 48 h, respectively.

Monte Carlo simulations were performed on replicate roughness networks representing rough surface with physical size of 34.4 × 34.4 mm (with 200 × 173 sites on hexagonal lattice and bond length of 0.2 mm), with the parameters of network as described from Wang and Or (2010). The hybrid individual-based model simulated growth and interactions among 60 cells that were inoculated at 3 sites (see Figure 2a) each consisting of 20 cells (10 of each competing species). The nutrient concentration across the entire simulation domain was initially constant, and subsequently we maintained constant concentrations only at the boundaries of the network throughout the simulation period. Nutrient distribution and diffusion are supported by the variable aqueous network resulted from various hydration states (Long and Or, 2005). The physiological parameters used for modeling growth, interactions and nutrient consumption of two competing bacterial species are summarized in Table 1 (Kreft *et al.*, 1998). Note the specific growth rate for the superior species (Sp1) is higher than for the inferior species (Sp2) reflecting the sole physiological advantage of Sp1 in nutrient interception and growth rate.

Table 1. Parameters describing bacterial growth and metabolism.

Parameters	Units	Values	
		Sp1	Sp2
μ_{max}: maximum specific growth rate	hr^{-1}	1.2	0.4
K_S: half-saturation constant	fg fl^{-1}[a]	1.2×10^{-6}	0.4×10^{-6}
Y_{max}: apparent yield at μ_{max}	fg mass (fg substrate)$^{-1}$	0.44	0.44
m: apparent maintenance rate	fg substrate (fg mass)$^{-1}$ hr^{-1}	0.18	
$\bar{V}_B$: median cell volume	fl	0.4	
$V_{B,d}$: cell volume at division	fl	$2\bar{V}_B$ /1.433	
$V_{B,min}$: minimal cell volume of an active bacterium	fl	$V_{B,d}$ /5	
ρ: cell density (dry mass)	fg fl^{-1}	290	
V: maximum cell velocity	µm s^{-1}	1	
C: substrate concentration	fg fl^{-1}	1×10^{-3}	

[a]: 1 fg = 1×10^{-15} g; 1 fl = 1×10^{-15} l.

The fitness of Sp2 relative to Sp1 was computed according to (Elena and Lenski, 2003),

$$RF = (\frac{W_2}{W_{02}}) / (\frac{W_1}{W_{01}}), \quad (2)$$

where W_{02} and W_2 are initial and final populations (simulated up to nutrient carrying capacity of a habitat) of Sp2 and W_{01} and W_1 are those of Sp1.

4.3 Results

4.3.1 BMicrobacterial growth and competition on rough surfaces under static hydration conditions

We first describe simulation results for surfaces under static hydration conditions as reference for simulations considering dynamic hydration status for similar mean aqueous phase content. Figure 2 depicts patterns and population growth curves of two competing bacterial species on rough surfaces under different (but static) hydration conditions. As expected, under wet conditions (matric potential value of -0.5 kPa), the total bacterial population expanded rapidly with total population size exceeding 10^5 cells within 70 hours after initial inoculation (Figure 2a). A small reduction in matric -2.0 kPa (Figures 2b and 2d); and finally, no significant bacterial growth was possible for -3.5 kPa potential value (more negative, thus drier surfaces) from -0.5 to -0.9 kPa resulted in a 25% decrease in population size; only a few hundred cells survived with subsequent reduction to for similar time frames. The highest population density was found at the

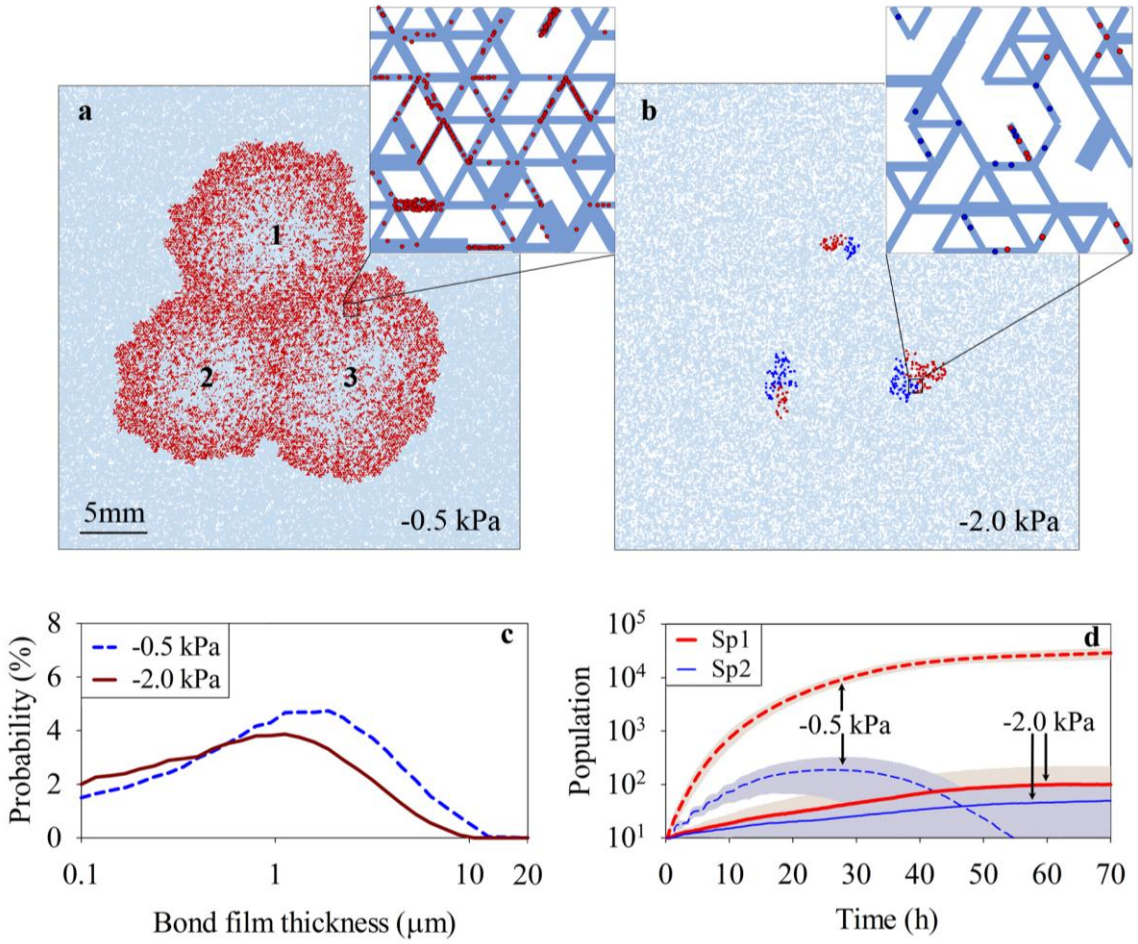

Fig. 2. Bacterial growth patterns and population dynamics on rough surfaces under different static hydration conditions. Simulated bacterial growth patterns under (a) wet (-0.5 kPa) and (b) dry (-2.0 kPa) 70 h after inoculations; (c) water configuration (expressed as the probability density of effective bond film thickness, with film thickness smaller than 0.1 μm not shown, see Figure 5c); and (d) bacterial population growth (mean ± s.d., n=30) under -0.5 kPa (dash lines) and -2.0 kPa (solid lines), respectively, Red and blue spots in (a) and (b) represent individual cells of Sp1 and Sp2. Numbers in (a) mark inoculation positions.

front of an expanding wave reflecting nutrient conditions and interception at the expanding front as seen in Figure 2a (Tsyganov and Ivanitsky, 2006; Saragosti *et al.*, 2011). In general, the thinning of effective aqueous film thickness (Figure 2c) and fragmentation of the aqueous phase with decreasing matric potential (Figure 1b) limit nutrient diffusive fluexes (Figure 1c) and suppress cell motion and dispersion and thus limit bacterial population growth. Simulations for static hydration conditions are in agreement with experimental observations (Drenovsky *et al.*, 2004; Dechesne *et al.*, 2008; Ponciano *et al.*, 2009; Dechesne *et al.*, 2010) and with recently published modeling results considering a single bacterial species on unsaturated rough surfaces (Wang and Or, 2010). Additionally, wet surface conditions (-0.5 kPa) supported rapid growth by the superior species (Sp1) that exhibited an exponential growth period immediately after inoculation followed by a gradual decrease in growth rate towards a stationary phase throughout

the rest of the simulation period (Figure 2d). In contrast, growth rates of the inferior species (Sp2) dropped rapidly attaining negative values 30 h after inoculation, leading to eventual extinction of Sp2 (Figures 2a and 2d). Drier condition (-2.0 kPa) suppressed growth rates for both species leading to similar population sizes 70 h after inoculation with similar spatial growth patterns indicative of coexistence (Figures 2b and 2d). Further reduction in matric potential value did not affect population coexistence albeit no significant growth of both species was simulated. Consistent with equivalent population growth sizes, comparable colony expansion rates of both species were simulated on drier rough surfaces, unlike the continuous decrease in colony expansion ratio of Sp2 relative Sp1 for simulations under wet surfaces with matric potential value of -0.5 kPa (Figure 3).

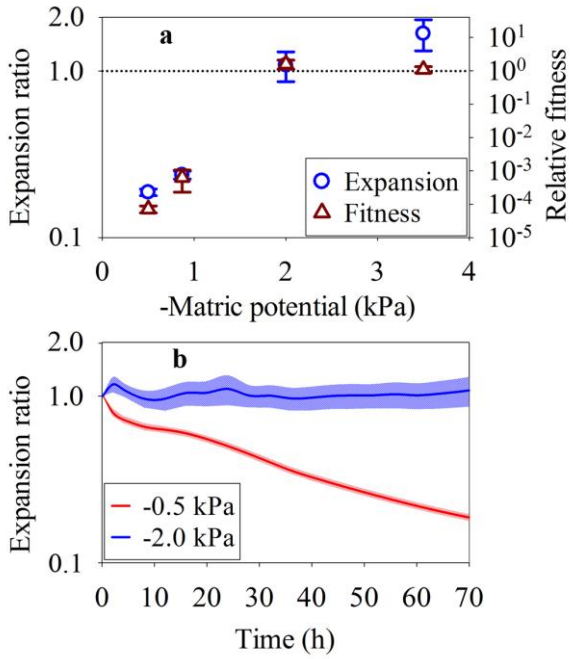

Fig. 3. Bacterial colony expansion ratio and relative fitness under different static hydration conditions. (a) Simulated bacterial colony expansion ratio of the inferior species (Sp2) relative to the superior species (Sp1) and relative fitness or Sp2 relative to Sp1 under various matric potential values (mean ± s.e.m., n=30); and (b) dynamics of colony expansion ratio of Sp2 relative to Sp1 as a function of elapsed time under wet and dry hydration conditions (mean ± s.e.m., n=30, shaded areas represent 1 s.e.m.).

4.3.2 Effects of hydration dynamics on microbial growth and species coexistence

Our primary focus was on quantifying the role of drying and wetting cycles on bacterial population growth relative to behavior under equivalent mean (static) hydration conditions. Figure 4 depicts snapshots of simulated bacterial growth patterns and population dynamics under static and dynamic hydration cycles (initial water potential was -2.0 kPa and was alternated between -2.0 and -0.5 kPa every 12 [short hydration cycle] and 48 h [long hydration cycle], respectively). Results show that the time required for similar colony sizes under short-

and long hydration-cycles was 144 and 192h, respectively, as compared with 50h for (equivalent) static hydration conditions. Hydration dynamics resulted in disproportional reduction in bacterial

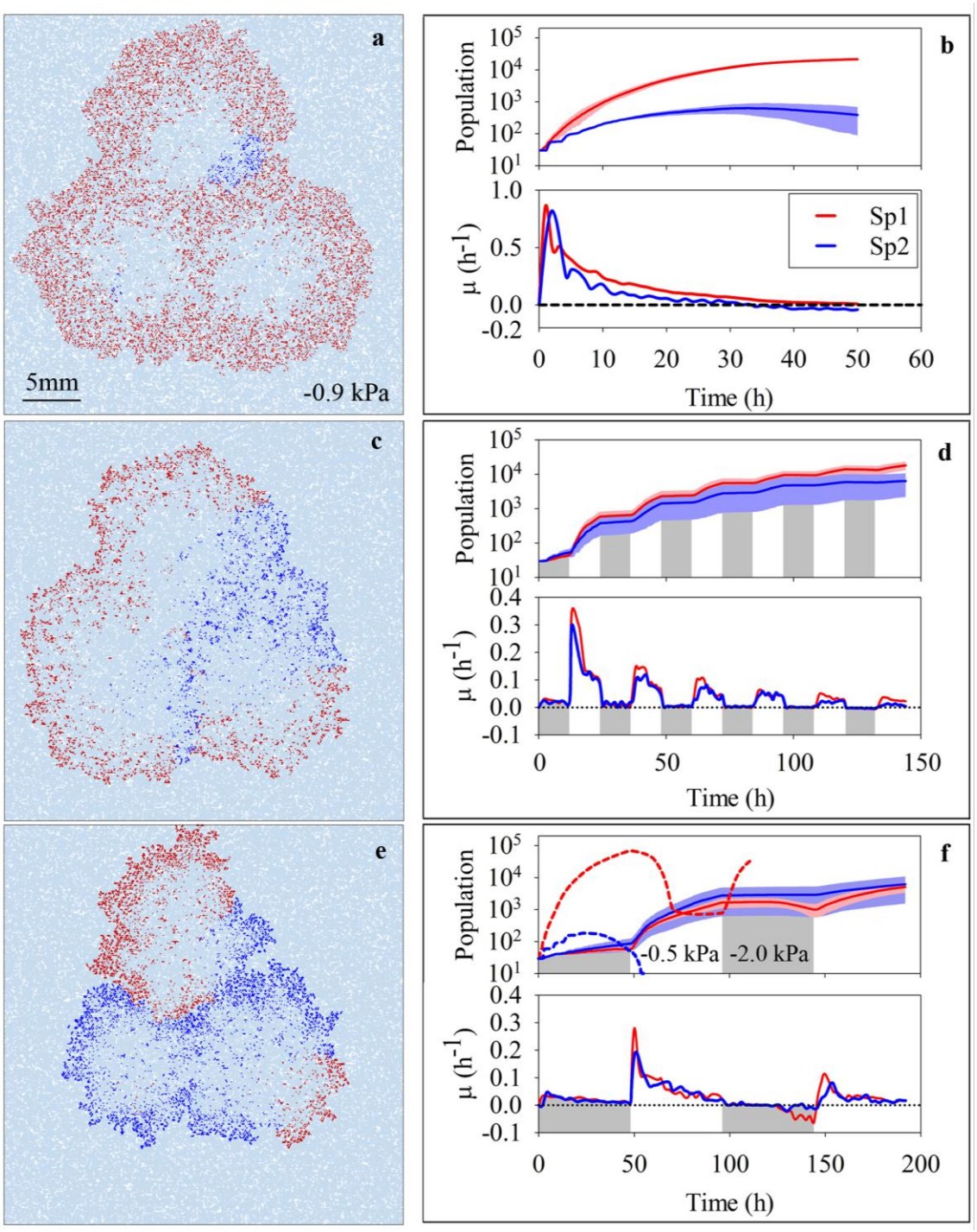

Fig. 4. Bacterial growth patterns and population dynamics under different hydration cycles. (**a**) Simulated bacterial growth patterns and (**b**) population growth and specific growth rates under median hydration conditions; and (**c**) and (**e**) growth patterns and (**d**) and (**f**) population growth and specific growth rates under short- and long-term dynamic hydration conditions, respectively (dashed curve in (f) illustrates population growth dynamics under hydration cycles started with wet event). Red and blue spots (lines) represent a Sp1 and Sp2, respectively. Shaded areas in (b), (d) and (f) represent one standard deviation of 3 replicates. Shaded columns in (d) and (f) mark dry episodes of matric potential value -2.0 kPa.

population growth during dry periods as evidenced by low specific growth rates, which were followed by rapid recovery in population size upon rewetting for all dynamic hydration scenarios (Figures 4d and 4f), consistent with experimental observations (Pesaro *et al.*, 2004; Iovieno and Bååth, 2008; Bapiri *et al.*, 2010). At the end of wet periods (96 h after inoculation for long hydration-cycle) nearly 90% of active cells inhabited domains with relatively large aqueous clusters supported by large water-filled channels. In contrast, most of the surviving bacterial populations were confined to relatively small (and deep) water-filled channels at the end of dry periods [144 h after inoculation for long hydration-cycle] (Figure 5). Not surprising, the superior species (Sp1) experienced a disproportionally larger reduction in population size due to hydration fluctuations than the reduction in total population size (Figures 5a and 5b). Simulations showed a significant increase in mean relative fitness (*RF*) of the inferior species (Sp2) relative to the superior species (Sp1) with *RF* values of 0.35 and 1.20 for short- and long dry-intervals, respectively, as compared with *RF*= 0.02 for static median hydration conditions. These changes reflect a transition from dominance by a superior species to coexistence of the two competing species, a change attributed solely to hydration dynamics (within the same roughness or pore spaces, Figure 4), in agreement with limited experimental observations (McLean and Huhta, 2000; Pesaro *et al.*, 2004). Remarkably, a change in the sequence of hydration dynamics (starting with a wet period) significantly altered the bacterial competition picture, as shown in Figure 4f, resulting in competitive exclusion of the inferior populations similar to that for static wet scenarios (Figures 2a and 2d).

4.4 Discussion

The ecological role of hydration dynamics on bacterial growth, community structure, and potential influences on species coexistence have been studied in various systems (Chesson, 2000; Ben-Jacob, 2003; Hibbing *et al.*, 2010). The new aspect of this study is in providing some of the first and direct insights into how hydration conditions and associated spatiotemporal variations affect bacterial coexistence and dynamics of community structure. The ease by which aquatic niches become fragmented and disconnected (under dry conditions) accentuates localized growth patterns with temporal sheltering for less competitive species conferring resistance against encroachment by competitors.

Suppression of population growth under dry conditions was attributed primarily to changes in aqueous phase configuration that affect both motion and diffusion pathways thereby limiting nutrient fluxes and interception for the competing populations and induce similar (diffusion limited) specific growth rates (Treves *et al.*, 2003; Zhou *et al.*, 2004; Iovieno and Bååth, 2008).

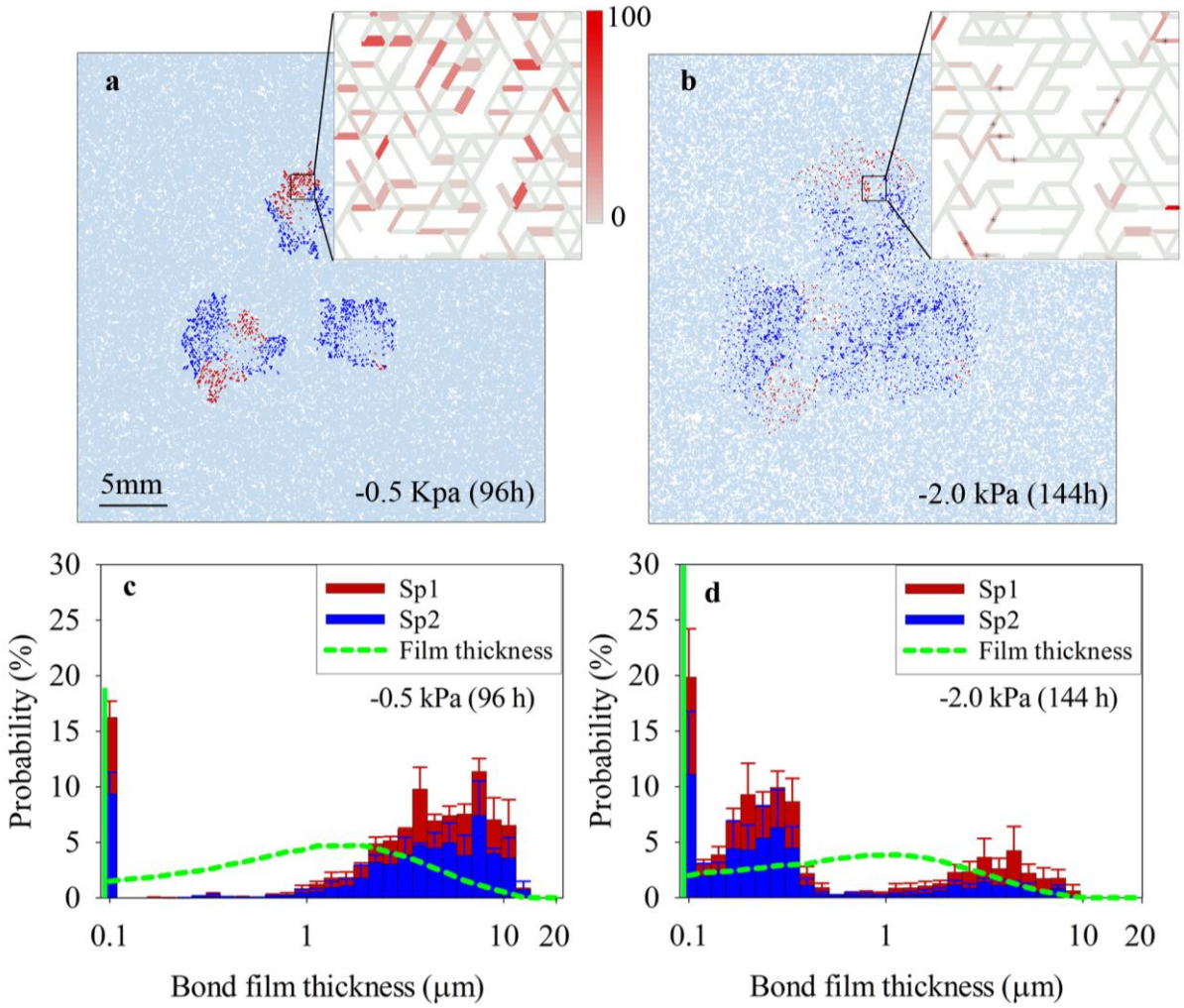

Fig. 5. Bacterial growth patterns and population distributions under different episode of long-hydration cycles. Simulated bacterial growth patterns at (a) 96 h (wet) and (b) 144 h (dry) after inoculations, with zoom-in images showing population densities [star symbols in enlarged inset of (b) mark channels/bonds with aqueous film thickness smaller than cell size]; and population spatial distributions (mean ± s.e.m., n=3, marked by the heights of red and blue columns for Sp1 and Sp2, respectively) and aqueous film thickness distributions under (c) wet and (d) dry episodes, respectively. Red and blue spots in (a) and (b) represent individual cells of Sp1 and Sp2. Solid green lines in (c) and (d) mark film thickness smaller than 0.1 μm.

Such mechanism of coexistence promotion by limited diffusive fluxes and aqueous phase fragmentation is consistent with limited available observations (Zhou *et al.*, 2002; Treves *et al.*, 2003; Ponciano *et al.*, 2009). For example, Zhou *et al.* (2002) found 2 to 3 orders of magnitude higher microbial diversity in unsaturated surface soils than in saturated soils. Additionally, restricted bacterial motility within thin aqueous films (dry conditions) limited dispersion distances and reinforced the critical role of localized diffusion pathways on chances of survival (Maennik *et al.*, 2009; Dechesne *et al.*, 2010; Wang and Or, 2010). The experimental results of Dechesne *et al.* (2008) reveal that for a small drop in matric potential of rough ceramic surfaces (from -0.5 to -3.6 kPa) colony expansion rates for motile bacteria dropped by 60 times! These

factors contributed to formation of nearly stationary growth patterns and formation of nutrient depleted regions that could not be traversed by competitive species (Long and Or, 2005) hence emergence of balanced population competition and gradually giving rise to coexistence. Under wet conditions (-0.5 kPa), the multitude of hydraulic connections among bacterial habitats maintained pathways for motile bacteria as well as supported high diffusion links for constant nutrient supply to expanding population fronts (Treves *et al.*, 2003; Zhou *et al.*, 2004). These relatively saturated and nutrient rich simulated scenarios provided Sp1 with a competitive advantage (Treves *et al.*, 2003; Hibbing *et al.*, 2010) that enabled it to expand faster and gradually enclose Sp2's enclaves thereby intercepting larger fraction of nutrients and tipping competition balance, resulting in competitive exclusion of Sp2. These results are consistent with the classical coexistence theories of niche stabilization and fitness equivalence (Adler *et al.*, 2007), whereby favorable growth environments (high nutrient fluxes, well connected and large aquatic habitats supporting significant cell motion, which are characteristics of wet surfaces) support expression of competitive advantage and lead to exclusion of inferior species. These often speculated by rarely quantified mechanisms of physico-chemical constraints restrict motility and nutrient fluxes within the fragmented aqueous phase giving rise to fitness equivalence among competing bacterial species (gradual loss of niche difference), and coexistence (Zhou *et al.*, 2002; Treves *et al.*, 2003; Dechesne *et al.*, 2008).

The disproportional sensitivity of densely populated regions to hydration dynamics (drying and wetting) acts to reset population imbalances. These simulation results are in agreement with experimental observations in which drying-rewetting conditions considerably increase bacterial diversity as compared with communities in unstressed and initially wet and fertile soils (Fierer and Schimel, 2002; Fierer *et al.*, 2003). While physiological traits allowed superior species to establish abundant presence in relatively larger and connected aqueous regions/pores (capitalizing on nutrient supply capacity) within wetting episodes; at the onset of dry periods, nutrient demand required in regions inhabited by large population density cannot be met by the new aqueous-based diffusion field, resulting in disproportionally large population decay [larger than would be expected for an equivalent reduction in mean flux] (Pesaro *et al.*, 2004; Iovieno and Bååth, 2008; Bapiri *et al.*, 2010). The situation for sparsely distributed "rural" populations inhabiting harsher domains is different, and simulation results show a large fraction of the population in these regions survived throughout dry episodes. Moreover, considering motility limitations induced by thinning films (Maennik *et al.*, 2009; Dechesne *et al.*, 2010; Wang and Or, 2010), these sparse and isolated populations are likely to exist in a stationary and sessile form (absent dispersion, expansion or mixing). Consequently, the unsymmetrical decline in

population size during drying episodes reinstates a balance in population sizes of the competing species and contributes to establishment of nearly stationary coexistence patterns by resetting the ecological clock.

Additionally, spatial preferences for dry and wet periods exhibited by bacterial population occupancy are reflections of the complex diffusion field and local nutrient carrying capacity and formation of resilient fraction of the population (less sensitive to hydration perturbations). These factors provide mechanistic explanation for experimental observations that soil drying-rewetting treatments may alter bacterial population dynamics and community structures (Fierer and Schimel, 2002; Fierer *et al.*, 2003; Iovieno and Bååth, 2008). Hence, dynamic hydration conditions temporally increase niche complexity in which location (or diffusion pathway) resilience may affect bacterial population response and even compensate for physiological traits and thus promote coexistence.

For the rare episodes of prolonged wetting in natural soils, the rapidly expanding population of competitive species may ultimately sweep through the domain including previously sheltered habitats and lead to competitive exclusion of inferior species as predicted by classical competition exclusion principles (Hutchinson, 1961). In practice, the ephemeral and very limited time window when soils are subjected to wet conditions (a few hours per year) reinforces the generality of the physico-chemical constraints imposed on nutrient diffusive flux heterogeneity and on motility. Thus sessile life form is expected to dominate soil bacterial life accentuating the ecological consequences of dynamic hydration conditions on bacterial population interactions and community structure across most soil types and climatic regions. The restricted duration of wet events in natural soil also imply severe constraints on distances traversed by motile bacteria into neighboring habitats, which are expected to be limited to a few pores even under favorable conditions (Soby and Bergman, 1983; Dechesne *et al.*, 2010), preventing successful invasions and thus competitive exclusion of weaker species. Although other agents such as roots and hypha, or concentrated flows in cracks and macropores may contribute to bacterial dispersion over large distances even in relatively dry soils, these would have limited influence along hot spots but are unlikely to alter structured residence of competing populations (Kohlmeier *et al.*, 2005).

Time averaged nutrient fluxes may be useful for estimations of total population sizes and carrying capacity of soil volumes (Drenovsky *et al.*, 2004; Long and Or, 2007, 2009; Dechesne *et al.*, 2008; Chesson, 2011), however, such averaging would not capture in local interactions discussed above that ultimately shape population dynamics and diversity. For example, inferences based on the average fitness of a species would predict competitive exclusion of

weaker species within a bacterial habitat (Carrero-Colón *et al.*, 2006; Chesson, 2011). The results revealed that highly localized, temporally variable and individual-level bacterial interactions, rather than median global values for a species, determine the dynamics and patterns of interacting bacterial populations in systems mimicking natural soils, consistent with organization principles for macroscale biological systems (Camazine *et al.*, 2001; Karsenti, 2008). Additionally, results show distinct effects of hydration sequences on bacterial coexistence indicative of sensitivity of responses of bacterial populations to initial conditions, which may cast some doubts on inferences based on steady state traditional population models, e.g., Lotka-Volterra model (Wangersky, 1978) and niche theories (Adler *et al.*, 2007) to describe complex soil bacterial dynamics.

Acknowledgements

We acknowledge the financial support of the Swiss National Science Foundation (200021-113442 and 200020-132154-1).

References

Adler PB, HilleRisLambers J, Levine JM. (2007). A niche for neutrality. *Ecol Lett* **10:** 95-104.

Banavar JR, Maritan A. (2009). Towards a theory of biodiversity. *Nature* **460**: 334-335.

Bapiri A, Bååth E, Rousk J. (2010). Drying-rewetting cycles affect fungal and bacterial growth differently in an arable soil. *Microb Ecol* **60:** 419–428.

Barton JW, Ford RM. (1997). Mathematical model for characterization of bacterial migration through sand cores. *Biotechnol Bioeng* **53:** 487-496.

Berkowitz B, Ewing RP. (1998). Percolation theory and network modeling applications in soil physics. *Surv Geophys* **19:** 23-72.

Ben-Jacob E. (2003). Bacterial self-organization: co-enhancement of complexification and adaptability in a dynamic environment. *Phil Trans R Soc A* **361:** 1283-1312.

Blunt MJ. (2001). Flow in porous media: pore-network models and multiphase flow. *Curr Opin Colloid Interface Sci* **6:** 197-207.

Camazine S, Deneubourg J, Franks NR, Sneyd J, Theraulaz G, Bonabeau E. (2001). *Self-organization in biological systems*, pp. 29–46, Princeton University Press: Princeton, NJ.

Carrero-Colón M, Nakatsu CH, Konopka A. (2006). Microbial community dynamics in nutrient-pulsed chemostats. *FEMS Microbiol Ecol* **57:** 1–8.

Chang WS, Halverson LJ. (2003). Reduced water availability influences the dynamics, development, and ultrastructural properties of *Pseudomonas putida* biofilms. *J Bacteriol* **185:** 6199-6204.

Chen J, Jin Y. (2011). Motility of Pseudomonas aeruginosa in saturated granular media as affected by chemoattractant. *J Contam Hydrol* **126:** 113-120.

Chesson P. (2000). Mechanisms of maintenance of species diversity. *Annu Rev Ecol Evol Syst* **31:** 343-366.

Chesson P. (2011). Ecological niches and diversity maintenance. In: Pavlinov IY (ed). *Research in biodiversity-models and applications*. Rijeka: InTech, pp 43-60.

Crawford JW, Harris JA, Ritz K, Young IM. (2005). Towards an evolutionary ecology of life in soil. *Trends Ecol Evol* **20:** 81-87.

Curtis TP, Sloan WT. (2004). Prokaryotic diversity and its limits: microbial community structure in nature and implications for microbial ecology. *Curr Opin Microbiol* **7:** 221-226.

Darnton NC, Berg HC. (2008). Bacterial flagella are firmly anchored. *J Bacteriol* **190:** 8223-8224.

Darrah PR. (1991). Measuring the diffusion coefficient of rhizosphere exudates in soil. I. The diffusion of non-sorbing compounds. *J Soil Sci* **42:** 413-420.

Dechesne A, Or D, Gulez G, Smets BF. (2008). The porous surface model, a novel experimental system for online quantitative observation of microbial processes under unsaturated conditions. *Appl Environ Microbiol* **74:** 5195-5200.

Dechesne A, Wang G, Güleza G, Or D, Smets BF. (2010). Hydration-controlled bacterial motility and dispersal on surfaces. *Proc Natl Acad Sci USA* **107:** 14369-14372.

Dens EJ, Van Impe JF. (2000). On the importance of taking space into account when modeling microbial competition in structured food products. *Math Comput Simulat* **53:** 443-338.

Drenovsky RE, Vo D, Graham KJ, Scow KM. (2004). Soil water content and organic carbon availability are major determinants of soil microbial community composition. *Microb Ecol* **48:** 424–430.

Elena SF, Lenski RE. (2003). Evolution experiments with microorganisms: the dynamics and genetic bases of adaptation. *Nat Rev Genet* **4:** 457-469.

Fenchel T. (2002). Microbial behavior in a heterogeneous world. *Science* **296:** 1068-1071.

Fierer N, Jackson R. (2006). The diversity and biogeography of soil bacterial communities. *Proc Natl Acad Sci USA* **103:** 626-631.

Fierer N, Lennon JT. (2011). The generation and maintenance of diversity in microbial communities. *Am J Bot* **98:** 439-448.

Fierer N, Schimel JP. (2002). Effects of drying-rewetting frequency on soil carbon and nitrogen transformations. *Soil Biol Biochem* **34:** 777-787.

Fierer N, Schimel JP, Holden PA. (2003). Influence of drying-rewetting frequency on soil bacterial community structure. *Microb Ecol* **45:** 63-71.

Gordon H, Haygarth PM, Bardgett RD. (2008). Drying and rewetting effects on soil microbial community composition and nutrient leaching. *Soil Biol Biochem* **40:** 302-311.

Hibbing ME, Fuqua C, Parsek MR, Peterson SB. (2010). Bacterial competition: surviving and thriving in the microbial jungle. *Nature Rev Microbiol* **8:** 15-25.

Hutchinson GE. (1961). The paradox of the plankton. *Am Nat* **95:** 137–145.

Iovieno P, Bååth E. (2008). Effect of drying and rewetting on bacterial growth rates in soil. *FEMS Microbiol Ecol* **65:** 400-407.

Karsenti E. (2008). Self-organization in cell biology: a brief history. *Nat Rev Mol Cell Biol* **9:** 255–262.

Kreft JU, Booth G, Wimpenny JWT. (1998). BacSim, a simulator for individual-based modelling of bacterial colony growth. *Microbiology-UK* **144:** 3275-3287.

Kohlmeier S, Smits THM, Ford RM, Keel C, Harms H, Wick LY. (2005). Taking the fungal highway: mobilization of pollutant-degrading bacteria by fungi. *Environ Sci Technol* **39:** 4640-4646.

Long T, Or D. (2005). Aquatic habitats and diffusion constraints affecting microbial coexistence in unsaturated porous media. *Water Resour Res* **41:** W08408.

Long T, Or D. (2007). Microbial growth on partially saturated rough surfaces: simulations in idealized roughness networks. *Water Resour Res* **43:** W02409.

Long T, Or D. (2009). Dynamics of microbial growth and coexistence on variably saturated rough surfaces. *Microb Ecol* **58:** 262-275.

Maennik J, Driessen R, Galajda P, Keymer JE, Dekker C. (2009). Bacterial growth and motility in sub-micron constrictions. *Proc Natl Acad Sci USA* **106:** 14861-14866.

McLean MA, Huhta V. (2000). Temporal and spatial fluctuation in moisture affect humus microfungal community structure in microcosms. *Biol Fertil Soils* **32:** 114–119.

Mitchell JG, Kogure K. (2006). Bacterial motility: links to the environment and a driving force for microbial physics. *FEMS Microbiol Ecol* **55:** 3-16.

Moldrup P, Olesen T, Komatsu T, Yoshikawa S, Schjønning P, Rolston DE. (2003). Modeling diffusion and reaction in soils: X. A unifying model for solute and gas diffusivity in unsaturated soil. *Soil Sci* **168:** 321-337.

O'Donnell AG, Young IM, Rushton SP, Shirley MD, Crawford JD. (2007). Visualization, modelling and prediction in soil microbiology. *Nat Rev Microbiol* **5**: 689-699.

Or D, Smets BF, Wraith JM, Dechesne A, Friedman SP. (2007). Physical constraints affecting bacterial habitats and activity in unsaturated porous media - a review. *Adv Water Resour* **30:** 1505-1527.

Pesaro M, Nicollier G, Zeyer J, Widmer F. (2004). Impact of soil drying-rewetting stress on microbial communities and activities and on degradation of two crop protection products. *Appl Environ Microbiol* **70:** 2577–2587.

Ponciano JM, La HJ, Joyce P, Forney LJ. (2009). Evolution of diversity in spatially structured *Escherichia coli* populations. *Appl Environ Microbiol* **75:** 6047-6054.

Prosser JI, Bohannan BJM, Curtis TP, Ellis RJ, Firestone MK, Freckleton RP, *et al.* (2007). The role of ecological theory in microbial ecology. *Nature* **5:** 384-392.

Reichenbach T, Mobilia M, Frey E. (2007). Mobility promotes and jeopardizes biodiversity in rock-paper-scissors games. *Nature* **448:** 1046-1049.

Saragosti J, Calvez V, Bournaveas N, Perthame B, Buguin A, Silberzan P. (2011). Directional persistence of chemotactic bacteria in a traveling concentration wave. *Proc Natl Acad Sci USA* **108:** 16235-16240.

Soby S, Bergman K. (1983). Motility and chemotaxis of *Rhizobium meliloti* in soil. *Appl Environ Microbiol* **46:** 995-998.

Stotzky G. (1997). Soil as an environment for microbial life. In: van Elsas JD, Trevors JT, Wellington EMH (eds). *Modern Soil Microbiology.* Marcel: New York, pp 1-20.

Treves DS, Xia BC, Zhou JZ, Tie JM. (2003). A two-species test of the hypothesis that spatial isolation influences microbial diversity in soil. *Microb Ecol* **45:** 20-28.

Torsvik V, Ovreas L. (2002). Microbial diversity and function in soil: from genes to ecosystems. *Curr Opin Microbiol* **5:** 240-245.

Torsvik V, Ovreas L. (2008). Microbial diversity, life strategies, and adaptation to life in extreme soils. In: Dion P, Nautiyal CS (eds). *Microbiology of Extreme Soils*. Springer: Berlin Heidelberg, pp 15-43.

Tsyganov MA, Ivanitsky GR. (2006). Solitonlike and nonsoliton models of interaction of taxis waves. *Biophysics* **51:** 887-891.

Vos M, Velicer GJ. (2008). Natural variation of gliding motility in a centimeter-scale population of *Myxococcus xanthus*. *FEMS Microbiol Ecol* **64:** 343-350.

Wangersky PJ. (1978). Lotka-Volterra population models. *Ann Rev Ecol Evol Syst* **9:** 189–218.

Wang G, Or D. (2010). Aqueous films limit bacterial cell motility and colony expansion on partially saturated rough surfaces. *Environ Microbiol* **12:** 1363-1373.

Wilson PDG, Brocklehurst TF, Arino S, Thuault D, Jakobsen M, Lange M, *et al.* (2002). Modelling microbial growth in structured foods: towards a unified approach. *Int J Food Microbiol* **73:** 275-289.

Zhou JZ, Xia BC, Huang HS, Palumbo AV, Tiedje JM. (2004). Microbial diversity and heterogeneity in sandy subsurface soils. *Appl Environ Microbiol* **70:** 1723-1734.

Zhou JZ, Xia BC, Treves DS, Wu LY, Marsh TL, O'Neill RV, *et al.* (2002). Spatial and resource factors influencing high microbial diversity in soil. *Appl Environ Microbiol* **68:** 326-334.

Chapter 5

A Hydration-Based Biophysical Index for the Onset of Soil Microbial Coexistence

Gang Wang and Dani Or

Scientific Reports **2**: 88, 2012 *DOI: 10.1038/srep00881*

Mechanistic exploration of the origins of the unparalleled soil microbial biodiversity represents a vast and uncharted scientific frontier. Quantification of candidate mechanisms that promote and sustain such diversity must be linked with microbial functions and measurable biophysical interactions at appropriate scales. We report a novel microbial coexistence index (*CI*) that links macroscopic soil hydration conditions with microscale aquatic habitat fragmentation that impose restrictions on cell dispersion and growth rates of competing microbial populations cohabiting soil surfaces. The index predicts a surprisingly narrow range of soil hydration conditions (very wet) that suppress microbial coexistence; and for most natural conditions found in soil hydration supports coexistence. The critical hydration conditions and relative abundances of competing species are consistent with limited experimental observations and with individual-based model simulations. The proposed metric offers a means for systematic evaluation of factors that regulate microbial coexistence in an ecologically consistent fashion.

5.1 Introduction

Soil is the most biologically active compartment of the biosphere, hosting unparalleled biodiversity at all scales[1-7]. Soil aqueous and biogeochemical environments are inherently heterogeneous and patchy[2,8], and thus delineate ecological spheres of influences that may separate microbial communities with respect to location, physiology, or genetics[1,3,9-11]. Complex pore spaces and fragmented aqueous habitats impose constraints on nutrient transport and on microbial motion in unsaturated soils whereby diffusion is the primary mechanism for nutrient supply relative to convection by rare infiltration episodes[8,12,13]. Additionally, pore space architecture and hydration conditions determine aqueous phase configuration thereof, play a key role in shaping microbial community dynamics and composition in soils[9-11]. Cell motion is usually limited, and is critical for survival and functioning in such patchy and heterogeneous environments[1,5,8,14-16]. Hydration constraints to motility and nutrient diffusion are expected to shape the dynamics and composition of the early phases of establishment of microbial communities on unsaturated rough surfaces inoculated by various processes (e.g., large convective flows)[1,5,8,12,13]. Recent studies have established relationships between hydration status that determine aqueous film properties and microbial flagellar motility[12,13].

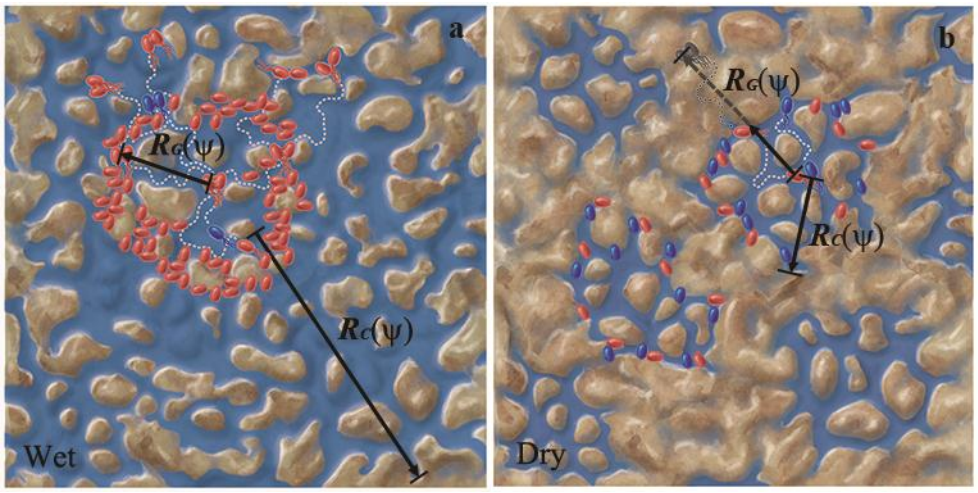

Fig. 1. Aqueous phase configuration on a schematic rough surface delineating connected cluster of sizes $R_C(\psi)$ and associated microbial mean generation length, $R_G(\psi)$ under (**a**) wet, and (**b**) dry conditions. Gray dash lines illustrate the additional distance required for a full generation length (additional time is required for cell division after reaching the aqueous cluster boundary). Red rods represented superior bacterial species and blue of inferior species, both are flagellated (dashed lines mark hypothetical cell trajectories).

We report a novel biophysical index for predicting hydration conditions that promote (or suppress) microbial coexistence on rough surfaces. We propose a framework for integrating

quantifiable biophysical variables, such as aquatic habitat size and connectivity, nutrient diffusion rate affecting microbial growth rates, and aqueous film thickness influencing microbial motility and dispersal distances, into a simple predictive index (see Fig. 1).

5.2 Methods

5.2.1 Aqueous-phase configuration on rough surface and analytical prediction

For the numerical simulations used to test the proposed analytical *CI*, we considered a model system of a rough soil surface represented by an equivalent network (with physical size of 34.4 × 34.4 mm with 200 × 173 sites on a hexagonal lattice) of simple roughness elements whose aqueous phase content and connectivity are functions of the matric potential and geometrical characteristics of the network[12,13]. An important ingredient in the foregoing analysis is the size of aqueous clusters defined as groups of interconnected pores or capillary channels that retain sufficiently thick aqueous film to support flagellar motility[12] and border "empty" channels with aqueous film too thin to support cell motion but available for nutrient diffusion[8,17]. The physical picture of the aqueous-phase is linked with how rough surfaces dry. As the ambient matric potential becomes lower (dryer), air-water interfaces recede deeper into crevices resulting in fragmentation of the previously connected aqueous network (Fig. 1a) into clusters of aqueous islands[8,12] (Fig. 1b). Consequently, the interplay of capillary forces and surface geometries shape details of the aqueous-phase network. However, the effective size of the largest aqueous cluster $R_C(\psi)$ is predictable from universality of percolation theory[17], and can be expressed as a function of the aqueous-phase content (controlled by the ambient matric potential, ψ),

$$R_C(\psi) = R_0\left(\frac{N_C(\psi)}{N_0}\right)^{1/\chi}, \tag{1}$$

where R_0 is radius of system size (for a finite domain), N_C is number of pores/channels of the maximum cluster, N_0 is number of total pores/channels of a system, and χ is a universal exponent dependent on the dimensionality of the network (see *Supplementary information*).

The aqueous cluster radius not only defines the size of an isolated microhabitat where competing microbial species may inhabit and interact, but it also determines the boundaries through which diffusive nutrient fluxes arrive and support life within the cluster.

5.2.2 Analytical solutions of nutrient diffusivity on rough surfaces

Another important consequence of aqueous phase fragmentation and film thinning is the reduction in effective nutrient diffusion (expressed as effective nutrient diffusion coefficient, D_{eff}). The relationship between mean water content on the surface ($\langle\theta(\psi)\rangle$, a function of matric

potential) and effective nutrient diffusion coefficient is expressed as[18] (see *Supplementary information*),

$$D_{eff}(\psi) = D_0 \frac{\langle \theta(\psi) \rangle^2}{\phi^{2/3}}, \quad (2)$$

where D_0 is nutrient diffusion coefficient in bulk water, and ϕ is the effective "porosity" generated by surface roughness (relative to a smooth surface, see *Supplementary information*). The averaged nutrient diffusive flux (represented by D_{eff}) is a measure of nutrient limitation to microbial growth rate that, in turns, determines microbial life history (see *Supplementary information*).

5.2.3 Microbial motility and generation length inhabiting unsaturated rough surfaces

Despite severe limitation to microbial flagellar motion within thin films and fragmented aqueous network, even minute changes in position within the network may play a critical role in the highly heterogeneous diffusion fields[1,5,14], where conditions for population growth or decay may be a few channels or pores apart[12]. Recent studies[12,13] have shown that microbial cell motion (expressed as mean flagellated cell velocity, $\langle V(\psi) \rangle$) was significantly restricted relative to flagellar motion in bulk water owning to the thinning of aqueous film that gives rise to additional viscous drag and capillary pinning forces according to,

$$\langle V(\psi) \rangle = \int_{\Omega_\alpha} \int_{\Omega_H} V_0 \frac{F_M - F_C - F_\lambda}{F_M} f^*(\alpha, H) d\alpha dH, \quad (3)$$

where V_0 is mean cell velocity in bulk water, F_M, F_C and F_λ are the viscous drag force opposing motion in bulk water, the viscous force associated with cell-surface hydrodynamic interactions, and the capillary pinning force, respectively, $f^*(\alpha,H)$ is bivariate probability density function of roughness elements spanning angle (α) and height (H) within the range of values Ω_α and Ω_H (see *Supplementary information*).

We may now combine these hydration based factors (cluster size, nutrient diffusion and cell motility) to estimate a characteristic distance traversed by a microbial cell during a single generation (until binary fission or a doubling time). We term this integrative variable as mean generation length (R_G) which explicitly incorporates intrinsic microbial growth characteristics with motility[18], and hydration status as (see *Supplementary information*),

$$\langle R_G(\psi) \rangle = \sqrt{2 \langle V(\psi) \rangle^2 \tau / \mu_{eff}}, \quad (4)$$

where μ_{eff} is effective microbial specific growth rate, and τ is the mean interval of microbial motile duration (see *Supplementary information*). Considering limitations imposed by aqueous

films for cell dispersal outside clusters, the boundaries of aqueous clusters are entry regions for nutrient fluxes supporting microbial life within the clusters. Consequently, species capable of establishing presence along these boundaries enhance their survivability relative to species in the cluster interior[19].

5.2.4 The definition of predictive microbial coexistence index

Based on this line reasoning, we propose a novel coexistence index (*CI*) defined as the ratio of microbial generation length $\langle R_G(\psi)\rangle$ to the effective radius of aqueous cluster $R_C(\psi)$, with both characteristic lengths dependent on hydration condition – matric potential value (see *Supplementary information*),

$$CI(\psi) = \langle R_G(\psi)\rangle / R_C(\psi)\,. \tag{5}$$

The proposed *CI* compares mean distance traversed by a cell during one generation with the effective size of aqueous clusters (islands) that may host multiple species. Note that $\langle R_G(\psi)\rangle$ reflects not only net motion but also potential for nutrient interception required for cell growth and division. The criticality of nutrient entry zone in a diffusion controlled environment makes presence of multiple species in this zone a defining factor for microbial coexistence. Under wet and favorable environmental conditions, physiologically superior species with fast growth rate may rapidly form a large population dominating presence along these boundaries at greater proportions than relatively slower growing species, and intercept a large fraction of nutrient fluxes from the boundaries. As a consequence, the resulting nutrient depletion at the interior of the microhabitat (aqueous cluster or island) would invariably lead to competitive exclusion of inferior species (Fig. 1a). In contrast, under drier conditions with fragmented aqueous-phase and reduced nutrient supply, microbial growth is limited below physiological capacity, lengthening microbial generation characteristic time (and length) relative to the size of the microhabitat thereof, enhances chances of arrival of diverse composition of species to the boundaries, giving rise to prolonged coexistence and more even species abundance (Fig. 1b). Overall, the model provides qualitative and quantitative estimates for the onset or loss of microbial coexistence, including relative abundance calculations in unsaturated soils (see *Supplementary information*).

5.3 Results

Figure 2 summarizes the variables used in deriving the proposed coexistence index. We first consider aqueous phase fragmentation expressed as aqueous cluster size as seen in Fig. 2a (with configurations shown also in Figs. 2d and 2e) as a function of water potential value and surface

geometry properties. Percolation theory[17] predicts that the size of continuous aqueous clusters is expected to decrease with decreasing water potential (as a surface dries) with a distinct and abrupt drop occurring at a critical water potential value close to -4.0 kPa, in excellent agreement with realizations of many different networks obtained from numerical simulation.

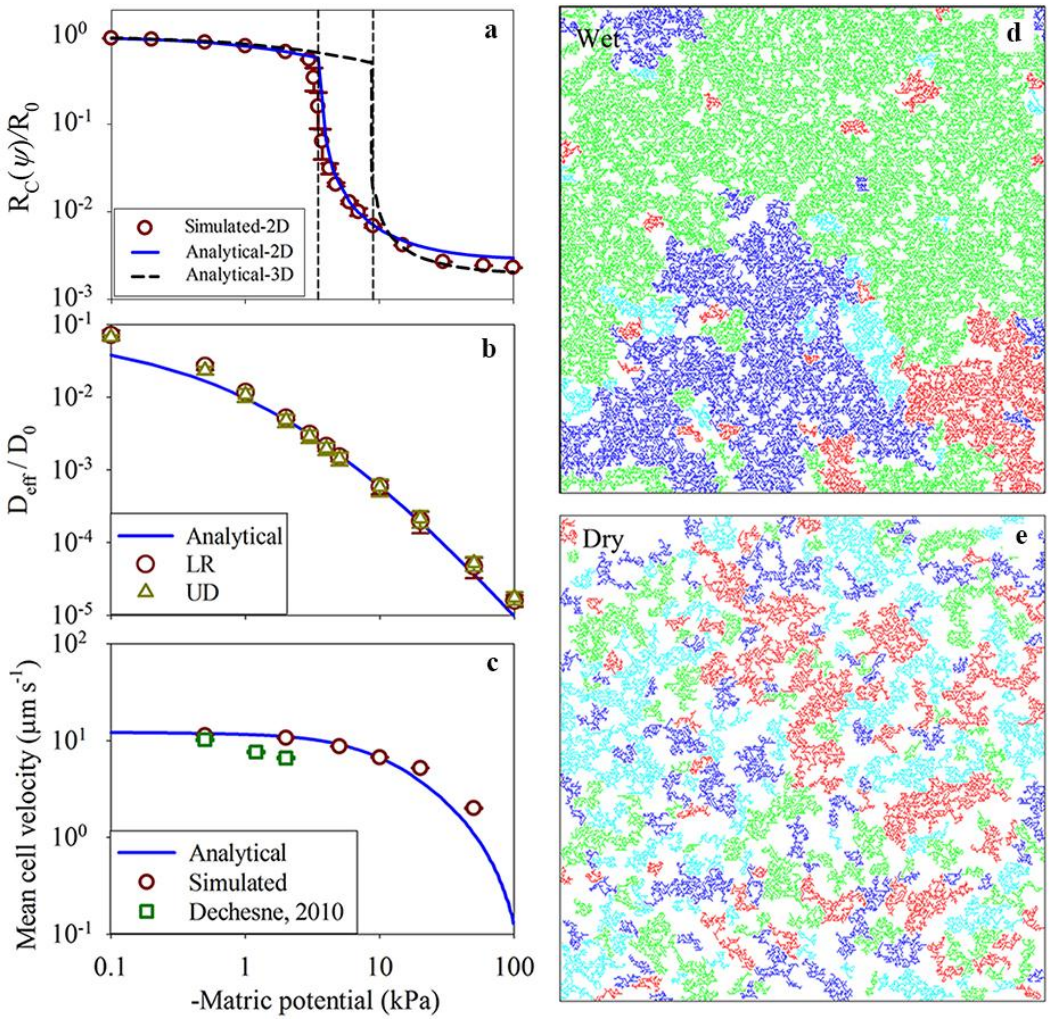

Fig. 2. (**a**) Predicted and simulated radii (mean±s.d., n=5) of aqueous clusters (normalized by maximum cluster size under saturation condition) as a function of matric potential, (**b**) predicted and simulated (mean±s.d., n=5) effective nutrient diffusion coefficients (normalized by diffusion coefficient of glucose in bulk water), UD and LR represent simulated diffusion coefficients with flux from upon to bottom and from left to right boundaries of a domain, respectively, (**c**) analytical prediction for mean cell velocity and comparisons with numerical simulations and experimental measurements (mean±s.e.m., n=34600 for simulation and n>248 for experiments), and aqueous cluster distributions on (**d**) wet and (**e**) dry surfaces, colors mark different clusters.

Invoking percolation theory, one may extend the predictions to volumes of connected aqueous clusters in 3D soil pore spaces (Fig. 2a and Supplementary Fig. S1). Accompanying the fragmentation of the aqueous-phase, a significant drop in effective nutrient diffusion coefficient[20] with decreasing water potential is predicted for various roughness networks, in good agreement with detailed simulation results (Fig. 2b). To complete the picture of hydration

effects on microbial functions on partially hydrated surfaces, we quantify effects of the macroscopic soil water potential on microbial flagellated motility (Eq. 3). Comparisons of analytically-derived predictions with direct observations[12] and detailed numerical simulations of cell motility considering many cells and different roughness networks show excellent agreement (Fig. 2c). The good agreement between simple analytical representations of key hydration-controlled processes motivates their joint use to predict hydration mediated microbial coexistence on rough surfaces.

The proposed *CI* postulates that existence of competing species within an aquatic island (cluster) critically depends on presence on the boundaries of such a cluster to intercept diffusing nutrients via aqueous films too thin to support flagellated motion. Figure 3 depicts analytical predictions of the proposed *CI* for multiple microbial populations on unsaturated rough surfaces based solely on surface roughness properties and microbial physiological traits (growth rates, motility, etc.) as mediated by hydration status (expressed by a macroscopic quantity – matric potential). An important advantage of the proposed *CI* is that the analytical prediction does not require details regarding the structure of diffusion fields nor specifics concerning population interactions and growth dynamics. *CI* values of less than unity for high matric potential values (wet conditions) indicate that distances (mean generation length) traversed by motile cells within one generation are shorter than aqueous cluster size (which, for wet conditions, could span a large fraction of the simulation domain). Low *CI* values also imply rapid increase in population size before reaching microhabitat boundaries. Consequently, the highly competitive species (superior species) may quickly dominate the boundaries, or even enclose slower growing species prior to reaching the boundaries and gradually intercept larger fractions of arriving nutrients thereby tipping competition balance, resulting in competitive exclusion of less effective competitors[5]. Figure 3b depicts the evolution of microbial relative abundance whereby the most competitive species dominate at *CI* values bellow unity (associated with wet surfaces). Under drier conditions (low matric potential values), predicted *CI* values gradually increase until a critical transition occurs at *CI*=1 marking conditions for onset of coexistence. These conditions are also marked by peak transition in population evenness values expressed by the widely used Simpson index[21]. The transition occurs across a surprisingly narrow range of matric potentials within a few kPa (Fig. 3a). Additionally, the theoretically derived relative fitness (*RF*) above the critical threshold of *CI* =1 (at around -4 kPa) becomes indicative of transition to coexistence mode among the microbial species (Fig. 3b). The performance of the *CI* was evaluated primarily based on Monte Carlo simulations using a mechanistic discrete individual-based model[12,13] simulating growth and life histories of large and multispecies microbial populations with typical

results shown in Fig. 3 and Supplementary Fig. S2. Remarkably, the simulation results reflecting behaviors of many individual cells responding to their local microenvironments were in reasonable agreement with the simplified analytical predictions (Fig. 3), and thus lend credence to the underlying assumptions in the basis of the proposed *CI*. The predictive index was also evaluated for limited experimental data[22] for two competing microbial species grown in soil (3D pore systems) under different hydration conditions. The comparison depicted in Fig. 4 shows that with decreasing matric potential, transition of the relative fitness of inferior species occurs at the expected critical *CI* =1 that marks hydration conditions for coexistence consistent with experimental observations[22].

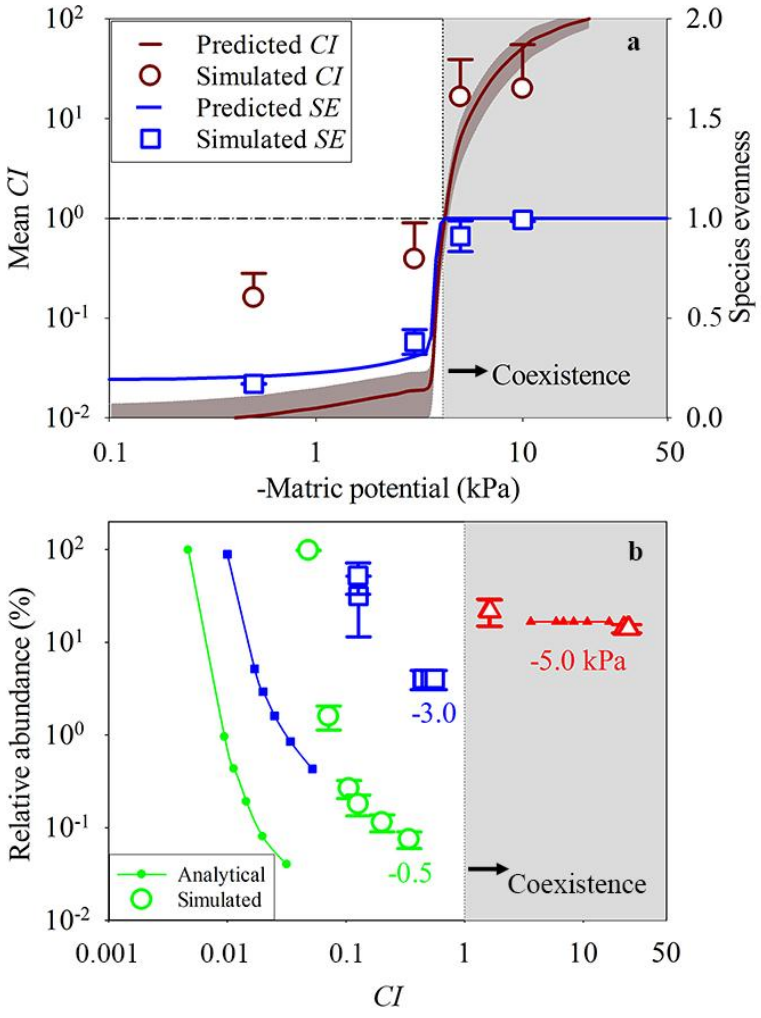

Fig. 3. (**a**) Analytical microbial *CI* predictions (mean±s.d., n=6, gray area marks 1 s.d.) and corresponding common Simpson species evenness (initial inoculation size of 100 cells of each species), and comparisons with simulated *CI* values (mean±s.d., n=384) and Simpson evenness (mean±s.d., n=16 mixed population inoculated colonies), and (**b**) analytical and simulated (mean±s.d., n=16 mixed population inoculated colonies) relative abundance as a function of *CI*. Note the trend towards evenness under drier conditions. The simulated abundance distributions were extracted from the same set of numerical simulations used for evenness indices presented in (a).

The analytical estimates of aqueous habitat fragmentation based on percolation theory (Eq. 1) were also used to estimate the numbers of aqueous clusters in soils yielding close agreement with numerical simulations, and are well constrained by total numbers of soil grains[23] (Supplementary Fig. S3). The aquatic and granular fragmentations provide estimates of distinct niches for accommodating the extremely diverse microbial populations consistent with the theories of spatial heterogeneity promote microbial diversity in soils[8,11,24,25]. Additionally, the

predicted sizes of aquatic habitats hosting competing microbial populations provide the basis for some of the coexistence calculations within the confines of aqueous clusters.

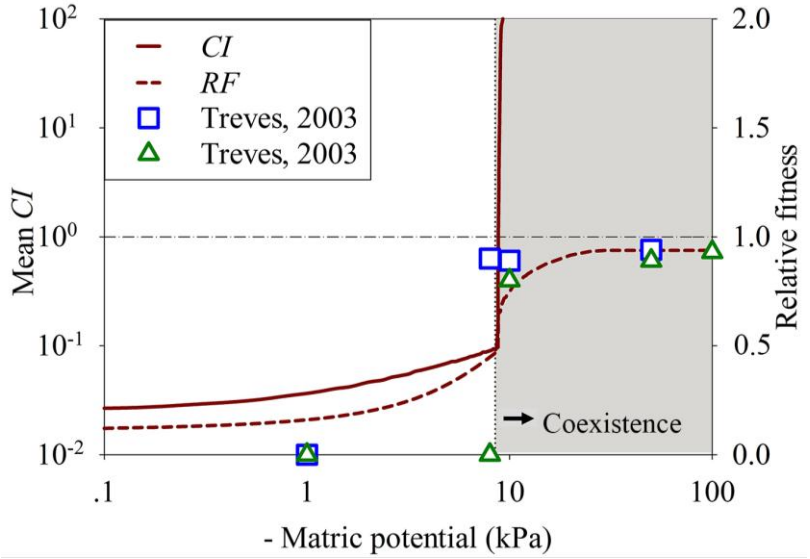

Fig. 4. Analytical *CI* predictions and calculated relative fitness (*RF)* (initial inoculation size of 100 cells of each species) for 3D porous media, and comparisons of *RF* with experimental data[20] ("triangle" and "square" symbols mark experimental data[20]).

5.4 Discussion

Although the notion that dry conditions induce spatial segregation is well established[8], the narrow range of hydration condition (a few kPa) at which the aqueous-phase becomes fragmented is surprising, and the generality of this strong fragmentation at a relatively wet state (in most soils and geographical regions) is important and not widely recognized. The *CI* prediction of lowering water matric potential increases microbial diversity is consistent with recently reported experimental observations[24-26]. For instance, the experimental results of Zhou *et al.*[26] reveal magnitude higher microbial diversity in unsaturated surface soils than in saturated deeper soils. Despite limited experimental information, the general agreement inspires confidence in the potential usefulness of this new *CI* for prediction of conditions promoting or limiting soil microbial coexistence and biodiversity based on simple traits and ambient conditions. In contrast with standard diversity metrics such as relative fitness[27], Shannon and Simpson indices[21] that are all based on analyzing experimental or simulation results, the proposed *CI* is a predictive metric entirely based on simple and measurable biophysical parameters. It is anticipated that the mechanisms postulated in the basis of the proposed *CI* are particularly important during early stages of microbial new colonization on surfaces by large convective events following extended dry periods (rewetting of surfaces)[5,8,28].

The practical implementation of the proposed *CI* in a predictive mode would require information regarding ranges of specific growth rates and motilities of microbial populations inhabiting soil surfaces. However considering the strong constraints imposed by aquatic habitat fragmentation and formation of thin water films, differences in motility among species are likely to be suppressed, thereby reducing parameter requirements for *CI* application to estimates of specific growth rate range. Nominally, the mean growth rate for a population would suffice to identify hydration conditions for onset of coexistence; however, estimates of relative abundance would require information on the range of specific growth rate values of a population, and the picture is likely to become more complex with consideration of hydration dynamics[29]

The narrow range of hydration conditions (a few kPa) for aqueous phase fragmentation and limited nutrient diffusion is relatively general, and leads to an almost universal transition to sessile microbial life due to cell pinning behind thin liquid films regardless of competitive advantages of a species. Additionally, conditions conducive to significant dispersal and population mixing are expected to be limited and rare in most soils (only a few hours several times per year even in temperate regions[3]), highlighting the inherent segregation in soils under natural climatic conditions and across all soil types. Despite numerous simplifications, the analytical *CI* represents a step towards linking the complex soil physical environment with microbial biodiversity in a predictive and ecologically consistent fashion, and offers a potential for addressing core issues in contemporary soil microbial ecology concerning soil and water resource quality, the fate of environmental contaminants, and global biogeochemical cycles[30,31].

Acknowledgements

We acknowledge the financial support of the Swiss National Science Foundation (200021-113442 and 200020-132154). We thank Jon Wraith (NHU) for comments on an earlier version of the manuscript, and Jonathan Levine, Stanislaus Schymanski and Peter Lehmann (ETHZ), and Jan Hopmans (UCD) for helpful discussions.

References

1. Fenchel, T. Microbial behavior in a heterogeneous world. *Science* **296**, 1068-1071 (2002).
2. Torsvik, V., Øvreås, L. & Thingstad, T. F. Prokaryotic diversity – magnitude, dynamics, and controlling factors. *Science* **296**, 1064-1066 (2002).
3. Young, I. M., Crawford, J. W., Nunan, N., Otten, W. & Spiers, A. in *Advances in Agronomy*, Sparks D. L. ed. (Academic Press, Burlington, 2008). pp. 81.
4. Fierer, N. & Jackson, R. B. The diversity and biogeography of soil bacterial communities. *Proc. Natl. Acad. Sci. U.S.A.* **103,** 626-631 (2006).
5. Hibbing, M. E., Fuqua, C., Parsek, M. R. & Peterson, S. B. Bacterial competition: surviving and thriving in the microbial jungle. *Nat. Rev. Microbiol.* **8**, 15-25 (2010).
6. Banavar, J. R. & Maritan, A. Towards a theory of biodiversity. *Nature* **460**, 334-335 (2009).
7. Prosser, J. I. *et al*. The role of ecological theory in microbial ecology. *Nature* **5**, 384-392 (2007).
8. Or, D., Smets, B. F., Wraith, J. M., Dechesne, A. & Friedman, S. P. Physical constraints affecting bacterial habitats and activity in unsaturated porous media – a review. *Adv. Water Resour*. **30**, 1505-1527 (2007).
9. Dion, P. Extreme views on prokaryote evolution. in *Microbiology of Extreme Soils*, Dion, P. & Nautiyal, C. S. eds. (Springer, Berlin Heidelberg, 2008). pp. 45-70.
10. Curtis, T. P. & Sloan, W. T. Prokaryotic diversity and its limits: microbial community structure in nature and implications for microbial ecology. *Curr. Opin. Microbiol.* **7**, 221-226 (2004).
11. Zhou, J. *et al.* Spatial and resource factors influencing high microbial diversity in soil. *Appl. Environ. Microbiol.* **68**, 326-334 (2002).
12. Dechesne, A., Wang, G., Gülez, G., Or, D. & Smets, B. F. Hydration-controlled bacterial motility and dispersal on surfaces. *Proc. Natl. Acad. Sci. U.S.A.* **107**, 14369-14372 (2010).
13. Wang, G. & Or, D. Aqueous films limit bacterial cell motility and colony expansion on partially saturated rough surfaces. *Environ. Microbiol.* **12**, 1363-1373 (2010).
14. Mitchell, J. G. & Kogure, K. Bacterial motility: links to the environment and a driving force for microbial physics. *FEMS Microbiol. Ecol.* **55**, 3-16 (2006).
15. O'Donnell, A. G., Young, I. M., Rushton, S. P., Shirley, M. D. & Crawford, J. D. Visualization, modelling and prediction in soil microbiology. *Nat. Rev. Microbiol.* **5**, 689-699 (2007).

16. Olson, M. S., Ford, R. M., Smith, J. A. & Fernandez, E. J. Ouantification of bacterial chemotaxis in porous media using magnetic resonance imaging. *Environ. Sci. Technol.* **38,** 3864-3870 (2004).
17. Berkowitz, B. & Ewing, R. P. Percolation theory and network modeling applications in soil physics. *Surv. Geophys.* **19**, 23-72 (1998).
18. Berg, H. C. ed. *Random walks in biology*. (Princeton Univ. Press, Princeton, 1983).
19. Ben-Jacob, E., Cohen, I. & Gutnick, D. L. Cooperative organization of bacterial colonies: from genotype to morphotype. *Annu. Rev. Microbiol.* **52,** 779-806 (1998).
20. Moldrup, P. *et al.* Modeling diffusion and reaction in soils: X. A unifying model for solute and gas diffusivity in unsaturated soil. *Soil Sci.* **168,** 321-337 (2003).
21. Hill, T. C. J., Walsh, K. A., Harris, J. A. & Moffett, B. F. Using ecological diversity measures with bacterial communities. *FEMS Microbiol. Ecol.* **43,** 1-11 (2003).
22. Treves, D. S., Xia, B., Zhou, J. & Tiedje, J. M. A two-species test of the hypothesis that spatial isolation influences microbial diversity in soil. *Microb. Ecol.* **45**, 20-28 (2003).
23. Wu, Q., Borkovec, M. & Sticher, H. On particle-size distribution in soils. *Soil Sci. Soc. Am. J.* **56,** 362-369 (1993).
24. Zhou, J., Xia, B., Huang, H., Palumbo, A. V. & Tiedje, J. M. Microbial diversity and heterogeneity in sandy subsurface soils. *Appl. Environ. Microbiol.* **70,** 1723-1734 (2004).
25. Carson, J. K. *et al.* Low pore connectivity increases bacterial diversity in soil. *Appl. Environ. Microbiol.* **76,** 3936-3942 (2010).
26. Zhou, J. Z. *et al*. Spatial and resource factors influencing high microbial diversity in soil. *Appl. Environ. Microbiol.* **68,** 326-334 (2002).
27. Elena, S. F. & Lenski, R. E. Evolution experiments with microorganisms: the dynamics and genetic bases of adaptation. *Nat. Rev. Genet.* **4**, 457-469 (2003).
28. Hall-Stoodley, L., Costerton, J. W. & Stoodley, P. Bacterial biofilms: from the natural environment to infectious diseases. *Nat. Rev. Microbiol.* **2,** 95-108 (2004).
29. Wang, G. & Or D. Hydration dynamics promote bacterial coexistence on rough surfaces. *ISME J.* (2012). doi:10.1038/ismej.2012.115.
30. Turbé, A. *et al.* Soil biodiversity: functions, threats and tools for policy makers. Bio Intelligence Service, IRD, and NIOO, Report for European Commission (DG Environment) (2010).
31. Evans, S. E. & Wallenstein M. D. Soil microbial community response to drying and rewetting stress: does historical precipitation regime matter. *Biogeochemistry* **109,** 101-116 (2012).

Supplementary information

Table S1. Physiological parameters for microbial growth, metabolism and nutrient concentrations.

Parameters	Units	Values*
μ_{max}: maximum specific growth rate	hr^{-1}	[0.2~1.2]†
K_S: half-saturation constant	mg l^{-1}	[0.2~1.2]×10^{-3}†
Y_{max}: apparent yield at μ_{max}	g dry mass (g substrate)$^{-1}$	0.44
m: apparent maintenance rate	g substrate (g dry mass)$^{-1}$ hr^{-1}	0.036
$\bar{V}_B$: median cell volume	fl	0.4
$V_{B,d}$: cell volume at division	fl	$2\bar{V}_B$ /1.433
$V_{B,min}$: minimal volume of an active cell	fl	$V_{B,d}$ /5
ρ: cell density (dry mass)	g l^{-1}	290
C: substrate concentration	mg l^{-1}	1

*: For 3D systems with extracted values from Treves *et al.*[1]

†: Bivariate uniform distribution with correlation coefficient of 0.01.

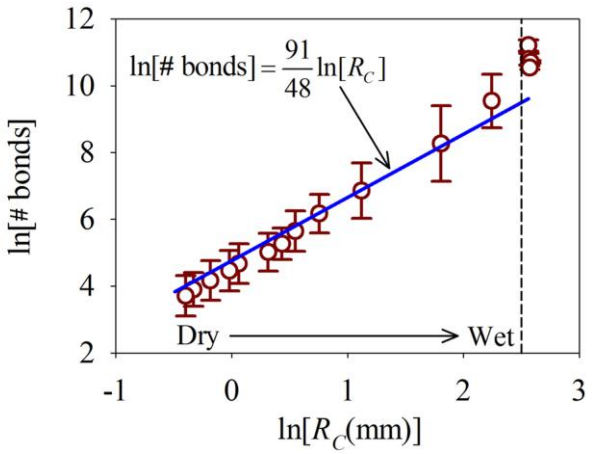

Fig. S1. Water filled pore cluster characteristics on unsaturated roughness networks. Simulated radius of the maximum water filled pore/channel cluster as a function of numbers of water filled pores/channels (mean±s.d., n=5), in agreement with numerical prediction by percolation theory[2]. Dashed line marks percolation threshold.

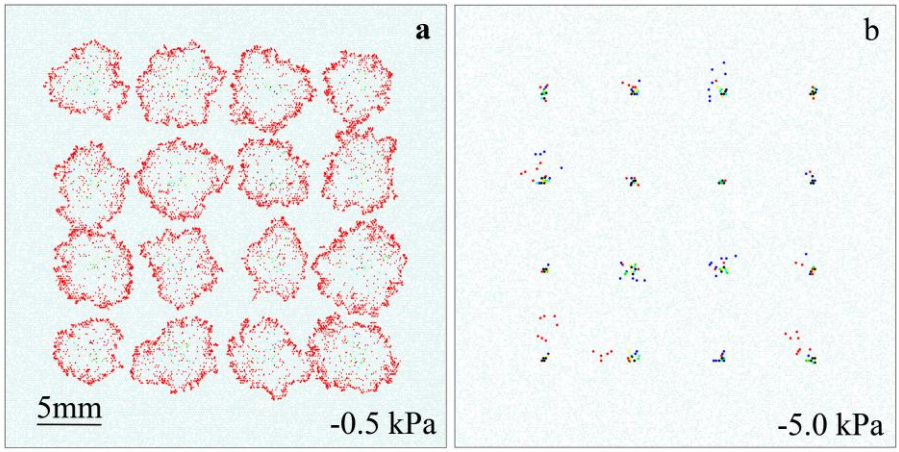

Fig. S2. **Simulated colony growth patterns of multiple competing microbial populations**. Colony growth patterns of a set of competing microbial species on unsaturated roughness network at 60 hr after inoculation under (**a**) -0.5 kPa, and (**b**) -5.0 kPa, respectively. Color spots represent the set of competing microbial species differentiated at intrinsic growth characteristics: maximum specific growth rate of species 1 (SP1) of 1.2 (red), SP2 of 0.6 (blue), SP3 of 0.5 (green), SP4 of 0.4 (cyan), SP5 of 0.3 (yellow) and SP6 of 0.2 hr^{-1} (black), and half saturation constant of SP1 of 1.2, SP2 of 0.6, SP3 of 0.5, SP4 of 0.4, SP5 of 0.3 and SP6 of 0.2 µg l^{-1}, respectively. Populations of 6 mixed species (each consisting 4 cells, totally 24 cells for each inoculation site) were inoculated within 16 sites on a roughness network at the beginning of a simulation.

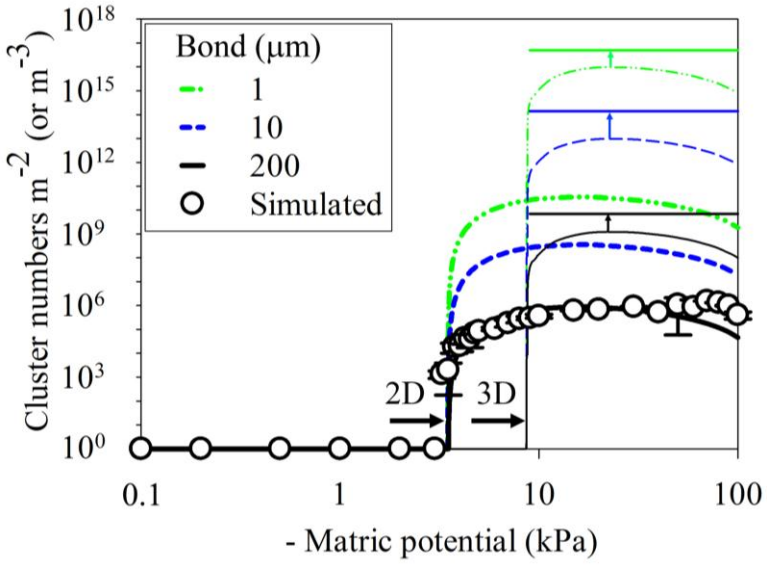

Fig. S3. A**nalytical aqueous cluster numbers for 2D surfaces and 3D soil volumes.** Predicted number of aqueous clusters for 2D surfaces (number per m^2) and for 3D soil volumes (number per m^3) with comparisons of numerical simulations (symbols) with measurements[3]. Color bars represent grain numbers per m^3 assuming grain diameters of 1, 10 and 200 µm, these are used as upper bounds for the maximum number of aqueous clusters per soil volume (m^3).

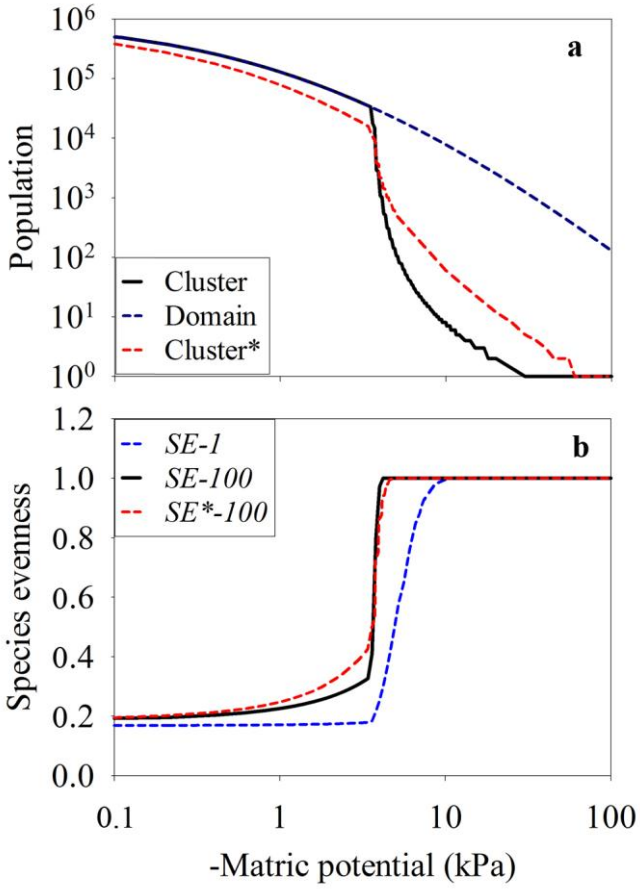

Fig. S4. A**nalytical nutrient-limited population capacities and species evenness.** (**a**) Analytical predictions of nutrient-limited population capacities per cluster and for the simulation domain, denoting 'Cluster*' for nutrient-limited population capacity per cluster calculated according to Eq. S22, and (**b**) analytical prediction of species evenness (*SE*) with initial inoculation size of 1 (*SE-1*) and 100 (*SE-100*) cells of each species, with '*SE*-100*' represents *SE* calculated according to Eq. S22 for population capacity per cluster with initial inoculation of 100 cells of each species.

Detailed methods

We considered microbial growth rate represented by the Monod function, with key biological parameters[4] listed in Supplementary Table S1,

$$\mu_{eff} = \frac{\mu_M C}{C+K} - m, \tag{S1}$$

where μ_M and μ_{eff} are the maximum and effective microbial specific growth rates, respectively, K is half-saturation constant marks the value of C at which an active cell achieves half of its maximal growth rate, m is microbial maintenance rate, and C is apparent nutrient concentration exposure to microbial population, which we considered to be proportional to nutrient diffusive flux (expressed as effective nutrient diffusion coefficient, D_{eff}),

$$\langle C \rangle = \frac{D_{eff}}{D_0} C_0, \tag{S2}$$

where D_0 is nutrient diffusion coefficient in bulk water, C_0 is nutrient concentration at boundaries, and D_{eff} is a function of mean volumetric water content ($\langle\theta(\psi)\rangle$) of rough surface[5],

$$D_{eff}(\psi) = D_0 \frac{\langle\theta(\psi)\rangle^2}{\phi^{2/3}}, \tag{S3}$$

where ϕ is the effective "porosity" generated by surface roughness (relative to smooth surface), which is calculated according to,

$$\phi = \frac{2\sqrt{3}}{3\langle H\rangle l} \int_{\Omega_\alpha} \int_{\Omega_H} H^2 \tan(\frac{\alpha}{2}) d\alpha dH, \tag{S4}$$

where $\langle H\rangle$ is the mean height of pores/channels (considering the effective height of the domain equals to the value of 3 times of the mean height of pores/channels), Ω_α and Ω_H are intervals of spanning angle and height of roughness element of the network, respectively, l is the length of a roughness element (pore/channel), α and H are spanning angle and height of a roughness element, respectively[6]. Mean volumetric water content ($\langle\theta(\psi)\rangle$) can be estimated as a function of ambient hydration status (matric potential, ψ) and surface roughness characteristics according to,

$$\langle\theta(\psi)\rangle = \int_{\Omega_\alpha} \int_{\Omega_H} \theta_{\alpha,H}(\psi) f(\alpha, H) d\alpha dH, \tag{S5}$$

with its variance $\sigma^2[\theta_{\alpha,H}(\psi)]$ as,

$$\sigma^2[\theta_{\alpha,H}(\psi)] = \int_{\Omega_\alpha} \int_{\Omega_H} (\theta_{\alpha,H}(\psi) - \langle\theta(\psi)\rangle)^2 f(\alpha, H) d\alpha dH, \tag{S6}$$

with $f(\alpha,H)$ of the bivariate probability density function of α and H, with correlation coefficient of ζ,

$$f(\alpha,H)=\frac{\exp[-\frac{1}{2(1-\zeta^2)}(\frac{(\ln(\pi-\alpha)-\langle\alpha\rangle)^2}{\sigma_\alpha^2}+\frac{(\ln H-\langle H\rangle)^2}{\sigma_H^2}-\frac{2\zeta(\ln(\pi-\alpha)-\langle\alpha\rangle)(\ln H-\langle H\rangle)}{\sigma_\alpha\sigma_H})]}{2\pi(\pi-\alpha)H\sqrt{(1-\zeta^2)\sigma_\alpha^2\sigma_H^2}},\text{(S7)}$$

where $\theta_{\alpha,H}(\psi)$ is volumetric water content of a roughness element with spanning angle α and height H[5], $\langle\alpha\rangle$ is the mean value of spanning angle for a roughness element. Functional relationships linking mean volumetric water content and matric potential (or relative humidity) are routinely determined in hydrologic studies. The effective growth rate of a specific microbial species (i) is written as,

$$\mu_{eff,i}=\frac{\mu_{M,i}C_0}{C_0+\frac{K_i\phi^{2/3}}{\langle\theta(\psi)\rangle^2}}-m_i. \quad \text{(S8)}$$

Equation S8 highlights dependency of microbial growth rate on environmental characteristics and physiological traits, and provides a means to estimate microbial mean generation time (binary fission or doubling time), $T_{G,i}$,

$$T_{G,i}=1/\mu_{eff,i}. \quad \text{(S9)}$$

The mean effective aqueous film thickness of a roughness network, $\langle d(\psi)\rangle$, is calculated as,

$$\langle d(\psi)\rangle=\int_{\Omega_\alpha}\int_{\Omega_H} d_{\alpha,H}(\psi)f(\alpha,H)d\alpha dH, \quad \text{(S10)}$$

where $d_{\alpha,H}(\psi)$ is effective aqueous film thickness of a roughness element of specified geometry (with spanning angle α and height H) that can be easily calculated[6]. It enables estimation of microbial cell velocity expressed as a function of mean aqueous film thickness according to, $V_{\alpha,H}(\psi)=V_0\frac{F_M-F_C-F_\lambda}{F_M}$, with V_0 of mean cell velocity in bulk water, F_M, F_C and F_λ are the viscous drag force opposing motion in bulk water (equal to the maximum flagellar propulsive force), the viscous force associated with cell-surface hydrodynamic interactions, and the capillary pinning force, respectively[5]. Microbial mean cell velocity on a roughness network is calculated as,

$$\langle V(\psi)\rangle=\int_{\Omega_\alpha}\int_{\Omega_H} V_0\frac{F_M-F_C-F_\lambda}{F_M}f^*(\alpha,H)d\alpha dH, \quad \text{(S11)}$$

where $f^*(\alpha,H)$ is bivariate probability density function of α and H considering six neighboring roughness elements,

$$f^*(\alpha,H)=\frac{\exp[-\frac{6}{2(1-\zeta^2)}(\frac{(\ln(\pi-\alpha)-\langle\alpha\rangle)^2}{\sigma_\alpha^2}+\frac{(\ln H-\langle H\rangle)^2}{\sigma_H^2}-\frac{2\zeta(\ln(\pi-\alpha)-\langle\alpha\rangle)(\ln H-\langle H\rangle)}{\sigma_\alpha\sigma_H})]}{\frac{\pi(\pi-\alpha)H}{3}\sqrt{(1-\zeta^2)\sigma_\alpha^2\sigma_H^2}}. \quad \text{S12)}$$

This in turn enables determination of microbial mobility defined as, $M_C = \langle V(\psi) \rangle^2 \tau / 2$, with τ the mean interval of microbial motile duration[7]. The mean square displacement of a cell within one generation time is estimated as[7],

$$\langle R^2 \rangle = 4 M_C T_G , \tag{S13}$$

which enables estimation of microbial mean generation (doubling) length as,

$$\langle R_G \rangle = \sqrt{2 \langle V(\psi) \rangle^2 \tau / \mu_{eff,i}} . \tag{S14}$$

The application of percolation theory to porous media represented by network models has yielded insight into physical behaviors at scales representing pores to larger/natural scales in porous media[2]. The dynamics of a spanning aqueous cluster via percolation transition into aqueous fragmentation is well described by percolation theory[2],

$$R_C(\psi) = R_0 (\frac{N_C}{N_0})^{1/\chi} , \tag{S15}$$

and

$$N_C(p) = \begin{cases} p_{C,a} (p_C - p)^{-\gamma}, & (p \le p_{C,a}) \\ N_0 p, & (p > p_{C,a}) \end{cases} , \tag{S16}$$

where N_C and N_0 are numbers of pores/channels of the maximum cluster and number of total pores/channels of a system, R_C and R_0 are effective radii of the maximum cluster and system size (for a finite domain), respectively, γ is an exponent having value of 43/18 for 2D and 1.80 for 3D systems, χ is statistical fractal with value of 91/48 for 2D systems and 2.52 for 3D systems, p_C is percolation threshold with value of 0.35 for 2D and 0.18 for 3D infinite systems, respectively, $p_{C,a}$ ($p_{C,a} = p_C - N_0^{-1/\gamma}$) is effective percolation threshold of finite systems, and p is probability of a pore/channel that has significant water retention that supports typical cell motility, which can be expressed as a function of hydration status (matric potential or relative humidity),

$$p(\psi) = \int_{\Omega_{\alpha*}} \int_{\Omega_{H*}} f(\alpha, H) d\alpha dH , \tag{S17}$$

where $\Omega_{\alpha*}$ and Ω_{H*} are ranges of spanning angle and height of roughness element, respectively, within which effective aqueous film thickness ($d_{\alpha,H(\psi)}$) of a roughness element is sufficient for typical cell motion – flagellar motility[6]. The number of water filled pore/channel clusters (N, minimum cluster number considering the maximum cluster size) can be expressed according to,

$$N(\psi) = \frac{N_0 p}{N_C} . \tag{S18}$$

The biophysical variables described above enable predictive and quantitative assessment of coexistence potential of multiple microbial species on a rough surface as a function of hydration status. We propose a single coexistence index (*CI*) defined as the ratio of microbial mean generation length to connected aqueous cluster size,

$$CI(\psi) = \langle R_G(\psi) \rangle / R_C(\psi) . \quad \text{(S19)}$$

This ratio compares the size of connected aqueous clusters (islands) hosting multiple species with cell displacement distances during one binary fission (generation), with displacement distance encapsulate both net motion and nutrient interception required for cell growth and division.

The modeled rough surface network under study is of physical size of 34.4 × 34.4 mm with 200 × 173 sites on hexagonal lattice[6]. Systematic testing of the proposed analytical *CI* was based primarily on a mechanistic hybrid individual-based model[6,8], considering explicitly autonomous cell motility, nutrient interception and cell growth, leading to trophic interactions among populations within hydration-controlled diffusion fields and aqueous films. We performed simulations on unsaturated model roughness networks[6], considering 6 motile microbial species differentiated by their intrinsic-growth characteristics, inoculated in 16 sites each consisting of 6 species (see Supplementary Fig. S2). The mean *CI* values extracted from a series of numerical simulations considered displacement distances by individual cells within one generation and the sizes of connected aqueous clusters on a simulated surface. Mean species evenness and mean relative abundance values extracted from numerical simulations were based on populations of 16 mixed inoculated colonies.

As a reference state we have considered population size of microbial species at a time where nutrient consumption has reached supply limit or capacity for an aqueous cluster. The population size at the nutrient-limiting state was used for estimating survivability within a prescribed domain, with the average elapsed time calculated according to:

$$W^* = \sum_i (W_{i0} 2^{\mu_{eff,i} T^*}) , \quad \text{(S20)}$$

where W_{i0} is initial population of microbial species i inoculated at the center of the aqueous cluster, $\mu_{eff,i}$ is effective specific growth rate of species i, and W^* is nutrient-limited population size for an aqueous cluster, which can be estimated from microbial physiological maintenance (assuming similar maintenance for all species) and the potential maximum nutrient flux arriving at boundary of the simulation domain and the number of aqueous clusters according to:

$$W^* = \begin{cases} \dfrac{12L_0 \langle H \rangle D_{eff}(\psi) \dfrac{C_0}{l}}{N_{2D}(\psi)} / \Delta m, & \text{(for 2D system)} \\ \dfrac{6L_0^2 D_{eff}(\psi) \dfrac{C_0}{l}}{N_{3D}(\psi)} / \Delta m, & \text{(for 3D system)} \end{cases}, \tag{S21}$$

where L_0 is the side length of the domain under consideration, C_0 is constant nutrient concentration at the boundary of the domain, Δm is the mean nutrient mass flux required for physiological maintenance of individual microbial cell, and $N(\psi)$ is the number of aqueous clusters. Alternatively, we may calculate the nutrient-limited population size of an aqueous cluster considering maximum nutrient flux arriving at boundary of a single (typical) cluster according to:

$$W^{*\prime} = \begin{cases} 6\pi R_C(\psi) \langle H \rangle D_{eff}(\psi) \dfrac{C_0}{l} / \Delta m, & \text{(for 2D system)} \\ 4\pi R_C^2(\psi) D_{eff}(\psi) \dfrac{C_0}{l} / \Delta m, & \text{(for 3D system)} \end{cases}. \tag{S22}$$

Comparisons of analytical predictions of the largest population size supported by diffusion for an aqueous cluster (Eqs. S21 and S22) and for the entire domain show consistent agreement for pre-percolation of the systems which diverge after percolation threshold due to aqueous phase fragmentation (Fig. S4a). Additionally, variation in initial inoculation size has minor influence in species evenness (Fig. S4b), reflecting the generality of the switch manner across a narrow range of hydration conditions.

The resolved species population sizes ($W_i = W_{i0} 2^{\mu_{eff,i} T^*}$) at T^* are subsequently used to estimate species evenness, abundance and fitness parameters. For the example of two species, the relative fitness (*RF*) of the inferior species (SP-I) relative to that of the superior species (SP-S) was calculated as[9],

$$RF = (\frac{W_I}{W_{I0}}) / (\frac{W_S}{W_{S0}}), \tag{S23}$$

where W_{I0} and W_I are initial and final populations of the inferior species, and W_{S0} and W_S are those of the superior species. Simpson species evenness (*SE*) was calculated as[10],

$$SE_{Simpson} = \frac{1}{Z \times \sum_i (w_i^2)}, \tag{S24}$$

where Z is number of total microbial species under consideration, w_i is relative abundance of species i, with $w_i = \dfrac{W_i}{\sum_i (W_i)}$, and W_i is the population of species i.

References

1. Treves, D. S., Xia, B., Zhou, J. & Tiedje, J. M. A two-species test of the hypothesis that spatial isolation influences microbial diversity in soil. *Microb. Ecol.* **45**, 20-28 (2003).
2. Berkowitz, B. & Ewing, R. P. Percolation theory and network modeling applications in soil physics. *Surv. Geophys.* **19**, 23-72 (1998).
3. Wu, Q., Borkovec, M. & Sticher, H. On particle-size distribution in soils. *Soil Sci. Soc. Am. J.* **56,** 362-369 (1993).
4. Kreft, J. U., Booth, G. & Wimpenny, J. W. T. BacSim, a simulator for individual-based modelling of bacterial colony growth. *Microbiol.* **144**, 3275-3287 (1998).
5. Moldrup, P. *et al.* Modeling diffusion and reaction in soils: X. A unifying model for solute and gas diffusivity in unsaturated soil. *Soil Sci.* **168,** 321-337 (2003).
6. Dechesne, A., Wang, G., Gülez, G., Or, D. & Smets, B. F. Hydration-controlled bacterial motility and dispersal on surfaces. *Proc. Natl. Acad. Sci. U.S.A.* **107**, 14369-14372 (2010).
7. Berg, H. C. ed. *Random walks in biology.* (Princeton Univ. Press, Princeton, 1983).
8. Wang, G. & Or, D. Aqueous films limit bacterial cell motility and colony expansion on partially saturated rough surfaces. *Environ. Microbiol.* **12**, 1363-1373 (2010).
9. Elena, S. F. & Lenski, R. E. Evolution experiments with microorganisms: the dynamics and genetic bases of adaptation. *Nat. Rev. Genet.* **4**, 457-469 (2003).
10. Hill, T. C. J., Walsh, K. A., Harris, J. A. & Moffett, B. F. Using ecological diversity measures with bacterial communities. *FEMS Microbiol. Ecol.* **43,** 1-11 (2003).

Chapter 6

Trophic Interactions and Self-organization of Microbial Consortia on Unsaturated Surfaces

Gang Wang and Dani Or

Trophic interactions shape community dynamics, and play key role in the onset and maintenance of biodiversity. Progress in resolving basic ecological questions concerning the origins and functioning of the immense biodiversity found in soil requires quantitative models integrating key biophysical processes and considering biological interactions at appropriate spatial and temporal scales. We study the role of trophic interactions in shaping microbial population dynamics and community structure and their impacts on microbially-mediated processes in unsaturated soils. An individual-based model that couples diffusion-reaction processes with hydration-mediated motility and nutrient diffusivity was developed to explicitly consider trophic interactions among mixed microbial populations at local scale of soil surfaces. Results reveal the increase in ecological niche dimensionality through spatial self-organization of microbial consortia Mediated through trophic interactions. The resulting spatial organization of different species reflected a complex interplay between the geometry of primary nutrient fluxes and evolving location and rate of release of byproducts essential for other members in the consortium. Not surprisingly, hydration conditions and spatial heterogeneity of rough surfaces impose diffusional and motility constraints that impeded and shape details and rates of self-organization. Concentration gradients and spatial structure of various substrates relative to species growth rates and survival are manifested in the emerging spatial patterns of consortia. We developed simple analytical metrics for predicting conditions necessary for successful microbial trophic interactions and emergence of meaningful community-level dynamics, in good agreement with numerical simulations of interacting microbial populations. The results provide insights into complexities expected in biostimulation of target soil volumes for bioremediation, and offer guidance for effective inoculation of interacting species based on soil hydration conditions.

6.1 Introduction

Microorganisms are the primary agents for many soil ecological functions and ecosystem services (Schink, 1997; Dejonghe *et al.*, 2003; Curtis and Sloan 2004; Pérez-Pantoja *et al.*, 2009; Oren, 2010), responsible for over 80% of total biogeochemical soil processes (Nannipieri and Badalucco, 2003). Soil microbes live in habitats of complex and dynamic physico-chemical environmental conditions, in which small scale spatial and temporal variations in nutrient source availability within complex pore spaces and variable hydration conditions shape microbial transport and nutrient source fluxes, and thus influence population growth and community dynamics in general (Curtis and Sloan 2004; Fenchel 2002; Young and Crawford 2004; Prosser *et al.*, 2007; Wang and Or, 2010). Recent advances in microbial biology revealed that trophically-interacting microbial communities, rather than individual species, control the primary interactions with local environments (McCann *et al.*, 1998; Woyke *et al.*, 2006; Miller *et al.*, 2010). Although trophic interactions have long been argued are key factors shaping the immense biodiversity and ecological functioning of macroscale plants and animal ecosystems in detail (Knight *et al.*, 2005; Harpole and Tilman, 2007; Alexandrou *et al.*, 2011; Cardinale, 2011), understanding of the origins of observed patterns and the interplay of mechanisms linking trophic processes and microbial dynamics remain sketchy and thus adding ambiguity to the picture of when certain microbial species are active and what affects the temporal discontinuity of their functional niches (Curtis and Sloan, 2004; Torsvik *et al.*, 2006; Prosser *et al.*, 2007).

Progress in establishing direct links between trophic processes coupling spatial and nutritional variables and microbial community dynamics and ecological implications requires quantitative modeling that integrates revision of elements of ecological theories and bio-physico-chemical processes at appropriate spatial and temporal scales (Prosser *et al.*, 2007; O'Donnell *et al.*, 2007; Banavar and Maritan, 2009; Gonzalez *et al.*, 2011; Morelli *et al.*, 2012).We study the role of trophic interactions on microbial population dynamics and community structure using an individual-based model (IBM) that couples diffusion-reaction processes with hydration-mediated motility and nutrient diffusivity. The model explicitly considers local-scale trophic interactions among species inhabiting unsaturated rough (soil) surfaces.

6.2 Methods

6.2.1 Modeling microbial growth on rough surfaces

We consider a 2D surface roughness capillary network for mimicking soil surfaces (Dechesne et al., 2010), with physical size of the network of 34.4 × 34.4 mm (with 200 × 173 sites on hexagonal lattice and bond length of 0.2 mm). The amount of aqueous phase retained within roughness elements and associated aqueous phase connectivity and aqueous phase cluster size can be expressed as functions of ambient matric potential values (or relative humidity) and surface roughness geometry and provide fundament supporting nutrient diffusive flux and microbial motility (Or *et al*., 2007; Wang and Or, 2010; Dechesne *et al*., 2010). We employ a hybrid form of the reaction-diffusion model for describing nutrient diffusion and microbial consumption (Kreft *et al.*, 1998; Dechesne *et al.*, 2010),

$$\begin{cases} \dfrac{\partial b}{\partial t} = D_b \nabla^2 b + \mu_{eff} b \\ \dfrac{\partial C}{\partial t} = D_C \nabla^2 C - \mu_{eff} b / Y \end{cases}, \tag{1}$$

with b of microbial number or concentration, C is nutrient concentration, D_b and D_C are diffusion coefficients of microbe and nutrient, respectively, t is elapsed time, Y is the yield term (linking microbial growth with consumed nutrient amount), and μ_{eff} is microbial effective specific growth rate, which is described according to the Monod equation as (Kreft *et al.*, 1998),

$$\mu_{eff} = \mu_0 \frac{C}{K_C + C} - m, \tag{2}$$

where μ_0 is microbial maximum specific growth rate, K_C is half-saturation constant (substrate concentration at which growth rate equals to half of the maximum growth rate), and m is specific maintenance rate. The mean-field microbial growth and dispersion in Eq. [1] was replaced by a discrete approximation using individual-based model (IBM) as described in (Kreft *et al.*, 1998). An inhibition form of the Monod equation for microbial growth with presence of inhibitor byproduct C^* (concentration) is expressed as (Bielefeldt and Stensel, 1999; Albanna *et al.*, 2012), $\mu_{eff} = \mu_0 \dfrac{C}{K_C(1 + C^* / K_I) + C} - m$, with K_I of inhibition constant.

Limitations of thin aqueous film in microbial flagellated motility (primary mode of microbial self-propulsion in planktonian form within aqueous films - Darnton and Berg, 2008) on rough surface are lumped into a function of cell size and film thickness, accounting capillary and hydrodynamic resistance to cell body, according to (Dechesne *et al.*, 2010),

$$V(\psi) = V_0 \frac{F_M - F_{Ca}(d(\psi)) - F_\lambda(d(\psi))}{F_M}, \tag{3}$$

where V_0 of mean cell velocity in bulk water, and F_M, F_{Ca} and F_λ are the viscous drag force opposing cell motion in bulk water (equal to the maximum flagellar propulsive force), the

viscous force associated with cell-wall hydrodynamic interactions, and the capillary pinning force, respectively. Note that receding air-water interfaces under drying conditions that results in thinning of film thickness also effectively disconnects microbial aqueous habitats and further limits microbial motion (Or *et al.*, 2007; Dechesne *et al.*, 2010). The limitations to individual cell motions and population self-organization on various unsaturated surfaces are incorporated in the IBM component of Eq. [1] and thus directly affect rates and organization of microbial consortia. Microbial trophic interaction efficiency is calculated as a ratio of total biomass of the bottom member and total byproduct mass produced by the top member of the trophic interaction chain (Christensen and Walters, 2004).

6.2.2 Modeling microbial trophic interactions on unsaturated surfaces

The nature of microbial activities are often subjected to complex trophic processes among involving populations that enable microbes to establish a homeostasis between neighbors and local environments for survival and for carrying complex ecological functions (Schink, 1997; Pérez-Pantoja *et al.*, 2009; Oren, 2010; Phelan *et al.*, 2012). The majority of trophic interactions concerns two types (Phelan *et al.*, 2012): commensal interaction, such that one organism benefits at or benefits to the others (Norlund *et al.*, 2009; Hasan *et al.*, 2011); or mutualistic interaction, in which both members cooperate and benefit each other (Dolfing and Tiedje, 1991; Schink, 1997; Lykidis *et al.*, 2011). To study soil microbial trophic interactions, we start with simple commensal interaction scenario, in which one microorganism (sp1) utilize initial nutrient (N1) and benefits another one (sp2) by producing the second nutrient (N2) supporting sp2's growth (see Fig. 1d); then we blend more trophic interactions into the model by introducing a third microorganism (sp3) which competes with sp2 for N4 (see Fig. 4d) for study more complex microbial community dynamics common in soils (Schink, 1997; Pérez-Pantoja *et al.*, 2009; Oren, 2010).

6.2.3 Analytical predictions in nutrient diffusion scale and microbial active motility range

Successful microbial self-organizations rely on interactions among neighboring populations and with local environments that are likely linked through essential nutrient acquisitions and/or environmental stimuli (Phelan *et al.*, 2012). The critical nutrient diffusion time T_B (when an active cell turns inactive due to consumption of cell-mass for maintenance with 0 nutrient supply) is determined by microbial metabolic maintenance rate of an active cell based on (Kreft *et al.*, 1998),

$$T_B = \frac{Q_{B0} - Q_{B\min}}{mQ_{B0}}, \quad (4)$$

where Q_{B0} and Q_{Bmin} are median and minimum biomass of an active cell, respectively.

The rate of microbial population-dispersion considering metabolic growth rate of μ_{eff} on two dimensional surfaces, $\vec{V}_R$, is described as (Skellam, 1951),

$$\vec{V}_R = \sqrt{4\mu_{eff} D_B}, \quad (5)$$

where D_B is microbial mobility (Berg, 1983), given as: $\langle V \rangle^2 \tau / 2$. Eq. [5] enables estimating the maximum population dispersion length during T_B as,

$$L_D = [2(\mu_0 \frac{C}{K_C + C} - m)\langle V \rangle^2 T_B{}^2 \tau]^{1/2}. \quad (6)$$

The largest possible displacement/distance (R_M) of a microbial cell during the critical time (T_B) without net metabolic cell growth is calculated according to (Berg, 1983),

$$R_M = (2\langle V \rangle^2 \tau T_B)^{1/2}, \quad (7)$$

where $\langle V \rangle$ is microbial mean cell velocity on a rough surface, and τ is the mean interval of microbial motile duration (Berg, 1983; Wang and Or, 2012. Equations [6] and [7] allow estimating the maximum dispersion length (L_T) of two trophically-interacting populations that allows successful establishment of a functional consortium as,

$$L_T = (2\langle V \rangle^2 \tau T_B)^{1/2} + [2(\mu_0 \frac{C}{K_C + C} - m)\langle V \rangle^2 T_B{}^2 \tau]^{1/2}. \quad (8)$$

A solution for diffusion from a point source on unsaturated surface can be described according to (Pattle, 1959),

$$C(R,t) = \frac{Q}{4\pi D_{eff} t} \exp(-\frac{R^2}{4D_{eff} t}), \quad (9)$$

where *C(R,t)* is the resulting nutrient concentration at a distance *R* from the point source and at time *t*; *Q* is nutrient mass at the point source at time 0; D_{eff} is effective nutrient diffusion coefficient on rough surface (Wang and Or, 2012).

The maximum nutrient uptake for an active cell at a distance *R* from point source at time T_B can be approximated as,

$$J_B = 2\pi \langle h \rangle D_{eff} C(R, T_B), \quad (10)$$

where $\langle h \rangle$ is effective aqueous film thickness on a rough surface (Wang and Or, 2012). Equation [10] provides an estimate for microbial cell survival potential whenever J_B is larger than nutrient acquisition for metabolic maintenance, and thus provides an estimate for the maximum nutrient

diffusion distance supporting minimal microbial nutrient acquisition for survival, expressed as,

$$R_D = [-4D_{eff}T_B \ln(\frac{2T_B Q_{B0} m}{Q\langle h\rangle Y})]^{1/2}, \quad (11)$$

where m is microbial maintenance rate.

These estimates (Equations [7] and [11]) could be used to estimate the maximum distance (R_T) between location of a nutrient point source and initial microbial inoculation position that would result in successful trophic interactions towards formation of consortia,

$$R_T = (2\langle V\rangle^2 \tau T_B)^{1/2} + [-4D_{eff}T_B \ln(\frac{2T_B Q_{B0} m}{Q\langle h\rangle Y})]^{1/2}. \quad (12)$$

We may interpret this distance as the minimal volumetric density for microbial inoculation or for bio-stimulation (using granular fertilizer, for example) that would promote trophic association and formation of consortia.

6.3 Results and Discussion

6.3.1 Microbial dynamics and self-organizations of trophically-interacting consortia

We performed systematic numerical simulations of trophically-interacting microbial populations and extracted information concerning patterns and population sizes as seen in snapshots depicted in Fig. 1. As expected, trophically-interacting microbial populations on homogeneous surfaces form stable and self-organized hierarchy patterns, with sp2 (the bottom species in the trophic interaction chain) consistently embedded in close proximity to sp1 (the top species of the trophic interaction chain), essentially conforming with the predicted trophic cascade (Fig. 1a). Initial inoculation positions of interacting species (separated inoculations of two species) may result in temporal suppression of sp2 population growth, however, over time, similar hierarchal patterns emerge reflecting self-organization (Figs. 1b and 1c). The highest population density was found at the periphery of expanding colonies due to favorable nutrient interception at the expanding front (Figs. 1a and 1b), consistent with experimental observations (Harshey, 2003; Macnab, 2003; Park *et al.*, 2003; Hiramatsu *et al.*, 2005). These straightforward simulation results provide a benchmark against which effects of trophic interactions for various spatial and nutritional heterogeneities and hydration variation are evaluated.

6.3.2 Hydration and spatial heterogeneity and nutrient concentrations affecting self-organization dynamics

Figure 2 illustrates simulation results for trophically-interacting microbial community cohabiting heterogeneous rough surfaces. The spatial self-organization patterns are similar to those for

homogeneous surfaces, however, the rates of population growth and colony expansion are greatly reduced, reflecting nutrient limitation and motility constraints. This is particular significant for sp2 whose metabolism relies exclusively on byproduct released by sp1. Not surprisingly, we found a delay in consortia self-organization time with increasing inoculation distance between two species. Under initial nutrient concentration of 0.1 mg/l, microbial population growth was significantly suppressed and time to self-organization prolonged (Figs. 2b and 2c). These results highlight the important roles of both microbial motility and nutrient diffusivity in facilitating trophic interactions among microbial communities. The results suggest that populations cohabiting hydrated rough surfaces (supporting microbial motility and nutrient diffusive transport, however limited), may self-organize in a manner similar to ideal surfaces (homogeneous) and thus enabling substantial coexistence of multiple species consistent with macroecological behavior of plant and animal ecosystems (Knight *et al.*, 2005; Harpole and Tilman, 2007; Dyer *et al.*, 2010; Alexandrou *et al.*, 2011; Cardinale, 2011). Such results may provide mechanistic explanation of macroecology principles based on rapid interactions among soil microbial communities (Gonzalez *et al.*, 2011).

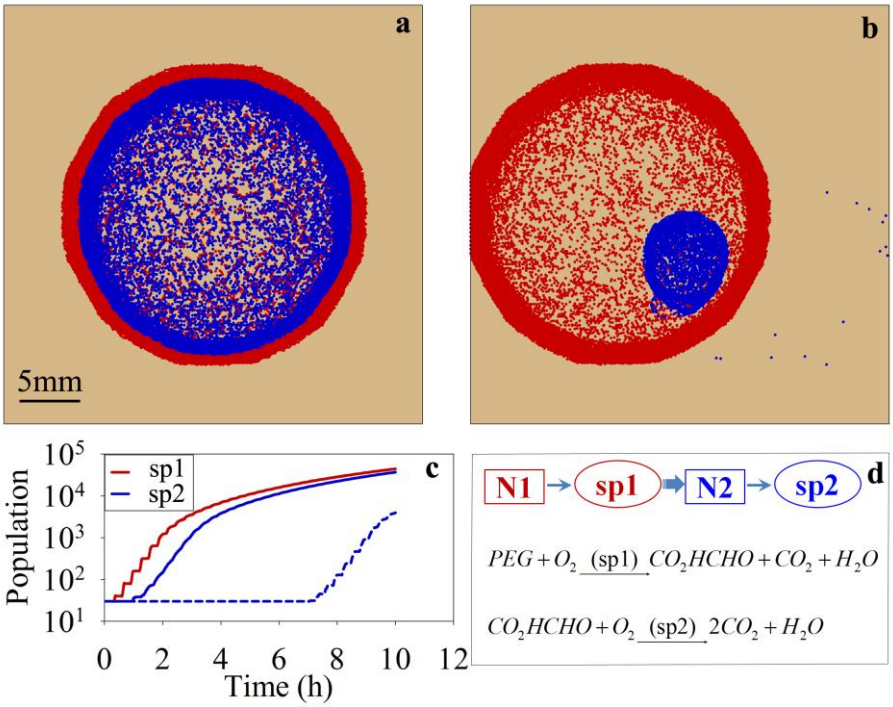

Fig. 1. Microbial grown patterns of two trophically-interacting populations on homogeneous surfaces under -0.5 kPa, with uniform initial nutrient configuration throughout simulation domain with (a) mixed, and (b) separated (with initial inoculations distance between sp1 and sp2 of 10 mm) initial inoculations of two species as sp1(red dots) and sp2 (blue), respectively), (c) population growth curves for mixed (solid lines) and separated initial inoculations (with sp1 has identical growth curves for mixed and separated scenarios), and (d) a schematic definition of trophic interactions and an example of microbial functional consortia (sp1: *Flabobacterium* sp.; and sp2: *Pseudomonas* sp., *Kawai, 2002*) degrading polyethyleneglycol (PEG)

In addition, nutrient limitations (low nutrient concentration) constrain population growth and dispersion ranges and consequently limit transport of excreted nutrient (N2) needed by sp2 thereby prolonging the time needed for consortium self-organization. This especially important while drying and associated capillary forces by air-water interfaces pin down microbial motions and simultaneously disconnect aqueous habitats. The simulation results are consistent with analytical predictions for maximal inoculation distance between two species that would result in successful trophic interactions under certain initial microhabitat conditions (Fig. 2d). Considering initial nutrient and surface hydration conditions for the simulation results in Fig. 2a, the analytically predicted maximum dispersion length (L_T) was larger than the most distant inoculation position and thus ensures successful interactions between sp2 and sp1 for all inoculation sites and formation of stable consortium (Figs. 2a and 2d). In contrast, for the same hydration and heterogeneity, the nutrient conditions for Fig. 2b predict smaller dispersion length than initial inoculation separation distance causing reduction in population size (Figs. 2b and 2d). These results illustrate the significance of nutrient flux (resulting from both nutrient diffusion and concentration) in facilitating microbial trophic interactions and thus affecting community dynamics and composition. This aspect is particularly important for capillary-pinned or non-motile community members (Knight *et al.*, 2005; Harpole and Tilman, 2007). Unlike the uniform nutrient fluxes from the domain boundaries in previous results, figures 3a-3d illustrate simulation results of trophically-interacting populations in the presence of spatially distributed nutrient point sources. We found stable self-organization of microbial growth patterns, with most of the microbial populations congregating around the point source regions. As expected, the time for self-organization was dependent on relative inoculation distance from the point source (Fig. 3a, white numbers mark arrival time to nutrient point sources). The results are in qualitative agreement with observations of rapid chemotactic responses of marine bacteria that swarm to exploit transient nutrient patches (Seymour *et al.*, 2010).

Spatial heterogeneity significantly increases the self-organization time (Figs. 3a and 3b). It took over 50 hrs for microbial populations to successfully access the second farthest point source, as compared with 9 hrs for homogeneous surfaces under similar conditions. Under lower matric potential values (drier surfaces with lower diffusive fluxes), microbial populations experienced considerably reduced growth rates and longer self-organization time. Consequently, less point nutrient sources were accessed, resulting in poorly self-organized consortia pattern (Figs. 3b and 3c). The analytical metric was in good agreement with numerical simulation results (Eq. [12]), as shown in Fig. 3e, with red arrows marking analytical predictions of maximum inoculation distance to a nutrient point source accessible by inoculated bacteria. The

numerical results and more significantly the analytical predictions offer mechanistic explanations for established ecological principles concerning the roles of fluxes of resources or organisms across interfaces between interacting populations in determining community dynamics and composition (Knight *et al.*, 2005).

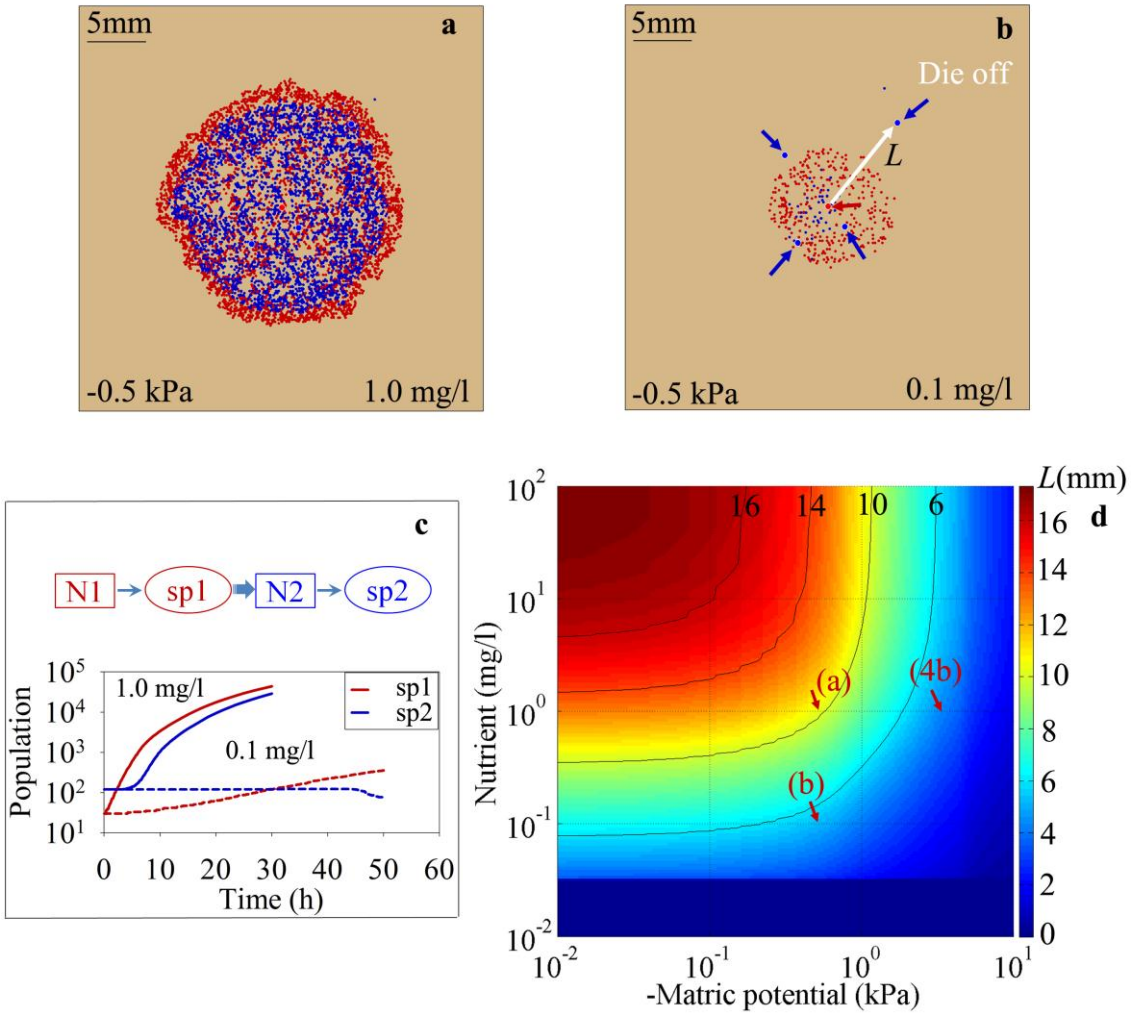

Fig. 2. Microbial grown patterns of two trophically-interacting populations on heterogeneous surfaces under uniform initial nutrient concentration of (a) 1.0 and (b) 0.1 mg/l, with initially separated microbial inoculations (red arrow in b marks inoculation position of sp1, and blue arrows mark inoculation positions of sp2 at distance of *L* to sp1, with its value of 2.0, 3.5, 6.0 and 9.0 mm, respectively), (c) corresponding population growth curves and a schematic definition of trophic interactions, (d) analytical predictions (Eq. [8]) in maximum inoculation distance that allow successful trophic interactions between two separated inoculated species, with red '(a)' and '(b)' mark initial conditions (nutrient and matric potential) for numerical simulations in a and b, and red '(4b)' marks initial conditions for simulations in Fig. 4b

6.3.3 Microbial dynamics and self-organizations with multitrophic interactions

Figure 4 depicts simulation results characteristic to multiple trophically-interacting species cohabiting heterogeneous surfaces. The spatial self-organization patterns are similar to those for two species consortia. Similarly, a decrease in surface hydration considerably suppresses

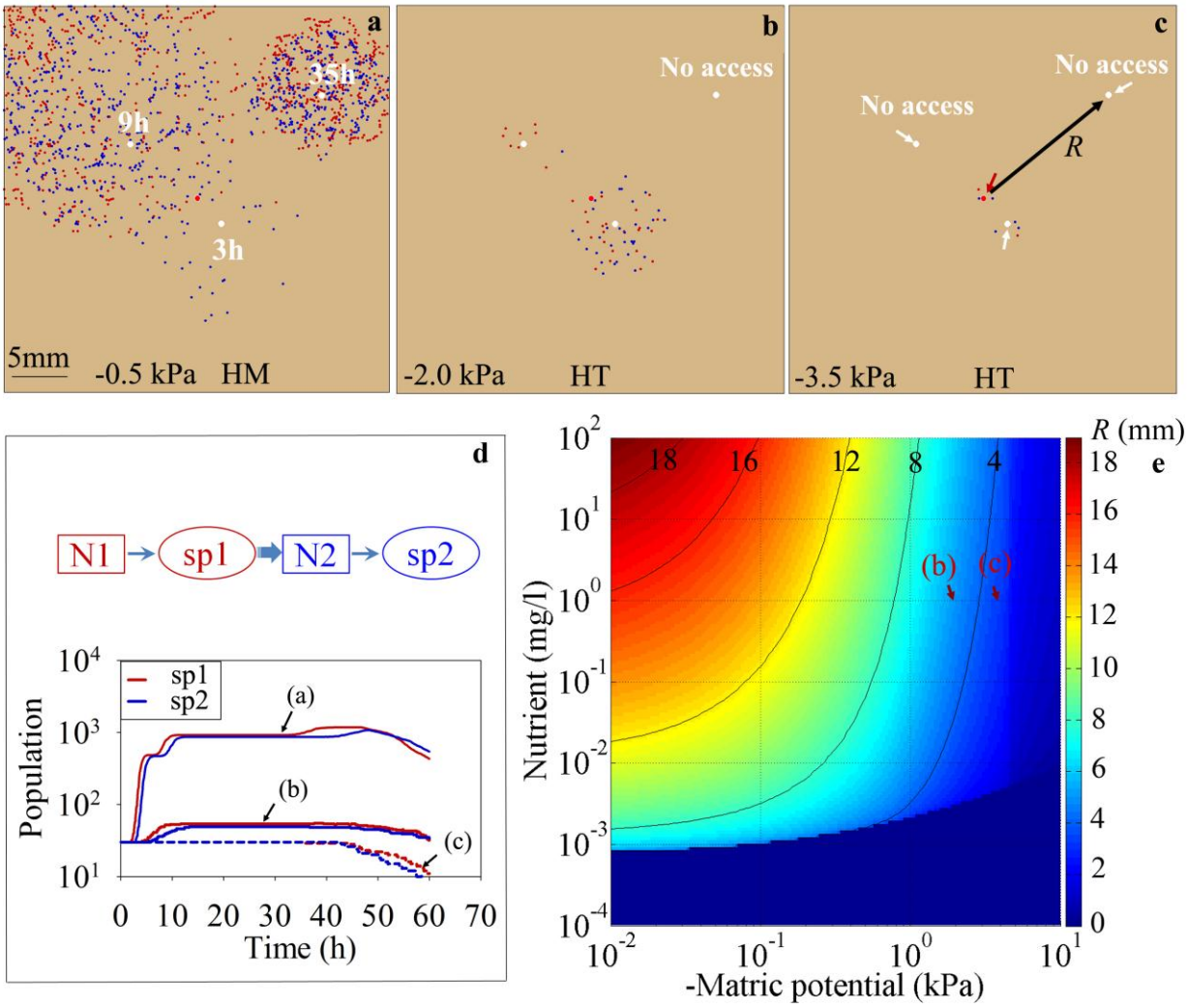

Fig. 3. Microbial grown patterns of two trophically-interacting populations on (a) homogeneous (HM) surface under -0.5 kPa, and on heterogeneous (HT) surface under (b) -2.0 and (c) 3.5 kPa, with initially point nutrient sources at distance *R* (marked by white arrows in c) from mixed initial inoculation (marked by red arrow in c) of 2.5, 7.5 and 14.0 mm, respectively, with initial concentration of nutrient-1 of 1.0 mg/l for all simulations, (d) corresponding population growth curves and a schematic definition of trophic interactions, and (e) analytical predictions (Eq. [12]) in maximum inoculation distance that allow successful trophic interactions between inoculated populations and point nutrient sources, with red '(b)' and '(c)' mark initial conditions (nutrient and matric potential) for numerical simulations in b and c

population growth, with no population simulated for matric potential value of -3.5 kPa. The suppression of microbial populations of sp2 and sp3 suggest also no successful trophic interactions established under dry conditions. For matric potential value of -3.5 kPa, sp2 and sp3 went extinct about 30 hours after inoculation, whereas population of sp1 started to decline 40 hours after inoculation (Fig. 4c). As for 2 species consortia, the potential for trophic interactions for 3 species is also governed by combination of diffusion, and dispersion distance predicted by the analytical expression as shown in Fig. 2d. For matric potential value of -0.5 kPa and initial nutrient concentration of 1 mg/l, the maximum inoculation separation distance is more than 9

mm thus enabling consortia establishment throughout the simulation domain. A decrease in matric potential value to -3.5 kPa resulted in microbial maximum dispersion length of around 4 mm, which was shorter than the initial inoculation distance of 6 mm, therefore, prohibiting trophic interactions and consortia establishment. The results resemble macroscale observation in plant and large organisms regarding foraging or dispersion distances relative to resource heterogeneity and connectivity (Jabot and Bascompte, 2012).

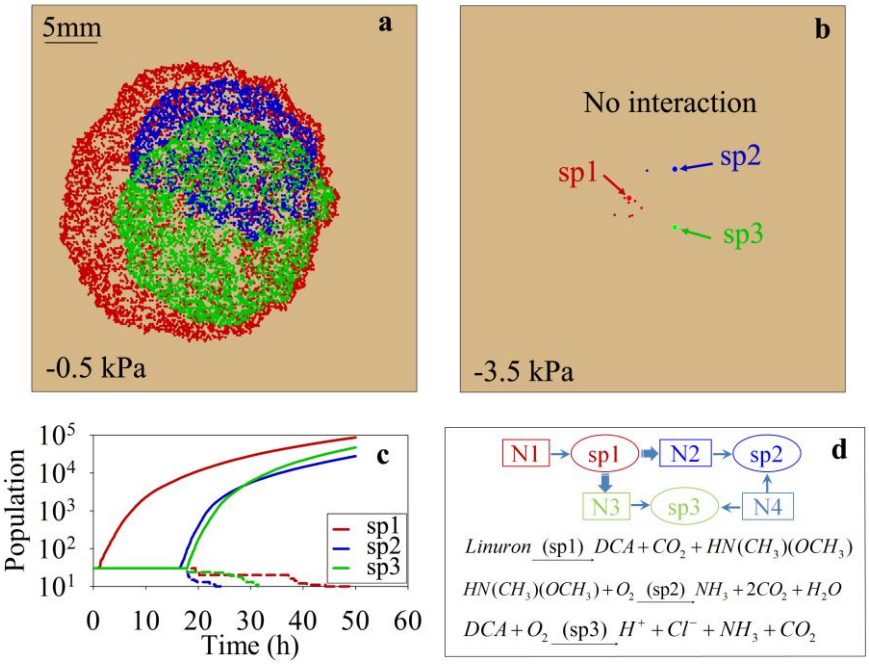

Fig. 4. Simulated growth patterns of trophically-interacting microbial species on heterogeneous (HT) rough surface under (a) -0.5 and (b) -3.5 kPa, with initial inoculation distance of 6 mm among 3 species (arrows in b mark inoculation sites), (c) corresponding population growth curves, and (d) a schematic definition of trophic interactions and an example of microbial functional consortia (sp1: *Variovorax sp.* WDL1; sp2: *H. sulfonivorans* WDL6; and sp3: *D. acidovorans* WDL34, from *Dejonghe et al., 2003*) degrading a pesticide 'linuron'

6.4 Summary and Conclusions

We developed a quantitative framework for systematic evaluation of trophic interactions in the spatial and temporal context and their impacts on microbial community dynamics and composition. Hydration provides the connecting agent for fluxes and dispersion pathways as expected in soil, and thus provide certain predictability for onset and patterns of microbial consortia shaped by diffusion and hierarchy of trophic interactions.

The quantitative estimates may have significant implications for soil resource management, biochemical cycles, and future bioremediation activities. For example, the resulting stable and self-organized coexistence of multiple microbial species support complex ecological functions, e.g., biodegradations of complex compounds (for example, polyethyleneglycol – PEG, and pesticides, such as linuron) that require cooperative metabolisms of multiple populations (Schink, 1997; McCann *et al.*, 1998; Woyke *et al.*, 2006; Miller *et al.*, 2010; Lykidis *et al.*, 2011; Fuchs *et al.*, 2011); and the nature of decreased species richness under dry conditions (common

in natural soil environments) likely reduces nutrient acquisitions of multi-populations resulting in less complete depletion of nutrient sources within an ecosystem and eventually extends microbial trophic processes, and thus enhance persistence of microbial communities cohabiting nutrient sparse soil environments essential for long-term ecosystem services (Cardinale *et al.*, 2006). The sensitivity of microbial growth and trophic organizations on nutrient source strength implies that initial inoculations and/or microbial augmentation are important for sufficient (also complete) biogeochemical processes in soils and other roughness systems (such as leaf surface or dry food materials). The initial microbial consortia construction and ongoing community dynamics mediated by environmental variables as predicted in this study are therefore important for successful bioremediation activities, and thus may play key factors for nutrient cycles at numerous ecosystem scales (Kato and Watanabe, 2010).

Acknowledgements

We acknowledge the financial support of the Swiss National Science Foundation (200021-113442 and 200020-132154).

References

A. Dechesne, G. Wang, G. Güleza, D. Or, B. F. Smets, Hydration-controlled bacterial motility and dispersal on surfaces. *Proc. Natl. Acad. Sci. USA* **107**, 14369-14372 (2010).

A. G. O'Donnell, I. M. Young, S. P. Rushton, M. D. Shirley, J. D. Crawford, Visualization, modelling and prediction in soil microbiology. *Nat. Rev. Microbiol.* **5**, 689-699 (2007).

A. Gonzalez *et al.*, Our microbial selves: what ecology can teach us. *EMBO Rep.* **12**, 775-784 (2011).

A. Lykidis, C. Chen, S. G. Tringe, A. C. McHardy, A. Copeland, N. C. Kyrpides, et al., Multiple syntrophic interactions in a terephthalate-degrading methanogenic consortium. *The ISME J.* **5**, 122-130 (2011).

A. Oren, in *Handbook of environmental engineering*, L. K. Wang, V. Ivanov, J. H. Tay, Y. T. Hung, Eds. (Springer, New York, 2010), Vol. 10.

A. R. Bielefeldt, H. D. Stensel, Biodegradation of aromatic compounds and TCE by a filamentous bacteria-dominated consortium. *Biodegradation* **10**, 1-13 (1999).

B. J. Cardinale *et al.*, Effects of biodiversity on the function of trophic groups and ecosystems. *Nature* **443**, 989-992 (2006).

B. J. Cardinale, Biodiversity improves water quality through niche partitioning. *Nature* **472**, 86-89 (2011).

B. Schink, Energetics of syntrophic cooperation in methanogenic degradation. *Microbiol. Mol. Biol. Rev.* **61**, 262-280 (1997).

C. Douarche, A. Buguin, H. Salman, A. Libchaber, *E. Coli* and oxygen: a motility transition. *Phys. Rev. Lett.* **102**, 198101 (2009).

C. J. Melián, J. Bascompte, P. Jordano, in *Aquatic food webs*, A. Belgrano, U. M. Scharler, J. Dunne, R. E. Ulanowica, Eds. (Oxford Univ. Press, New York, 2005), pp. 19-24.

D. Or, B. F. Smets, J. M. Wraith, A. Dechesne, S. P. Friedman, Physical constraints affecting bacterial habitats and activity in unsaturated porous media - a review. *Adv. Water Resour.* **30**, 1505-1527 (2007).

D. Pérez-Pantoja, B. González, D. H. Pieper, in *Handbook of Hydrocarbon and Lipid Microbiology*, T. McGenity, J. R. Meer, V. Lorenzo, K. N. Timmis, Eds. (Springer, Heidelberg, 2010), pp. 800-829.

D. Reznick, M. J. Bryant, F. Bashey, R- and K-selection revisited: the role of population regulation in life-history evolution. *Ecology* **83**, 1509-1520 (2002).

F. Hiramatsu *et al.*, Patterns of expansion produced by a structured cell population of *Serratia Marcescens* in response to different media. *Microbes Environ.* **20**, 120-125 (2005).

F. Jabot, J. Bascompte, Bitrophic interactions shape biodiversity in space. *Proc. Natl. Acad. Sci. USA* **109**, 4521-4526 (2012).

F. Kawai, Microbial degradation of polyethers. *Appl. Microbiol. Biotechnol.* **58**, 30-38 (2002).

G. Fuchs, M. Boll, J. Heider, Microbial degradation of aromatic compounds – from one strategy to four. *Nat. Rev. Microbiol*. **9**, 803-816 (2011).

G. Wang, D. Or, Aqueous films limit bacterial cell motility and colony expansion on partially saturated rough surfaces. *Environ. Microbiol.* **12**, 1363-1373 (2010).

I. M. Young, J. W. Crawford, Interactions and self-organization in the soil-microbe complex. *Science* **304**, 1634-1637 (2004).

J. Dolfing, J. M. Tiedje, Kinetics of two complementary hydrogen sink reactions in a defined 3-chlorobenzoate degrading methanogenic co-culture. *FEMS Microbiol. Ecol.* **86**, 25-32 (1991).

J. G. Skellam, Random dispersal in theoretical populations. *Biometrika* **38**, 196-218 (1951).

J. Huisman, F. J. Weissing, Biodiversity of plankton by species oscillations and chaos. *Nature* **402**, 407-410 (1999).

J. I. Prosser *et al.*, The role of ecological theory in microbial ecology. *Nature* **5**, 384-392 (2007).

J. R. Banavar, A. Maritan, Towards a theory of biodiversity. *Nature* **460**, 334-335 (2009).

J. R. Seymour, R. Simó, T. Ahmed, R. Stocker, Chemoattraction to dimethylsulfoniopropionate throughout the marine microbial food web. *Science* **329**, 342-345.

J. W. Crawford, J. A. Harris, K. Ritz, I. M. Young, Towards an evolutionary ecology of life in soil. *Trends Ecol. Evol.* **20**, 81-87 (2005).

K. L. I. Norlund, *et al*., Microbial architecture of environmental sulfur processes: a novel syntrophic sulfur-metabolizing consortia. *Environ. Sci. Technol*. **43**, 8781-8786 (2009).

K. McCann, A. Hastings, G. R. Huxel, Weak trophic interactions and the balance of nature. *Nature* **395**, 794-798 (1998).

L. A. Dyer, T. R. Walla, H. F. Greeney, J. O. Stireman III, R. F. Hazen, Diversity of interactions: a metric for studies of biodiversity. *Biotropica* **42**, 281-289 (2010).

L. D. Miller *et al*., Establishment and metabolic analysis of a model microbial community for understanding trophic and electron accepting interactions of subsurface anaerobic environments. *BMC Microbiol*. **10**, 149 (2010).

L. G. Morelli, K. Uriu, S. Ares, A. C. Oates, Computational approaches to developmental patterning. *Science* **336**, 187-191 (2012).

M. A. Alexandrou *et al*., Competition and phylogeny determine community structure in Müllerian co-mimics. *Nature* **469**, 84-88 (2011).

M. Albanna, M. Warith, L. Fernandes, Kinetics of biological methane oxidation in the presence of non-methane organic compounds in landfill bio-covers. *Waste Manage.* **30**, 219-227 (2012).

M. E. Hibbing, C. Fuqua, M. R. Parsek, S. B. Peterson, Bacterial competition: surviving and thriving in the microbial jungle. *Nat. Rev. Microbiol.* **8**, 15-25 (2010).

N. C. Darnton, H. C. Berg, Bacterial flagella are firmly anchored. *J. Bacteriol*. **190**, 8223-8224 (2008).

P. Nannipieri, L. Badalucco, in *Handbook of Processes and Modeling in the Soil Plant System*, D. K. Benbi, R. Niedere, Eds. (Haworth, Binghamton, New York, 2003), pp. 57-82.

R. M. Harshey, Bacterial motility on a surface: many ways to a common goal. *Annu. Rev. Microbiol.* **57**, 249-273 (2003).

S. A. Hasan, M. I. M. Ferreira, M. J. Koetsier M. I. Arif, D. B. Janssen DB, Complete biodegradation of 4-fluorocinnamic acid by a consortium comprising *Arthrobacter* sp. strain G1 and *Ralstonia* sp. strain H1. *Appl. Environ. Microbiol*. **77**, 572-579 (2011).

S. Kato, K. Watanabe, Ecological and evolutionary interactions in syntrophic methanogenic consortia. *Microbes Environ*. **25**, 145-151 (2010).

S. Park, P. M. Wolanin, E. A. Yuzbashyan, P. Silberzan, J. B. Stock, R. H. Austin, Motion to form a quorum. *Science* **301**, 188-188 (2003).

T. Fenchel, Microbial behavior in a heterogeneous world. *Science* **296**, 1068-1071 (2002).

T. M. Knight, M. W. McCoy, J. M. Chase, K. A. McCoy, R. D. Holt, Trophic cascades across ecosystems. *Nature* **437**, 880-883 (2005).

T. P. Curtis, W. T. Sloan, Prokaryotic diversity and its limits: microbial community structure in nature and implications for microbial ecology. *Curr. Opin. Microbiol.* **7**, 221-226 (2004).

T. Woyke *et al.*, Symbiosis insights through metagenomic analysis of a microbial consortium. *Nature* **443**, 950-955 (2006).

V. Christensen, C. J. Walters, Ecopath with Ecosim: methods, capabilities and limitations. *Ecol. Model.* **172**, 109-139 (2004).

V. H. Smith, Effects of resource supplies on the structure and function of microbial communities. *Anton. Leeuw. Int. J. G.* **81**, 99-106 (2002).

V. Torsvik, L. Øvreås, in *Modern Soil Microbiology*, J. D. van Elsas, J. K. Jansson, J. T. Trevors, Eds. 2nd edn. (Taylor, Boca Raton, 2006), pp 23-54.

V. V. Phelan, W. Liu, K. Pogliano, P.C. Dorrestein, Microbial metabolic exchange – the chemotype-to-phenotype link. *Nat. Chem. Biol*. **8**, 26-35 (2012).

W. Dejonghe *et al.*, Synergistic degradation of linuron by a bacterial consortium and isolation of a single linuron-degrading variovorax strain. *Appl. Environ. Microbiol*. **69**, 1532-1541 (2003).

W. S. Harpole, D. Tilman, Grassland species loss resulting from reduced niche dimension. *Nature* **446**, 791-793 (2007).

G. Wang, D. Or, A Hydration-Based Biophysical Index for the Onset of Soil Microbial Coexistence. *Scientific Reports* **2**: 88, 2012 *DOI: 10.1038/srep00881*.

R. E. Pattle, Diffusion from an instantaneous point source with a concentration-dependent coefficient. *Quart. J. Mech. Appl. Math*. **7**, 407-409 (1959).

Chapter 7

Summary and Outlook

7.1 Summary

We have successfully developed a hybrid model that couples an individual-based modeling approach with diffusion-consumption elements for simulating microbial growth, nutrient consumption, and trophic interactions on rough surfaces. The model explicitly considers surface geometrical features and variable hydration conditions that determine aqueous-phase configurations essential for microbial growth and nutrient diffusion. The model resolves spatial- and temporal nutrient diffusion fields defined by boundary conditions and surface heterogeneity, and local nutrient interception by microbial populations. It explicitly tracks motions and life histories of microbial cells considering primary hydrodynamic and capillary constraints to motility. The model enables systematic estimation of the effects of hydration status and surface geometrical properties on microbial cell motility and impacts on microbial colony growth and expansion, and the influence of variable hydration conditions on microbial population dynamics and species coexistence on partially hydrated rough surfaces. We also studied the effects of trophic interactions on shaping microbial population dynamics and community composition, and their impacts on microbial ecological functioning in unsaturated soils. We draw the following primary conclusions:

1. Bacterial flagellar motility on unsaturated soil surfaces is severely limited due to physical constraints imposed by coupling surface geometrical features and hydration conditions. Experimental measurements of many individual cells inhabiting partially-hydrated porous ceramic surfaces have shown a rapid decrease in cell motility (expressed as mean cell velocity) with decreasing surface matric potential value; and within a few kPa of matric potential value, cell motility nearly ceased. The constraints on cell motility contribute to and control bacterial colony expansion on unsaturated rough surfaces.
2. Our mechanistic simulation model demonstrated that capillarity and water configuration resulting from hydration conditions and pore space features play key roles limiting cell motility by imposing cell-wall hydrodynamic interactions and capillary pinning forces on individual cells inhabiting partially-hydrated rough surfaces. The motility constraints combined with nutrient diffusion limitation control bacterial growth and colony development on rough surfaces. The simulation results defined a surprisingly narrow range of hydration

conditions where motility confers an ecological advantage upon bacteria living on natural surfaces.

3. Hydration variations mediate environmental conditions of microhabitats. The range of hydration conditions that may confer physical and ecological advantages to superior microbial populations and support competitive exclusion of less efficient populations is surprisingly narrow (within a few kPa of matric potential value). The rapid fragmentation of soil aqueous phase under natural conditions suppresses microbial growth and cell dispersion thereby balancing performance of competing populations. Additionally, hydration fluctuations intensify localized interactions leading to promotion of coexistence by affecting disproportionally densely populated regions during dry periods thereby affecting microbial population dynamics far beyond responses predicted from equivalent stationary hydration values.
4. Based on the knowledge gained from the systematic study of microbial life on unsaturated rough surfaces, we have successfully developed a novel biophysically-based metric capable of predicting conditions suitable for microbial species coexistence and diversity in soils, based on solely quantifiable biophysical variables. These include aqueous-phase capillary retention on rough surfaces, thinning of liquid films and formation of disconnected aquatic clusters, along with the resulting ranges of microbial self-motion and dispersion, and constraints on diffusion-supported microbial growth. These biophysical ingredients are integrated into a novel predictive index with potentially broad applicability encompassing natural soil surfaces, dry food products and other partially hydrated rough surfaces. The model predicts a surprisingly narrow range of hydration conditions that mark a sharp transition from suppression to promotion of microbial species coexistence irrespective of soil type or details of surface roughness geometry for the onset of microbial coexistence consistent with limited experimental data and with individual-based simulation models.
5. Simulation models of trophic interactions among multiple microbial populations cohabiting rough surfaces revealed that trophic interactions increase ecological niche dimensionality through spatial self-organization among microbial consortia. Spatial organization is strongly influenced by the geometry of primary nutrient fluxes and by the nature and rate of release of byproducts essential for other members in the consortium. Not surprisingly, hydration conditions and spatial heterogeneity impose diffusion constraints and motility limitations that influence levels and rates of self-organization. Concentration gradients and inhibitory functions of various substrates relative to species growth rates and tolerance levels are clearly manifested in the emerging spatial patterns of consortia.

The study lies at the intersection of environmental microbiology, vadose zone hydrology, and soil physics. The quantitative results offer a great potential for improved mechanistic understanding of microbiological interactions in the most active compartment of the biosphere by cutting across disciplinary boundaries and offering new insights into long standing environmental questions that are critical to soil and water resource quality, the fate of biogenic and anthropogenic contaminants, and global biogeochemical cycles. Specifically, the results shed light onto the origins of the unparalleled biodiversity maintained in soil. The proposed frameworks (the hybrid model and predictive coexistence index) further constitute useful instruments for guiding future experiments and data collection.

7.2 Outlook

An important and poorly studied aspect of soil microbial biology is its temporal components. Molecular-based estimates of microbial diversity in soils are likely to represent a genetic potential, most of which may be associated with inactive organisms. Even mild temporal fluctuations in hydration conditions common in many soils of temperate regions may exert significant influence on microhabitats and microbial functions in unsaturated soils. The range of water potentials (and relative humidity - RH) supporting growth and activity of microbial life is surprisingly narrow. Desiccation extremes require significant physiological adjustments and adaptation strategies. The present consensus is that under extreme desiccation conditions the best survival strategy is for microorganisms to completely abolish their metabolism during the most unfavorable period, and switch into a dormant state until conditions improve. Consequently, many microorganisms developed resting stages or spores. In the dormant state, spores undergo no detectable metabolism and exhibit a higher degree of resistance to inactivation under extremely stressed conditions. Sporulation is genetically expensive and misses growth opportunities even at low resource levels. *Commitment to the spore stage occurs at some point but seems to be a progression of events which, once completed, prevents reversion; the point of no return is the accumulation of successive survival events* – Roszak and Colwell, 1987. There are microorganisms that neither sporulate nor encyst, and yet can be isolated from unfavorable environments. Such microorganisms persist as vegetative (dormant) cells but use up their energy reserves slowly due to reduced metabolic activity. Establishing quantitative links between survival strategies in soils subjected to different frequencies and extremes (magnitude) of desiccation stress and the corresponding microbial population dynamics and coexistence of multiple strategies remains unexplored at the process level. It is also at the core of the idea of a “flickering” active diversity and is thus intimately linked to the temporal dimension of

ecological niche. Another most common microbial response to extreme environmental fluctuations is formation of biosynthesized extracellular polymeric substances (EPS) in which cells are embedded, forming aggregates or sessile colonies attached to solid surfaces. Soil bacterial aggregation and pooling of resources prove a successful adaptation to variations in hydration status and in nutrient availability, and enhances cooperative genetic and metabolic exchanges. The ubiquity of such microbially excreted EPS across many different environmental conditions and habitats is attributed to its key role in environmental adaptation in particular anchoring, nutrient entrapment, and maintenance of favorable hydration conditions. EPS support higher water retention and consequently higher nutrient diffusion rates within EPS-rich microenvironments relative to surrounding soil under dry conditions. Given the ecological importance of this ubiquitous modification of microbial immediate environment, information regarding the role and function of EPS in the vadose zone that supports much of the microbial diversity, plant life, and nutrient cycling, is limited. In particular, quantitative description of mechanisms by which EPS confers desiccation resistance or enhances recovery following desiccation for a diverse group of prokaryotes in partially-saturated terrestrial habitats remains obscure (especially at the scale of a microbial aggregate or colony attached to soil surface). Particularly important is the link between EPS hydro-chemical characteristics that make it a "universal" interface between microbes and their environments, and its capacity to improve microbial existence under transient desiccation conditions in the vadose zone.

Based on these open research questions, we propose the following steps in future research:

1. To extend our modeling framework for elucidating long term bacterial survival strategies in response to extreme hydration dynamics associated with different climatic regions in the world. Specifically, to quantify success of sporulation vs. temporary dormancy strategies in response to exposure to prescribed patterns of desiccation conditions with variable extent and duration (climatic data derived) on simulated microbial population size and composition.
2. To integrate physical aspects of EPS production and resulting interfacial hydration and transport properties into modeling microbial function and survival in unsaturated soil subjected to dynamic hydration patterns.

GANG WANG, PhD – Curriculum Vitae

PERSONAL INFORMATION

Gang Wang
ETH Zurich
Institute of Terrestrial Ecosystems (ITES)
8092-Zurich, Switzerland
Tel: +41 44 633 6013
E-mail: gang.wang@env.ethz.ch

SUMMARY OF RESEARCH INTERESTS

My research interest focuses on the causes and consequences of microbial diversity; biofilm modeling and bacterial evolution; mass flow and transport in porous media, and on interfaces between pore scale physical processes and biological activity in soils; environmental measurement technology, waste management and bioremediation, and microbial community ecology of N and C cycling and global climate changing.

I have authored and co-authored 12 refereed publications (*ISI citations over 300*), 1 manuscript in review and 1 manuscript in preparation, and 16 proceeding papers and abstracts.

EDUCATION

Ph.D. Environmental Sciences
ETH Zurich, Switzerland. 2012 (*PhD defense on May, 2012*), supervisor Prof. Dr. Dani Or

M.Sc. Applied Chemistry
University of Science & Technology of China, Hefei, China. 2005

B.A. Chemical Engineering
University of Science & Technology of China, Hefei, China. 2002

PROFESSIONAL EXPERIENCE

2008 – 2012	Research assistant	ETH Zurich, Switzerland
2005 – 2007	Research Director	China National Center for Quality Supervision and Test of Standard Parts, China
2002 – 2005	Research assistant	University of Science & Technology of China
2001 – 2002	Research assistant	University of Science & Technology of China

PROFESSIONAL AFFILIATIONS

American Geophysical Union (AGU)

European Geosciences Union (EGU)

American Society for Microbiology (ASM)

Federation of European Microbiological Societies (FEMS)

PUBLICATIONS

SCIENTIFIC JOURNALS (Refereed) --

1. **Wang G** and D Or. Trophic interactions and self-organization of microbial consortia on unsaturated surfaces. (in preparation)
2. Lazouskaya V, D Or, **G Wang**, LP Wang, JL Caplan, and Y Jin. Colloid mobilization by fluid displacement fronts in channels. (Submitted)
3. **Wang G** and D Or. 2012. A hydration-based biophysical index for the onset of soil microbial coexistence. *Scientific Reports* **2**: 88, 2012 *DOI: 10.1038/srep00881*.
4. **Wang G** and D Or. 2012. Hydration dynamics promote bacterial coexistence on rough surfaces. *ISME J.* doi:10.1038/ismej.2012.115.
5. **Wang G** and D Or, 2010. Aqueous films limit bacterial motility and colony expansion on partially saturated rough surfaces. *Environ. Microbiol.* 12, 1363. (*9 cit - ISI*)
6. Dechesne A, **G Wang**, G Gülez, D Or and BF Smets. 2010. Hydration controlled bacterial motility and dispersal on surfaces. *PNAS* 107, 14369. (11 *cit - ISI*)
7. Mu Y, HQ Yu, **G Wang**. 2007. Evaluation of three methods for enriching H-2-producing cultures from anaerobic sludge. *Enzyme Microb. Technol.* 40, 947. (56 *cit - ISI*)
8. Mu Y, HQ Yu, **G Wang**. 2007. A kinetic approach to anaerobic hydrogen-producing process. *Water Res.* 41, 1152. (34 *cit - ISI*)
9. Mu Y, **G Wang,** HQ Yu. 2006. Kinetic modeling of batch hydrogen production process by mixed anaerobic cultures. *Bioresour. Tecnnol.* 97, 1302. (37 *cit - ISI*)
10. Mu Y, **G Wang,** HQ Yu. 2006. Response surface methodological analysis on biohydrogen production by enriched anaerobic cultures. *Enzyme Microb. Technol.* 38, 905. (51 *cit - ISI*)
11. Mu Y, HQ Yu, **G Wang.** 2006. Permeabilities of anaerobic CH_4-producing granules. *Water Res.* 40, 1811. (5 *cit - ISI*)
12. **Wang G,** Y Mu, HQ Yu. 2005. Response surface analysis to evaluate the influence of pH, temperature and substrate concentration on the acidogenesis of sucrose-rich wastewater. *Biochem. Eng. J.* 23, 175. (40 *cit - ISI*)
13. Hu ZH, **G Wang**, HQ Yu. 2004. Anaerobic degradation of cellulose by rumen microorganisms at various pH values. *Biochem. Eng. J.* 21, 59. (30 *cit - ISI*)
14. Fu RQ, TW Xu, **G Wang**, WH Yang, and ZX Pan. 2003. PEG-catalytic water splitting in the interface of a bipolar membrane. *J. Colloid Interf. Sci.* 263, 386. (32 *cit - ISI*)

PROCEEDINGS AND ABSTRACTS --

1. **Wang G** and D Or. 2012. A hydration-based biophysical index for the onset of soil microbial coexistence. ITES rDAY, 2012, Zurich, Switzerland.
2. **Wang G** and D Or. 2012. Self-organization of microbial consortia via trophic interactions on hydrated rough surfaces. ISME14 Roundtable meeting, 2012, Copenhagen, Denmark.
3. Lazouskaya V, **G Wang**, D Or and Y Jin. Colloid mobilization by displacement fluid fronts in porous media. Gordon Research Seminar 2012, Flow & Transport in Permeable Media, Les Diablerets, Switzerland.
4. **Wang G** and D Or. 2012. A biophysical index for predicting hydration-mediated microbial diversity in soils. EGU2012, 2012, Vienna, Austria.

5. **Wang G** and D Or. Hydration-induced diffusion and motility constraints promote microbial diversity in unsaturated soil. ZHydro seminar 2011, Zurich, Switzerland.
6. **Wang G** and D Or. 2011. Constrained motility and nutrient diffusion shape bacterial colony morphology on partially hydrated rough surfaces. FEMS2011, 2011, Geneva, Switzerland.
7. Jin Y, V Lazouskaya, **G Wang** and D Or. 2010. Mechanisms of colloid retention and mobilization in unsaturated porous media. CESAR 2010, 2010, Viborg, Denmark.
8. **Wang G** and D Or. 2010. Hydration affects motility and nutrient diffusion and governs microbial coexistence on rough surfaces. CESAR 2010, 2010, Viborg, Denmark.
9. **Wang G** and D Or. Heterogeneous nutrient fields shape microbial competition on rough sources. ITES seminar 2010, Zurich, Switzerland.
10. Jin Y, D Or, F Moebius and **G Wang.** 2010. Colloid mobilization by displacement fluid fronts in porous media. EGU2010, 2010, Vienna, Austria.
11. **Wang G** and D Or. 2010. Heterogeneous diffusion of two nutrients shape growth and dispersal patterns of competing bacterial species grown on partially saturated rough surfaces. RAISEBIO2010, 2010, Leipzig, Germany.
12. **Wang G** and D Or. 2009. Hydration effects on microbial motility and coexistence on unsaturated rough surfaces. SGM2009, 2009, Neuchâtel, Switzerland.
13. Dechesne A, **G Wang**, D Or, D Gulez and Barth F Smets. 2009. Individual- and population-scale swimming motility on unsaturated surfaces: experimental quantification and biophysical modeling. FEMS2009, 2009, Gothenburg, Sweden.
14. **Wang G** and D Or. 2009. Microbial growth and coexistence on diffusion-limited unsaturated rough surfaces. EGU2009, 2009, Vienna, Austria.
15. **Wang G** and D Or. 2008. Capillarity and liquid configuration limit bacterial motility on unsaturated rough surfaces. AGU2008, 2008, San Francisco, CA, USA.
16. **Wang G**, Y Mu, HQ Yu. 2004. A kinetic approach to anaerobic hydrogen-producing process. Proceedings of 1st National Symposium on Pollution Control and Resource Reuse. 2004, Shanghai, China.